

Michael Buchsteiner, BSc

**Biomimetic Models for Acetylene Hydratase:
Alkyne Activation on Tungsten Centers**

MASTERARBEIT

zur Erlangung des akademischen Grades

Diplom-Ingenieur

Masterstudium Technische Chemie

eingereicht an der

Technischen Universität Graz

Betreuerin

Univ.-Prof. Dr. Nadia C. Mösch-Zanetti

Institut für Chemie, Bereich Anorganische Chemie

Karl-Franzens-Universität Graz

EIDESSTATTLICHE ERKLÄRUNG

Ich erkläre an Eides statt, dass ich die vorliegende Arbeit selbstständig verfasst, andere als die angegebenen Quellen/Hilfsmittel nicht benutzt, und die den benutzten Quellen wörtlich und inhaltlich entnommenen Stellen als solche kenntlich gemacht habe. Das in TUGRAZonline hochgeladene Textdokument ist mit der vorliegenden Masterarbeit identisch.

10.05.2018
Datum

H. Buchsteiner
Unterschrift

ACKNOWLEDGEMENT

I would like to express my deepest gratitude to a number of people who reliably accompanied and supported me throughout my studies in Graz. All of you made my final degree not only possible, but contributed to an extraordinary experience in my life.

First of all I would like to thank my supervisor Univ.-Prof. Dr. Nadia C. Mösch-Zanetti for making it possible to carry out this work in her research group and for giving me such a fascinating and future-oriented topic. This thesis would not have been possible without her professional guidance and without such a great working environment. I owe my deepest gratitude to Carina Vidovič, MSc for taking another master student in her tungsten team. Without numerous discussions and her enormous support this thesis would not have materialized in such a way. I also sincerely thank Ass.-Prof. Dr. Jörg Schachner for his guidance into the world of Inorganic Chemistry. He massively contributed to my enthusiasm for Inorganic Chemistry in the summer of my 4th semester and he always made sure that fun and jokes do not go short in the daily business. Furthermore I have greatly benefited from Dr. Lydia M. Peschel, who accepted me as her bachelor student and introduced me into her tungsten chemistry. Her guidance and her supervision during my Bachelor's thesis were essential for the success of my master thesis. It is very sad, that she can no longer be with us. Additionally I would like to express my greatest appreciation to Ao.Univ.-Prof. Dr. Ferdinand Belaj for measuring my crystals and for solving my crystal structures, to Ing. Bernd Werner for measuring my numerous NMR samples and to our technicians Doris Eibinger and Nathalie Kowaliuk-Breg for providing required chemicals and glassware that quickly. They have made their essential support available in a number of ways. In addition, there are a number of people who were not directly involved in my daily work, but provided valuable support, encouragement or just made the daily work within the group very enjoyable: Stefan Holler, MSc with insightful discussions about organic chemistry, Mike Tüchler, MSc and Dr. Antoine Dupé with invaluable support and comments, our apprentices Alexander Zernig and Tanja Scheer by cleaning all my dirty glassware and by delivering my NMR samples, Dr. Simon Walg, Dr. Niklas Zwettler, Melanie Ramböck, MSc, Dr. Hristo Varbanov, Madeleine Ehweiner, MSc and Isabel

Fuchs by being such valuable and supportive colleagues. Thank you for creating such a great working environment!

My studies would not have been possible without the support of my family and my friends. Special thanks to my parents for encouraging me in all my plans, giving me good advice and for fulfilling all my wishes. Last but not least I would like to thank my friends, especially Mario Lang and Franz Strauß, for our numerous organic synthesis evenings, which drove me to get better in synthetic chemistry and for the great time with them throughout my studies. You all have made my years of study extraordinary!

TABLE OF CONTENTS

List of Abbreviations	3
Abstract	4
Zusammenfassung	5
1. Introduction	6
1.1 Synthesis of Acetaldehyde in Nature and Industry	6
1.1.1 Industrial Synthesis of Acetaldehyde: The Wacker Process	7
1.1.2 Enzymatic Synthesis of Acetaldehyde	8
1.2 Tungsten in Enzymes	9
1.3 <i>Acetylene Hydratase</i>	10
1.3.1 Molecular Structure of <i>Acetylene Hydratase</i>	10
1.3.2 Mechanistic Considerations	11
1.4 Alkyne Activation on Metal Centers	13
1.5 The Bonding Situation in Metal-Alkyne and Metal-Carbonyl Complexes ..	15
1.5.1 Metal-Alkyne Complexes	15
1.5.2 Metal-Alkyne-Carbonyl Complexes	16
1.5.3 Metal-Oxo-Alkyne Complexes	18
1.6 Biomimetic Models for <i>Acetylene Hydratase</i>	19
1.6.1 Tungsten(II)-Alkyne Complexes	19
1.6.2 Tungsten(IV) Complexes as Models for <i>Acetylene Hydratase</i>	22
1.6.3 Oxotungsten(IV)-Alkyne Chemistry	24
2. Objectives	26
3. Results and Discussion	28
3.1 Ligand Synthesis	28
3.1.1 Synthesis of Sodium 4-Methylpyridine-2-thiolate	28
3.1.2 Synthesis of Sodium 4,6-Dimethylpyrimidine-2-thiolate	29
3.2 Tungsten(II) Precursor Synthesis	30

3.3	Complex Synthesis	31
3.3.1	Synthesis of $[W(CO)_3L_2]$	31
3.3.2	Synthesis of $[W(CO)(H\equiv H)L_2]$	34
3.3.3	Oxidation of $[W(CO)(H\equiv H)L_2]$ to $[WO(H\equiv H)L_2]$	42
3.4	Reactivity of $[WO(H\equiv H)L_2]$	47
3.4.1	Catalytic Acetylene Hydration	47
3.4.2	Reactivity of $[WO(H\equiv H)L_2]$ with various Nucleophiles / Electrophiles ..	50
4.	Conclusion	53
5.	Experimental Section	55
5.1	General	55
5.2	Precursor Synthesis	58
5.3	Ligand Synthesis	59
5.4	Complex Synthesis	61
6.	References	68
7.	Appendix	73
7.1	Crystallographic Data and Structure Refinement	73

LIST OF ABBREVIATIONS

4-Me-SPy	4-Methylpyridine-2-thiolate
6-Me-SPy	6-Methylpyridine-2-thiolate
Asp	Aspartic acid
bp	Boiling point
cat.	Catalyst
D	Donor
DABCO	1,4-Diazabicyclo[2.2.2]octane
Et	Ethyl
L	Any bidentate monoanionic ligand
M	Any metal
MA	Maleic acid anhydride
mCPBA	<i>meta</i> -Chloroperoxybenzoic acid
Me	Methyl
Me-SPym	4,6-Dimethylpyrimidine-2-thiolate
mnt	1,2-Dicyanoethylenedithiolate
n-Pr	n-Propyl
Nu	Nucleophile
OTf	Trifluoromethanesulfonate
ox.	Oxidation
PyN-O	Pyridine- <i>N</i> -oxide
rt	Room temperature
SPhoz	2-(4'-Dimethyloxazolin-2'-yl)-thiophenolate
SPy	Pyridine-2-thiolate
THF	Tetrahydrofuran
TMAO	Trimethylamine- <i>N</i> -oxide
Tp'	Hydridotris(3,5-dimethylpyrazolyl)borate
X	Any halogen

ABSTRACT

A novel biomimetic structural model for the enzyme *Acetylene Hydratase* is presented. In order to mimic the sulfur-rich active site, the literature known ligands 4-methylpyridine-2-thiolate (**L1**, 4-Me-SPy) and 4,6-dimethylpyrimidine-2-thiolate (**L2**, Me-SPym) were employed. Both ligands were chosen to stabilize tungsten-acetylene adducts similar to the literature-known 2-(4-dimethyloxazolin-2'-yl)thiophenolate ligand. Especially the electron-poor ligand 4,6-dimethylpyrimidine-2-thiolate was applied to provoke a nucleophilic attack on a coordinated acetylene.

Starting from the well-known tungsten(II) precursors $[\text{W}_2\text{Br}_4(\text{CO})_7]$ (**P1**) and $[\text{WBr}_2(\text{CO})_3(\text{NCMe})_2]$ (**P2**) the tungsten tris-carbonyl complexes $[\text{W}(\text{CO})_3(\text{Me-SPym})_2]$ (**C2**) and $[\text{W}(\text{CO})_3(4\text{-Me-SPy})_2]$ (**C1**) were synthesized. The tris-carbonyl complexes were further reacted with acetylene to give $[\text{W}(\text{CO})(\text{H}\equiv\text{H})(\text{Me-SPym})_2]$ (**C4**) when employing **C2**. In the case of **C1** the complex underwent acetylene insertion into the W-N bond to obtain $[\text{W}(\text{CO})(\text{H}\equiv\text{H})(=4\text{-Me-SPy})(4\text{-Me-SPy})]$ (**C3**). Furthermore compound **C3** was found to eliminate acetylene with time in solution to give $[\text{W}(\text{CO})(\text{H}\equiv\text{H})(4\text{-Me-SPy})_2]$ (**C5**). The complex **C5** was additionally also synthesized via the ligand addition method from a precursor mixture of $[\text{WBr}_2(\text{CO})(\text{H}\equiv\text{H})(\text{NCMe})_2]$ with $[\text{WBr}_2(\text{CO})(\text{H}\equiv\text{H})_2(\text{NCMe})]$ (**P3**). The tungsten(IV) complexes $[\text{WO}(\text{H}\equiv\text{H})(\text{Me-SPym})_2]$ (**C6**) and $[\text{WO}(\text{H}\equiv\text{H})(4\text{-Me-SPy})_2]$ (**C7**) were obtained by controlled oxidation with the oxygen-atom-transfer reagent pyridine-*N*-oxide.

The investigation of **C3** towards oxidation and of **C6** and **C7** towards methyl lithium, piperidine, sodium methanolate, water, methyl iodide and pyridine-*N*-oxide did not result in the desired reactivity.

All compounds were fully characterized by ^1H and ^{13}C NMR spectroscopy, IR spectroscopy and single crystal X-ray diffraction analysis. Compared to free acetylene, the coordination towards the tungsten center in **C3-C7** results in a significant elongation of the acetylenic $\text{C}\equiv\text{C}$ bond, as well as in a drastic downfield shift of acetylenic ^1H and ^{13}C NMR signals. These results point towards an enhanced electrophilicity on acetylenic carbons.

ZUSAMMENFASSUNG

Ein neues strukturelles Modell für das Enzym Acetylen Hydratase wird vorgestellt. Um die schwefelreiche Umgebung des aktiven Zentrums nachzubilden, wurden die literaturbekannten Liganden 4-Methylpyridin-2-thiolat (**L1**, 4-Me-SPy) und 4,6-Dimethylpyrimidin-2-thiolat (**L2**, Me-SPym) eingesetzt. Beide Liganden wurden ausgewählt, um Wolfram-Acetylen Addukte, ähnlich zum literaturbekannten Liganden 2-(4-Dimethyloxazolin-2'-yl)thiophenolat, zu stabilisieren. Besonders der elektronenarme Ligand 4,6-Dimethylpyrimidin-2-thiolat wurde ausgewählt, um die Reaktivität des koordinierten Acetylen gegenüber einem nukleophilen Angriff zu steigern.

Beginnend mit den bekannten Wolfram(II) Vorstufen $[W_2Br_4(CO)_7]$ (**P1**) und $[WBr_2(CO)_3(NCMe)_2]$ (**P2**) wurden die Wolfram-triscarbonyl Komplexe $[W(CO)_3(Me-SPym)_2]$ (**C2**) und $[W(CO)_3(4-Me-SPy)_2]$ (**C1**) synthetisiert. Die Triscarbonyl-Komplexe wurden mit Acetylen umgesetzt, um, im Falle von **C2**, den Komplex $[W(CO)(H\equiv H)(Me-SPym)_2]$ (**C4**) zu erhalten. Im Falle des Komplexes **C1** erfolgt zusätzlich eine Acetylen Insertion in die W-N Bindung zu $[W(CO)(H\equiv H)(=4-Me-SPy)(4-Me-SPy)]$ (**C3**). Verbindung **C3** eliminiert Acetylen mit der Zeit in Lösung und bildet $[W(CO)(H\equiv H)(4-Me-SPy)_2]$ (**C5**). Der Komplex **C5** wurde zusätzlich ausgehend von einer Mischung aus den Vorstufen $[WBr_2(CO)(H\equiv H)(NCMe)_2]$ und $[WBr_2(CO)(H\equiv H)_2(NCMe)]$ (**P3**) über die Methode der „Ligand-Addition“ hergestellt. Die Wolfram(IV) Komplexe $[WO(H\equiv H)(Me-SPym)_2]$ (**C6**) und $[WO(H\equiv H)(4-Me-SPy)_2]$ (**C7**) wurden über kontrollierte Oxidation mit dem Sauerstofftransferreagenz Pyridin-*N*-oxid erhalten.

Die Untersuchung von **C3** gegenüber der Oxidation und von **C6** und **C7** gegenüber Methylolithium, Piperidin, Natriummethanolat, Wasser, Methyljodid und Pyridine-*N*-oxid lieferte nicht die gewünschte Reaktivität.

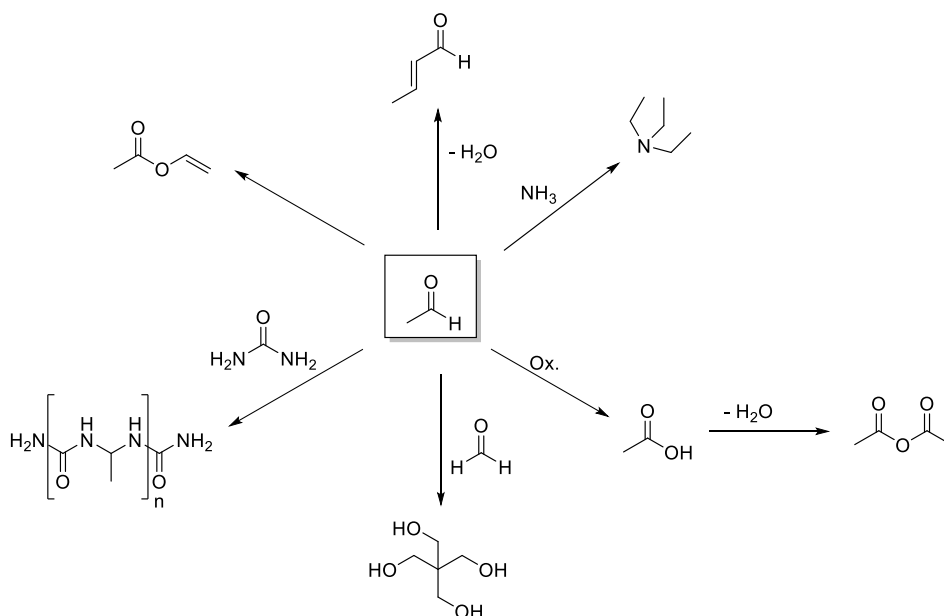
Alle Verbindungen wurden umfänglich mittels 1H - und ^{13}C -NMR-Spektroskopie, IR-Spektroskopie und Einkristall-Röntgenstrukturanalyse charakterisiert. Die Koordination von Acetylen zum Wolfram-Zentrum in **C3-C7** führt, im Vergleich zum freien Acetylen, zu einer signifikant verlängerten $C\equiv C$ Bindung sowie zu tieferem Feld verschobenen 1H - und ^{13}C -NMR Acetylen-Signalen. Diese Ergebnisse sprechen für eine gesteigerte Elektrophilie an den Acetylen-Kohlenstoffatomen.

1. INTRODUCTION

1.1 SYNTHESIS OF ACETALDEHYDE IN NATURE AND INDUSTRY

Acetaldehyde is one of the industrially most important aldehydes with a worldwide consumption of $766 \cdot 10^3$ t/year.^[1] It is a low-boiling liquid (bp = 20.16 °C) and readily undergoes all organic reactions known for aldehydes, like acetalization with alcohols, schiff-base formation with amines, oxidation to carbonic acids and aldol reactions.^[1]

As shown in Scheme 1 acetaldehyde is mainly used as precursor for the production of basic chemicals. For example it reacts with urea via a condensation reaction to give a widely used resin.^[2] With amines acetaldehyde reacts to alkylamines. Additionally croton aldehyde, a prochiral Michael acceptor, and vinyl acetate, a polymer building block, are accessible from acetaldehyde.^[3] Derivatives of pentaerythritol, also obtained starting from acetaldehyde, have found huge chemical application in transformer oil, paints and also cosmetics.^[4] Acetaldehyde can also be oxidized using oxygen to give, depending on the catalyst, acetic acid or acetic acid anhydride directly.^[1,5]

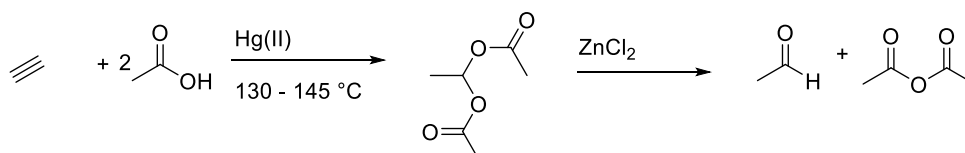


Scheme 1. Utilization of acetaldehyde in the synthesis of basic chemicals.^[1,2]

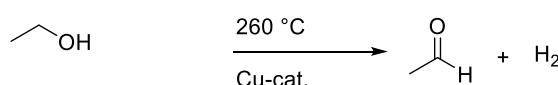
1.1.1 INDUSTRIAL SYNTHESIS OF ACETALDEHYDE: THE WACKER PROCESS

In the early 20th century the commercial production of acetaldehyde started.^[1] An overview of possible routes for the industrial synthesis of acetaldehyde is given in Scheme 2. Traditionally acetaldehyde is obtained from ethanol via dehydrogenation and oxidation using high-temperature processes.^[1] Additionally it was also synthesized via hydration of acetylene using toxic Hg(II) salts as catalysts and either HNO₃ (Chisso process) or Fe₂(SO₄)₃ (wet oxidation process from Hoechst) for the regeneration of Hg(II).^[1] This reaction initially gives the enol, which then tautomerizes to acetaldehyde. Rarely acetaldehyde was also synthesized in two step processes via a vinyl ether (BASF) or via ethylidene diacetate (société chimique des usines du rhône).^[1]

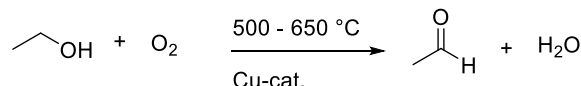
■ **Production via ethylidene diacetate (société chimique des usines du rhône): developed 1914**



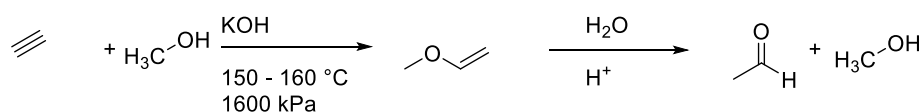
■ **Dehydrogenation of ethanol: 1918 - 1939**



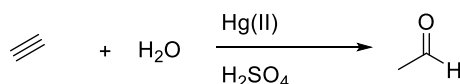
■ **Oxidation of ethanol (Verba Chemie process): until 1940s**



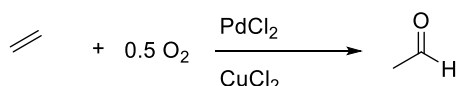
■ **Production via vinyl ether (Repe process, BASF): 1939 - 1945**



■ **Hydration of acetylene (wet oxidation process (Hoechst), Chisso process): 1912 - 1962**



■ **Wacker process: since 1959**

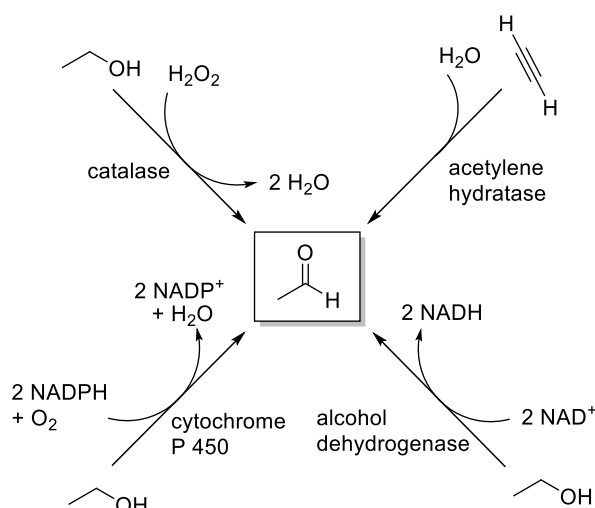


Scheme 2. Overview of processes for the industrial synthesis of acetaldehyde.^[1]

Since the discovery of the Wacker process, using a homogeneous PdCl₂ / CuCl₂ catalyst system for the net-oxidation of ethylene to acetaldehyde, in 1959 by the “Consortium der chemischen Industrie GmbH”, all other routes for the production of acetaldehyde were diminished.^[1,6]

1.1.2 ENZYMATIC SYNTHESIS OF ACETALDEHYDE

In nature, acetaldehyde is mainly synthesized by four enzymes (Scheme 3).^[7] Three of those enzymes generate it by oxidation of ethanol: The enzyme alcohol dehydrogenase, found in the liver, generates acetaldehyde by metabolising ethanol.^[7,8] To a minor extent acetaldehyde is also generated by cytochrome P450 and catalase.^[7,8]



Scheme 3. Synthesis of acetaldehyde in nature.^[7-9]

Compared to the other enzymes in Scheme 3 *Acetylene Hydratase* is very unique, as it synthesizes acetaldehyde not through the oxidation of ethanol and, apart from nitrogenase, is the only enzyme that accepts acetylene as substrate.^[9,10] *Acetylene Hydratase* was isolated from the strictly anaerobic fermenting bacterium *Pelobacter acetylenicus* by the group of B. Schink.^[9] It performs a net-hydration reaction of acetylene to acetaldehyde (Scheme 3). This reaction was found to be highly exergonic ($\Delta G^0 = -111.9$ kJ/mol).^[11] Nevertheless a catalyst, such as the enzyme *Acetylene Hydratase*, is required for this reaction because of kinetic inhibition.

Acetylene Hydratase belongs to the quite limited family of tungsten-dependent enzymes, which covers roughly about 18 enzymes.^[12]

1.2 TUNGSTEN IN ENZYMES

Tungsten is a group 6 element, relatively abundant on earth (average concentration of 10^{-4} ppm) and predominantly found as oxides of the type $M(+II)WO_4$ (e.g. scheelite $CaWO_4$, wolframite $(Mn, Fe)WO_4$, stolzite $PbWO_4$).^[12,13] It is also the only element of the third transition row which is found in enzymes, typically in the oxidation states of +IV to +VI.^[12,14] Tungsten and to a larger extent its lighter homologue molybdenum are often involved in catalysis.^[15] In nature both elements are typically regarded as chemically similar elements, albeit tungsten is predominantly used by extremophilic bacteria.^[12,16,17]

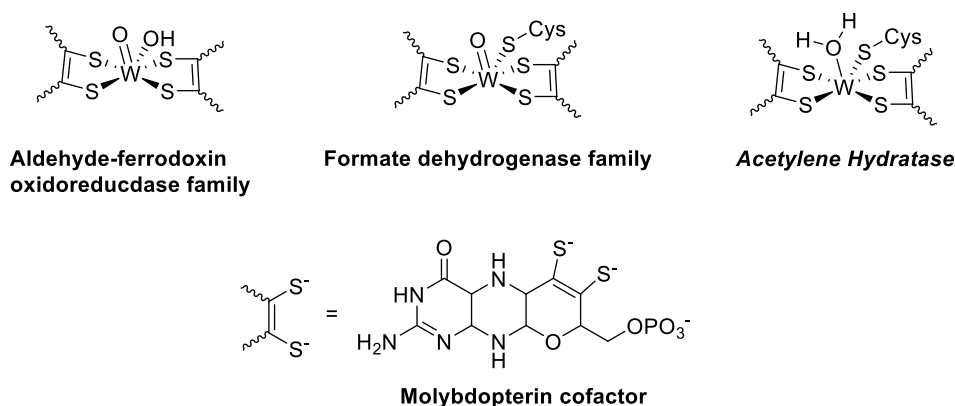


Figure 1. The three classes of tungstoenzymes (top), all of them utilizing the molybdopterin cofactor (bottom).^[18]

Tungstoenzymes are most commonly divided into three classes, all of them utilizing the molybdopterin cofactor (Figure 1, bottom).^[12,16,18] Members of the first class, aldehyde-ferrodoxin oxidoreductase family, catalyze the oxidation of aldehydes to their corresponding carbonic acids.^[16] The second class is the formate dehydrogenase family and comprises enzymes that catalyze the reduction of CO_2 or the reverse reaction, the oxidation of formate to CO_2 .^[12,18] The third group only comprises *Acetylene Hydratase*, which was first isolated from the strictly anaerobic fermenting bacterium *Pelobacter acetylenicus*.^[9] *Pelobacter acetylenicus* is found in marine freshwater sediments and lives on acetylene as its sole source of energy.^[19]

As mentioned in Scheme 3 *Pelobacter acetylenicus* uses *Acetylene Hydratase* for the initial step of the fermentation of acetylene to acetaldehyde.^[9] In contrast to the active sites of the aldehyde-ferredoxin oxidoreductase family as well as of the formate dehydrogenase family, *Acetylene Hydratase* contains a tungsten(IV) center, instead of tungsten(VI).^[18]

1.3 ACETYLENE HYDRATASE

1.3.1 MOLECULAR STRUCTURE OF ACETYLENE HYDRATASE

The crystal structure of *Acetylene Hydratase* was solved at 1.26 Å resolution in 2007 by the group of O. Einsle.^[20,21] As depicted in Figure 2 *Acetylene Hydratase* has a monomeric structure.^[21] Similar to all tungstoenzymes, the active site of *Acetylene Hydratase* contains two molybdopterin cofactors (Figure 2).^[21]

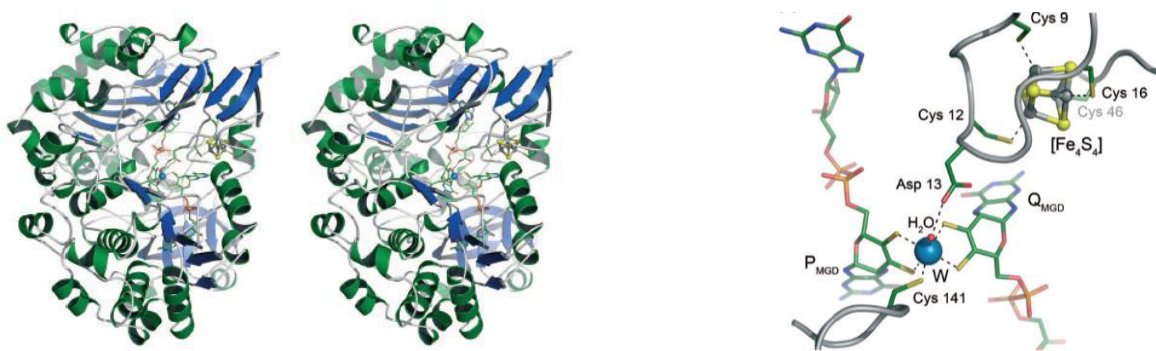
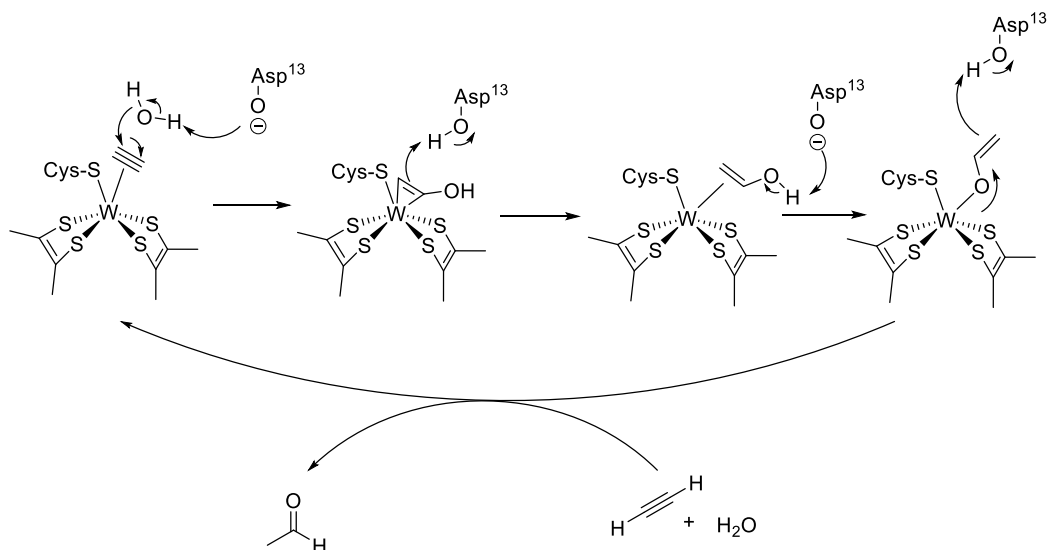


Figure 2. Overall structure of *Acetylene Hydratase* (right) and its active site (left). Picture taken from Ref.^[21]

Furthermore, a cysteine residue from the protein backbone and a water molecule are coordinated towards the tungsten center.^[21] Interestingly under ambient atmosphere *Acetylene Hydratase* is only active in the presence of strong reducing agents like titanium(III) citrate and dithionite.^[9] Although it was reported to be air stable, no enzyme activity was detected in assays under atmospheric oxygen or without the reducing agents.^[9]

1.3.2 MECHANISTIC CONSIDERATIONS

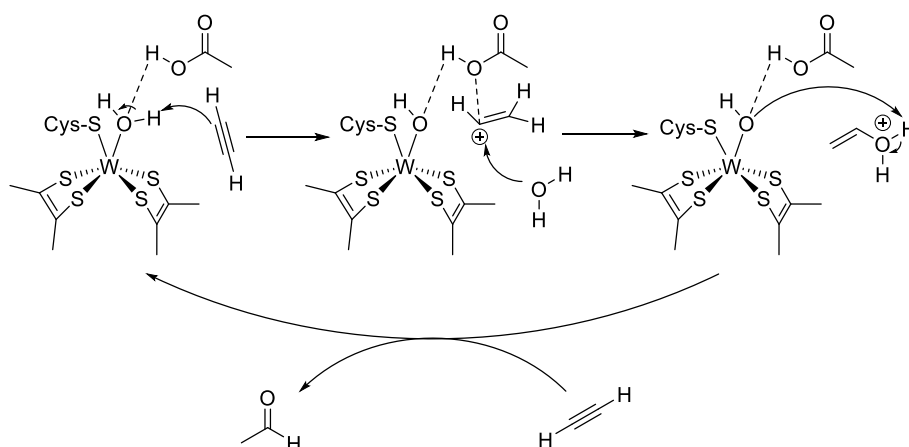
The mechanism of *Acetylene Hydratase* is still under discussion.^[19] Four different reaction mechanisms have been proposed in literature, they are differentiated between first shell and second shell mechanisms. In the first shell mechanism acetylene and all reaction intermediates are coordinated towards the tungsten center, whereas in the second shell mechanism they are not.^[19]



Scheme 4. First shell mechanism proposed by Himo and coworkers.^[22]

Three first shell mechanisms have been suggested by the groups of Himo, Hillier and Bayse, including a multistep mechanism via a vinylidene and a carbene.^[22–24] In all these mechanisms acetylene is activated towards a nucleophilic attack of a water molecule by coordination to the tungsten center (Scheme 4).^[19] An enol is subsequently formed, which finally tautomerizes to give acetaldehyde.

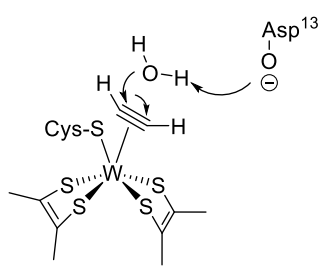
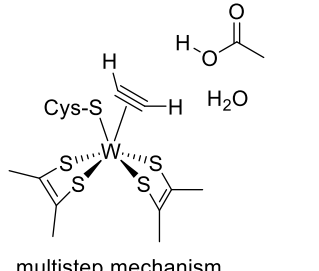
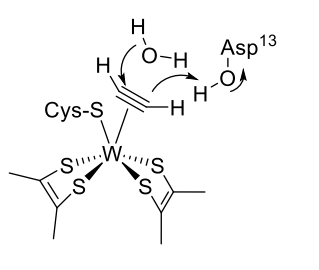
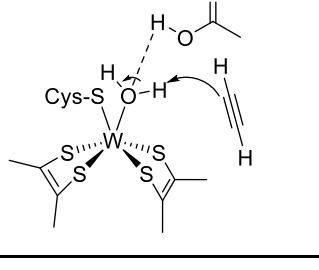
The only second shell mechanism for *Acetylene Hydratase* was proposed in 2007 by the Einsle group together with the enzyme's crystal structure (Scheme 5).^[21] The authors suggest that the water molecule, which is coordinated to the tungsten center, forms a hydrogen bond to the nearby Asp¹³ residue. Hence the water becomes very acidic and the acetylene is protonated. The formed vinyl cation reacts with an additional water molecule to form an enol like in the first shell mechanism, which then tautomerizes to acetaldehyde.



Scheme 5. Second shell mechanism proposed by O. Einsle and co-workers.^[21]

Table 1 gives a summary of all proposed mechanisms for *Acetylene Hydratase*. All four mechanisms were investigated using DFT calculations.^[22,24] The first shell mechanism of the Bayse group and the second shell mechanism of the Einsle group seem to be implausible, as the calculated activation energies were evaluated as too high.^[23,24] Considering the calculated activation energies, the first shell mechanism suggested by Himo and coworkers seems to be most likely.^[22,25–28] This is also supported by the fact that the initial step of first shell mechanisms, the acetylene coordination, was calculated to be exergonic (-5.4 kcal/mol).^[22]

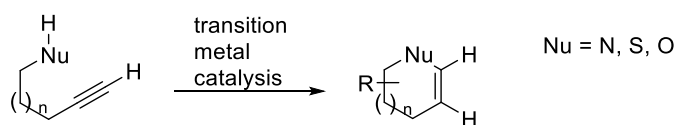
Table 1. Summary of proposed mechanisms and calculated energy barriers.

Key step	Activation energy	Reference
	16.9 kcal/mol ^[22]	Himo group. ^[22,25] Thiel group. ^[26–28]
 multistep mechanism	34.0 kcal/mol ^[24]	Hillier group. ^[24]
	41.0 kcal/mol ^[24]	Bayse group. ^[23]
	43.9 kcal/mol ^[24]	Einsle group. ^[21]

1.4 ALKYNE ACTIVATION ON METAL CENTERS

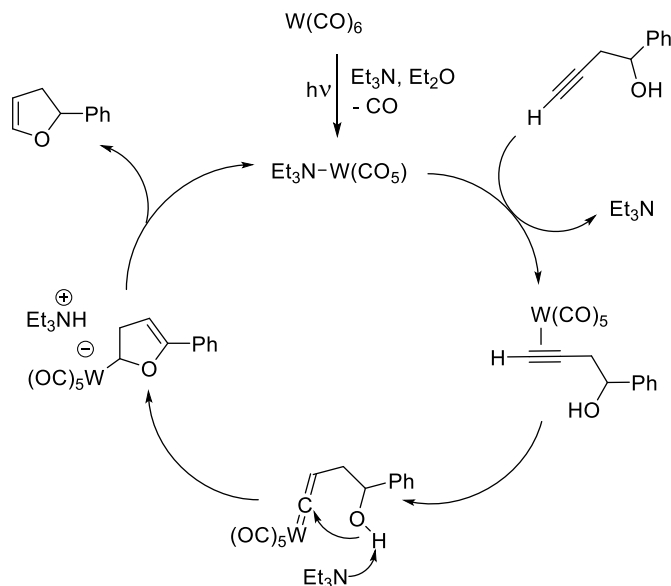
Alkyne activation on metal centers and subsequent attack of a nucleophile, as the proposed key step in enzymatic acetylene hydration,^[22–24] have been numerous reported in literature, including also their application in natural product synthesis.^[29] Especially for the synthesis of heterocycles alkyne activation is an alternative strategy to traditional ring closing reactions.^[29,30,31] Intramolecular ring closures, similar to the one depicted in Scheme 6, have been reported using complexes of Ti^[32], Zn^[32], Y^[32], Ln^[32], Ru^[32,33,34], Rh^[32,35], Pd^[32,36,37], Cu^[32], Au^[32,38–41], Mo^[32,34,42,43], Cr^[32], W^{[32,34,42–}

44], Pt^[32,34,37,45,46], Ir^[35,47,48], Re^[34]. There also exist a handful examples of an intermolecular attack of an activated alkyne using Pt,^[45,49] Ir,^[48] Au^[50] and Rh-catalysts.^[51] To the best of our knowledge a nucleophilic attack of an unsubstituted acetylene, as in the mechanistic proposal of acetylene hydration of the Einsle group,^[21] has never been reported.



Scheme 6. Application of π -acid catalysis in heterocyclic chemistry.^[30]

The reported examples of alkyne activation using group 6 metals are of high relevance,^[32,34,43,44,52] as *Acetylene Hydratase* also has a group 6 metal in its active site.^[21] However, this chemistry is limited to catalysts of the type [LM(CO)₅] (M = Mo, W; L = Et₃N, THF, DABCO), which are in situ generated from M(CO)₆ (M = Mo, W) and the respective ligand under UV-irradiation.^[32,44] Moreover only examples of an intramolecular nucleophilic attack are reported.^[32,34,42–44]



Scheme 7. Proposed mechanism for Mo- and W-dependent intramolecular alkyne activation.^[53,54]

The mechanism of this ring closure using Mo- and W-carbonyl complexes as π -acid catalysts has already been studied.^[53,54] A proposed catalytic cycle is depicted in

Scheme 7. It involves activation of the alkyne by coordination to the metal center, followed by formation of a vinylidene, intramolecular nucleophilic attack on the vinylidene and decooordination of the product as key steps.^[53]

1.5 THE BONDING SITUATION IN METAL-ALKYNE AND METAL-CARBONYL COMPLEXES

1.5.1 METAL-ALKYNE COMPLEXES

The Chatt-Dewar-Duncanson model, originally introduced to describe the bonding situation in Pt-alkene complexes and extensively used for the description of olefin complexes,^[55,56] can also be applied for the description of the metal-alkyne bond.^[57,58] In Figure 3 the well-known molecular orbital diagram of acetylene as well as the interactions of the relevant orbitals with a metal center are depicted. It shows that acetylene has two filled π -orbitals, oriented perpendicular to each other.^[59]

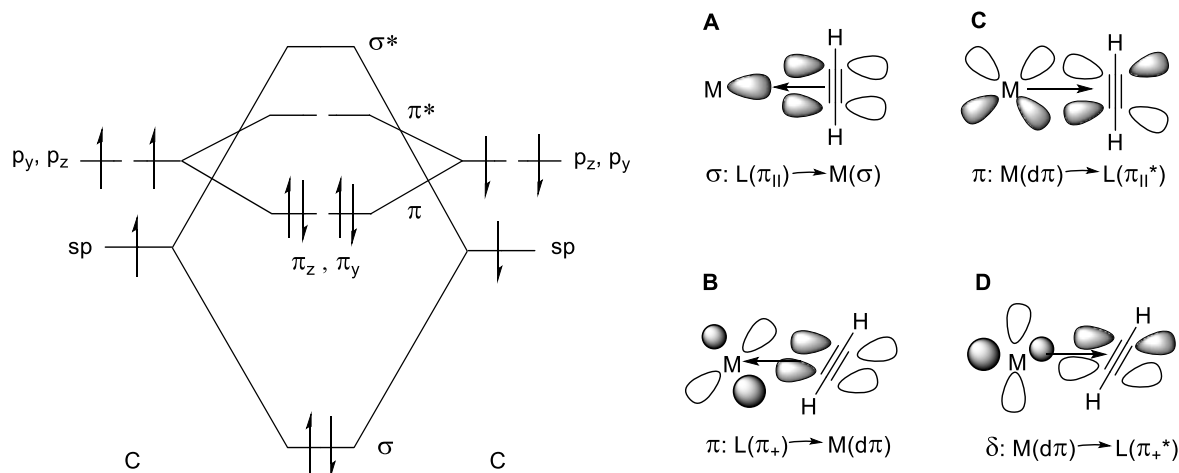
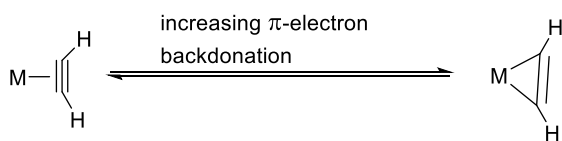


Figure 3. Molecular orbital diagram of acetylene and possible bonding interactions with a metal center.^[60]

The electrons in one of these π -orbitals perform a σ -electron transfer to the metal center (Figure 3, A). The other π -orbital overlaps with a metal orbital to perform a π -electron donation (Figure 3, B). The lowest unoccupied molecular orbitals of acetylene are its two π^* -orbitals, also standing perpendicular to each other.^[59] These orbitals are prone to π -backdonation (Figure 3, C) and to a δ -overlap (Figure 3, D).^[61]

Acetylene as ligand can either be considered as a neutral 2-electron donor (pure σ -electron transfer, Figure 3, A) or as a neutral 4-electron donor (π -overlap and σ -electron transfer, Figure 3, A and B).^[59,61,62]



Scheme 8. Schematic representation of the Chatt-Dewar-Duncanson model on metal-alkyne complexes. Increasing π -electron backdonation leads to the formation of a metallacyclopropane.

As illustrated in Scheme 8, the metallacyclopropane is formed with increasing π -electron backdonation. This leads to a distortion of the originally 180° angle of the $C\equiv C-H$ bond in uncoordinated acetylene because of the reduced triple bond character. Additionally the $C\equiv C$ bond is weakened upon coordination, because electron density is on the one hand donated from the binding π -orbital to the metal center and on the other hand electron density is pushed into the antibonding π^* -orbital (Figure 3).

1.5.2 METAL-ALKYNE-CARBONYL COMPLEXES

The principle of σ -donation and π -backbonding of the Dewar-Chatt-Duncanson model can also be applied to carbonyl complexes.^[55,63,64] Figure 4 shows a schematic drawing of the molecular orbital diagram of CO (left) as well as the possible interactions of the CO ligand with a transition metal center (right).

The CO ligand can also form σ - and π -interactions with the metal center, similar to the alkyne ligand (see section 1.5.1). The occupied σ^*_s -orbital overlaps with a metal orbital to perform a σ -electron transfer (Figure 4, A).^[60] Additionally, the electrons in the π_p -orbitals can also form weak π -interactions with the metal center (Figure 4, B).^[60,63] Finally, a π -electron backdonation can occur into the π^*_p -orbital of CO (Figure 4, C). Hence, σ -electron transfer strengthens the CO bond, while π -electron backdonation weakens the CO bond, as it fills an antibonding orbital. Additionally, the

formed π -bond using electrons of the π_p -orbital weakens the CO bond, as the electrons come from a bonding orbital.

As all these interactions affect the CO stretching frequency in the IR spectrum, a summary of their impact is given in Table 2.

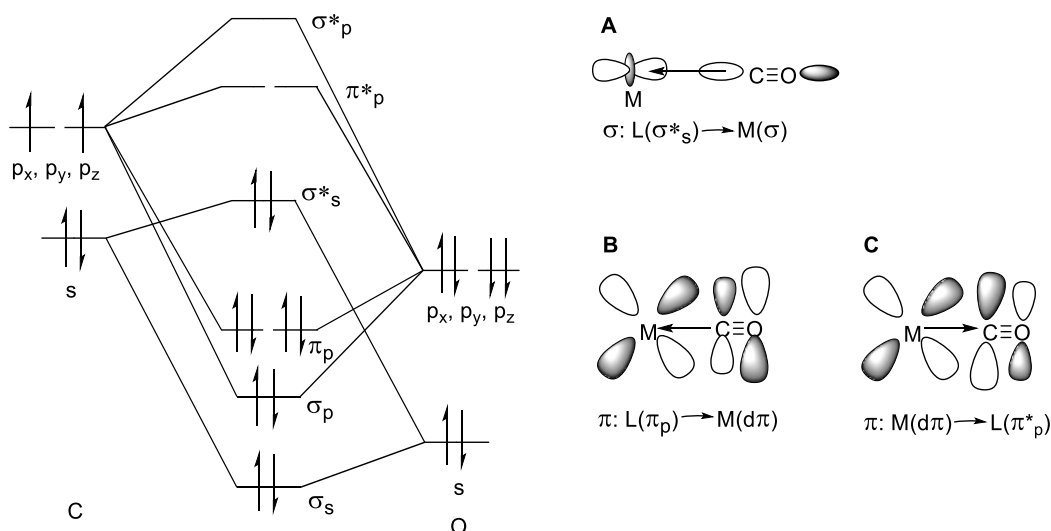


Figure 4. Molecular orbital diagram of CO (left) and possible bonding interactions with a transition metal center (right).^[60,63,64,65]

Table 2. Summary of bonding interactions between metal and CO ligand and their influence on M-C and C-O bond.

Interaction	M-C bond length	C-O bond length	IR ν_{C-O}
$\sigma: L(\sigma^*_s) \rightarrow M(\sigma)$	decreases	decreases	increases
$\pi: L(\pi_p) \rightarrow M(d\pi)$	decreases	increases	decreases
$\pi: M(d\pi) \rightarrow L(\pi^*_p)$	decreases	increases	decreases

The bonding situation in metal-alkyne-carbonyl complexes has been previously described.^[58] $[W(CO)(H-\equiv H)(S_2CNEt_2)_2]$ and $[W(CO)(H-\equiv H)(SPhoz)_2]$ have both CO and alkyne ligand in an approximately parallel arrangement.^[66,67] Templeton and coworkers attribute this to the fact that a 3-center-2-electron bond with $d\pi$ of the metal as the donor orbital and π^*_p of CO and π^*_{II} of acetylene as acceptor orbitals is formed (Figure 5).^[58] Therefore, this leads to a net-energy gain compared to a 90° arrangement. Thus, the below shown parallel arrangement of CO and alkyne is usually adopted.

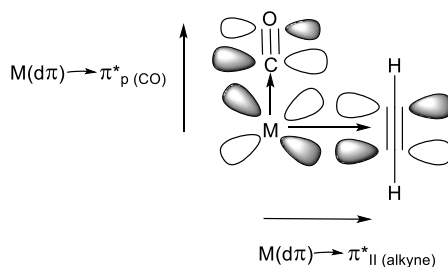


Figure 5. Schematic drawing of the possible 3-center-2-electron bond between metal, alkyne- and CO-ligand in a parallel arrangement of CO and alkyne.^[58]

1.5.3 METAL-OXO-ALKYNE COMPLEXES

Similarly to metal-alkyne-carbonyl complexes, the bonding in metal-oxo-alkyne complexes has been studied too.^[57] The possible interactions of metal orbitals with ligand orbitals are shown in Figure 6. Two 2-center-2-electron bonds of the transition metal d-orbital with the oxo ligand and the alkyne ligand respectively can be formed (Figure 6, A and B).^[57] In addition to that a 3-center-4-electron bond between a π -orbital of the W-O bond, the bonding orbital of the alkyne and the metal orbital is possible (Figure 6, C).^[57] In contrast to transition metal carbonyl alkyne complexes (section 1.5.2),^[58] this leads to a stabilization of the alkyne ligand in an approximately 90° angle to the W-O bond.

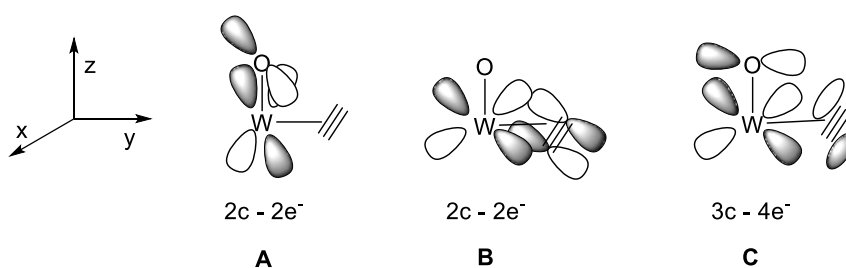


Figure 6. Bonding interactions in metal-oxo-alkyne complexes.^[57]

1.6 BIOMIMETIC MODELS FOR *ACETYLENE HYDRATASE*

Bioinorganic chemistry seeks for a deeper understanding of mechanisms and properties of transition metal-containing enzymes. Therefore so-called biomimetic complexes, which are transition metal complexes with a ligand system as similar as possible to the coordination environment in the active site of the enzymes, are synthesized. These biomimetic complexes are simplified models of enzymes, which allow mechanistic studies, studies on oxidation states and studies concerning the ligand system.

In enzyme modeling chemistry one has to differentiate between structural and functional models. A structural model usually does not show enzyme activity, but mimics the coordination sphere of the active site. Therefore structural models are used to study the chemical behavior of the enzyme's active site. In contrast to that a functional model can use a totally different coordination sphere of the active site as long as it performs the catalytic reaction of the enzyme. Functional models are important to get knowledge about the mechanism and the role of the metal. The combination of the two modeling approaches is a structural-functional model. Such a combined model shows catalytic activity as well as characteristic structural features of the enzyme. A complex which fulfills both can therefore be regarded as a simplified template of the enzyme.

In the following sections literature-known examples of tungsten-acetylene complexes, which are highly relevant for biomimetic modelling of *Acetylene Hydratase*, will be presented.

1.6.1 TUNGSTEN(II)-ALKYNE COMPLEXES

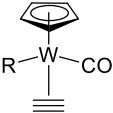
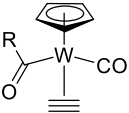
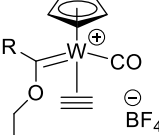
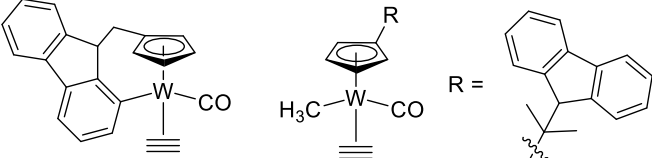
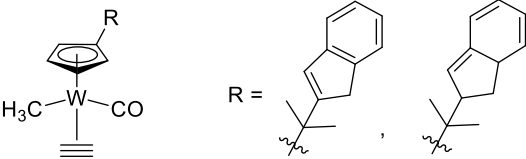
Tungsten(II)-acetylene chemistry started in the late 70's, where Alt and co-workers reported the chemistry of tungsten(II)-carbonyl-acetylene complexes stabilized by a cyclopentadienyl ligand.^[68–73] The author synthesized $[\text{W}(\text{CO})_2(\text{Cp})(\text{H}\equiv\text{H})(\text{CH}_3)]$, the first tungsten(II)-acetylene complex, by a photochemical reaction of the seven-coordinate $[\text{W}(\text{CO})_3(\text{H}\equiv\text{H})(\text{CH}_3)]$ with acetylene. The chemistry of $[\text{W}(\text{CO})_2(\text{Cp})(\text{H}\equiv\text{H})(\text{CH}_3)]$ and its derivatives was intensively investigated until the 90s.^[68–74] Later on, also tungsten-acetylene complexes using sulfur-rich dithiocarbamate-ligands

were reported in 1978, where the group of McDonald succeeded in isolating $[\text{W}(\text{CO})(\text{H}-\equiv\text{H})(\text{S}_2\text{CNEt}_2)_2]$ starting from the phosphine-precursor $[\text{W}(\text{CO})_2(\text{PPh}_3)(\text{S}_2\text{CNEt}_2)]$.^[66] Additionally the authors also reported the first crystal structure of a tungsten(II) acetylene complex, revealing a parallel arrangement of CO and acetylene (section 1.5.2).^[66]

In 1997 the group of Templeton entered into tungsten-acetylene chemistry with the first report of a tungsten-acetylene complex stabilized by the scorpionate ligand hydrido-tris(pyrazolyl)borate (Tp').^[75] Subsequently the reactivity of $[\text{Tp}'\text{W}(\text{CO})(\text{H}-\equiv\text{H})\text{I}]$ and its derivatives has been intensively studied by the Templeton group.^[75–80] Lately Peschel et al. succeeded in synthesizing a novel tungsten-acetylene system using 2-(4',4'-dimethyloxazoline-2'-yl)thiophenolate (SPhoz) as ligand.^[67] $[\text{W}(\text{CO})(\text{H}-\equiv\text{H})(\text{SPhoz})_2]$ was synthesized from $[\text{W}(\text{CO})_2(\text{SPhoz})_2]$, which reacts readily under acetylene atmosphere.^[67] Although the SPhoz ligand system is different in terms of reactivity compared to dithiocarbamates, a parallel arrangement of CO and acetylene similar to $[\text{W}(\text{CO})(\text{H}-\equiv\text{H})(\text{S}_2\text{CNEt}_2)_2]$ was observed.^[67]

A complete summary of literature-known tungsten(II)-acetylene complexes, sorted by the year of publication, is given in Table 3.

Table 3. Summary of literature-known monomeric tungsten(II)-acetylene complexes.

Compound	Year	Crystal structure	Reference
 $R = \text{Me, Et, n-Pr, n-Bu}$	1977		[68,70,71]
 $R = \text{Me, Et, n-Pr, n-Bu}$			
$[\text{W}(\text{CO})(\text{H}-\equiv\text{H})(\text{S}_2\text{CNEt}_2)_2]$	1978	X	[66,81]
$[\text{W}(\text{CO})_2(\text{H}-\equiv\text{H})\text{I}_2\text{L}]$ (L = PMe_3 , AsMe_3)	1982		[82]
 $R = \text{Me, Et, n-Pr, n-Bu}$	1983		[70,72]
$[\text{W}(\text{MA})(\text{H}-\equiv\text{H})(\text{S}_2\text{CNR}_2)_2]$ (R = Me, Et)	1985		[83]
 $R =$	1991		[69]
 $R =$	1993		[73]
$[\text{Tp}'\text{W}(\text{CO})_2(\text{H}-\equiv\text{H})][\text{OTf}]$, $[\text{Tp}'\text{W}(\text{CO})(\text{H}-\equiv\text{H})\text{I}]$	1997		[75]
$[\text{Tp}'\text{W}(\text{CO})(\text{H}-\equiv\text{H})(\text{R})]$ (R = CN, CNBF_3)	1998		[79]
$[\text{Tp}'\text{W}(\text{CO})(\text{H}-\equiv\text{H})(\text{R})][\text{O}_3\text{SCF}_3]$ (R = CN-Me, CN-H, CO)			
$[\text{W}(\text{CO})(\text{H}-\equiv\text{H})(\text{SPhoz})_2]$	2015	X	[67]
$[\text{Tp}'\text{W}(\text{CO})(\text{H}-\equiv\text{H})(\text{R})][\text{OTf}]$ (R = NC-Me, $\text{N}(\text{CH}_3)=\text{CHCH}_3$, $\text{N}(\text{CH}_2\text{CH}_3)=\text{CHCH}_3$)		X	
$[\text{Tp}'\text{W}(\text{CO})(\text{H}-\equiv\text{H})(\text{N}=\text{CHCH}_3)]$	2016		[76]
$[\text{Tp}'\text{W}(\text{CO})(\text{H}-\equiv\text{H})(\text{R})][\text{BF}_4]$ (R = NHCHCH_3 , $\text{N-CH}(\text{CH}_3)(\text{CPh}_3)$, $\text{N-CH}(\text{CH}_3)\text{C}(\text{C}_6\text{H}_4\text{OCH}_3)\text{-Ph}_2$)		X	

1.6.2 TUNGSTEN(IV) COMPLEXES AS MODELS FOR *ACETYLENE HYDRATASE*

As *Acetylene Hydratase* is a tungsten(IV) dependent enzyme with the sulfur-rich molybdopterin cofactor in its active site,^[21] tungsten(IV)-acetylene complexes ideally with a sulfur-rich coordination sphere qualify as structural models. Furthermore tungsten(IV) complexes that catalyze acetylene hydration can be regarded as functional models for the enzyme.

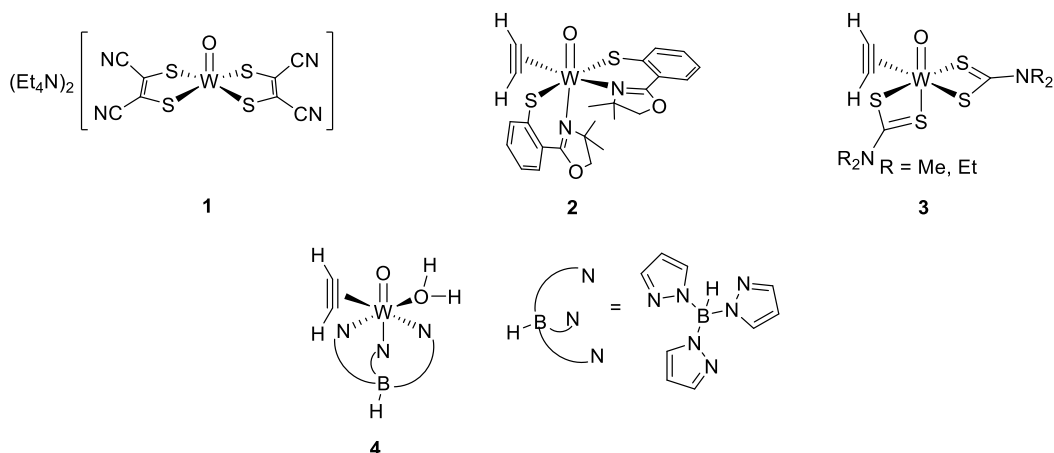


Figure 7. Complexes which qualify as biomimetic models for *Acetylene Hydratase*.^[57,67,78,84,85]

Figure 7 summarizes the known structural and functional models for *Acetylene Hydratase*.^[86] Only one functional model for *Acetylene Hydratase* is known in literature. Complex 1 was synthesized in 1996 and reported to be a functional model of *Acetylene Hydratase* in 1997,^[84,85] 10 years prior to the crystallization of *Acetylene Hydratase* in 2007.^[21] In 2017 the catalytic activity of 1 was reinvestigated by Hintermann and coworkers.^[87] However, the results of Sarkar could not be reproduced.^[87]

Additionally to the functional model of the Sarkar group three structural models (Figure 7: Compounds 2, 3 and 4) are reported in literature.^[57,67,78] Model 2, reported in 2015 by the group of Mösch-Zanetti, shows reversible acetylene decooordination upon light exposure to form the five-coordinate species $[WO(SPhoz)_2]$.^[67] This behavior has not yet been reported for *Acetylene Hydratase*, but gives important information about chemical behavior of tungsten(IV)-acetylene complexes with a

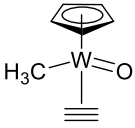
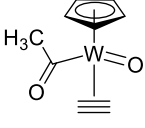
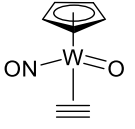
sulfur-rich coordination sphere and is highly relevant as product decoordination is also a key step in the catalytic cycle of acetylene hydration.^[9,19-21]

Model 3 has already been reported in 1981 by the group of Templeton. It uses a dithiocarbamate ligand to stabilize the acetylene adduct.^[57] Although 3 does not show catalytic activity it is the closest structural analog of the active site of *Acetylene Hydratase*, as it also has four sulfur atoms in the first coordination sphere of tungsten(IV).^[57]

Model 4, synthesized in 2000 also by Templeton and co-workers, does not have a sulfur rich ligand system similar to *Acetylene Hydratase*, but has a water molecule as well as acetylene coordinated to the tungsten center.^[78] Therefore this model is of high structural importance, as both reactants necessary for acetylene hydration are coordinated towards the tungsten center. Until now no crystal structures of 3 and 4 have been reported, which makes propositions concerning the degree of acetylene activation (C-C bond length and C-C-H bond angle) and comparisons to other model compounds impossible.

Furthermore few tungsten(IV)-acetylene complexes, which do not qualify as models for *Acetylene Hydratase*, are known. A complete list of all known tungsten(IV)-acetylene complexes is given in Table 4.

Table 4. Summary of literature-known monomeric tungsten(IV) acetylene complexes.

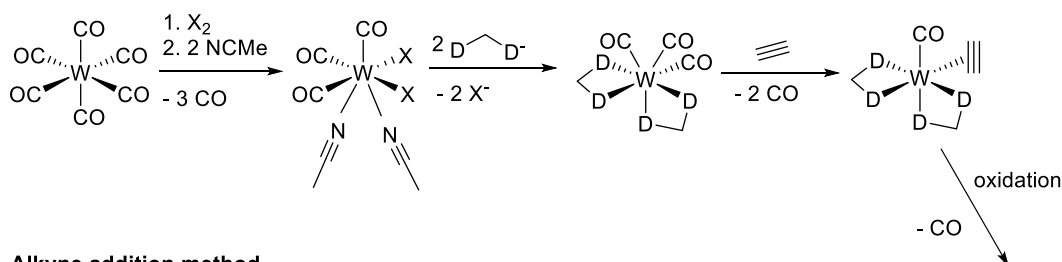
Compound	Year	Crystal structure	Reference
$[\text{WO}(\text{H}-\equiv\text{H})(\text{S}_2\text{CNR}_2)]$ (R = Me, Et)	1981		[57]
	1986		[74]
	1986		[74]
	1986		[74]
$[\text{WCl}_4(\text{H}-\equiv\text{H})(\text{Et}_2\text{O})]$	1989		[88]
$[\text{W}(\text{PMe}_2\text{Ph})_2(\text{H}-\equiv\text{H})(\text{NAr})_2]$ (Ar = diisopropylphenyle)	1993		[89]
$[\text{Tp}'\text{WOI}(\text{H}-\equiv\text{H})]$	1999		[77]
$[\text{Tp}'\text{WO}(\text{H}_2\text{O})(\text{H}-\equiv\text{H})][\text{OTf}]$			
$[\text{Tp}'\text{WO}(\text{H}-\equiv\text{H})][\text{OTf}]$	2000		[78]
$[\text{Tp}'\text{WO}(\text{OH})(\text{H}-\equiv\text{H})]$			
$[\text{WO}(\text{H}-\equiv\text{H})(\text{SPhoz})_2]$	2015	X	[67]

1.6.3 OXOTUNGSTEN(IV)-ALKYNE CHEMISTRY

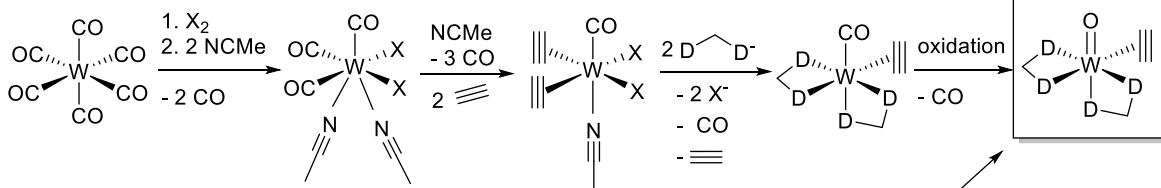
Possible synthetic routes for the synthesis of biomimetic oxotungsten(IV)-acetylene complexes are summarized in Scheme 9. A distinction has to be made between ligand addition method, alkyne addition method and the reduction method. The ligand addition method and the alkyne addition method are well established in literature and within the group, whereas no examples for the synthesis of oxotungsten(IV)-alkyne complexes via the reduction method are reported.

The synthesis of the tungsten(II) precursor $[\text{W}_2\text{Br}_4(\text{CO})_7]$, as well as the 7-coordinate acetonitrile adduct $[\text{WBr}_2(\text{CO})_3(\text{NCMe})_2]$ for the alkyne and ligand addition method are well known in literature.^[90–93] Additionally the alkyne addition method has already been successfully employed for the synthesis of $[\text{WO}(\text{H}-\equiv\text{H})(\text{SPhoz})_2]$,^[67,90] $[\text{WO}(\text{H}-\equiv\text{H})(\text{S}_2\text{CNR}_2)]$ (R = Me, Et)^[57,66,94] and $[\text{Tp}'\text{WO}(\text{OH})(\text{H}-\equiv\text{H})]$.^[75,77,78]

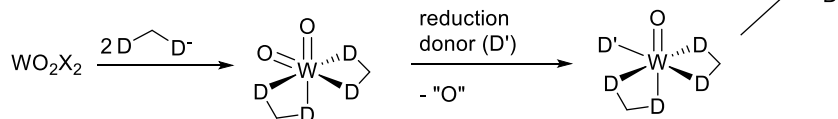
Ligand addition method



Alkyne addition method



Reduction method



Scheme 9. Possible synthetic routes towards tungsten-oxo-alkyne complexes.^[67,88–90,92,93,95]

The bis-alkyne precursors $[\text{WBr}_2(\text{CO})(\text{R}-\equiv\text{R})_2(\text{NCMe})]$ ($\text{R} = \text{Me}, \text{Ph}$) have been isolated by Baker et al. in 1994.^[95,96] Furthermore, preliminary results of the Möscher-Zanetti group show that the bis-acetylene precursor $[\text{WBr}_2(\text{CO})(\text{H}-\equiv\text{H})_2(\text{NCMe})]$ is also accessible in a mixture with $[\text{WBr}_2(\text{CO})(\text{H}-\equiv\text{H})(\text{NCMe})_2]$.^[92]

One example for the reduction route for the synthesis of tungsten(IV) complexes exists in literature, although no tungsten(IV)-oxo-acetylene complexes have been synthesized via this approach. $[\text{WCl}_4(\text{H}-\equiv\text{H})_2]$ was synthesized from WCl_6 via reduction in acetylene atmosphere to form $\text{C}_2\text{Cl}_2\text{H}_2$ as side product.^[88]

The oxidation of tungsten-carbonyl complexes to their corresponding oxo-complexes has already been conducted. The groups of Young and Möscher-Zanetti used pyridine-*N*-oxide for the synthesis of the complexes $[\text{Tp}'\text{W}(\text{CO})\text{O}\{\text{S}_2\text{P}(\text{OPr}^i)_2-\text{S}\}]$ and $[\text{WO}(\text{H}-\equiv\text{H})(\text{SPhoz})_2]$ respectively.^[67,97] Additionally Young reported the oxidation of $[\text{Tp}'\text{W}(\text{CO})_2\text{I}]$ to $[\text{Tp}'\text{W}(\text{CO})\text{OI}]$ using molecular oxygen.^[97] Finally the group of Templeton used the peracid mCPBA for oxidation of carbonyl complexes.^[80]

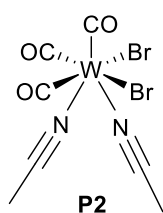
2. OBJECTIVES

The mechanism of the tungstoenzyme *Acetylene Hydratase* is still unresolved. Nevertheless three different first shell mechanisms and one second shell mechanism have been proposed.^[21–24] A strategy to gain further insight into the mechanism of *Acetylene Hydratase* is the synthesis of model compounds with a sulfur-rich coordination sphere similar to the molybdopterin cofactor in the active site of *Acetylene Hydratase*.^[21] Three oxo-tungsten(IV)-acetylene complexes which serve as a structural model for *Acetylene Hydratase* have been published.^[57,67,78] However, no acetylene hydration reactivity of these complexes is reported.^[57,67,78] $[\text{Et}_4\text{N}]_2[\text{W}^{\text{IV}}\text{O}(\text{mnt})_2]$ is the only tungsten(IV)-complex with a sulfur-rich coordination sphere which was found to perform catalytic acetylene hydration, although no tungsten-alkyne intermediate was observed.^[84,85] However, the results could not be reproduced.^[87] Without a reliable functional model the synthesis of structural-functional models for *Acetylene Hydratase* is crucial to gain further insights into the mechanism of its acetylene hydration. Bidentate S,N-ligands on an oxo-tungsten(IV)-acetylene center seem to be beneficial for acetylene activation, because reversible acetylene coordination with the S,N-ligand SPhoz has already been observed in the compound $[\text{WO}(\text{H}\equiv\text{H})(\text{SPhoz})_2]$ (section 1.5.3).^[67]

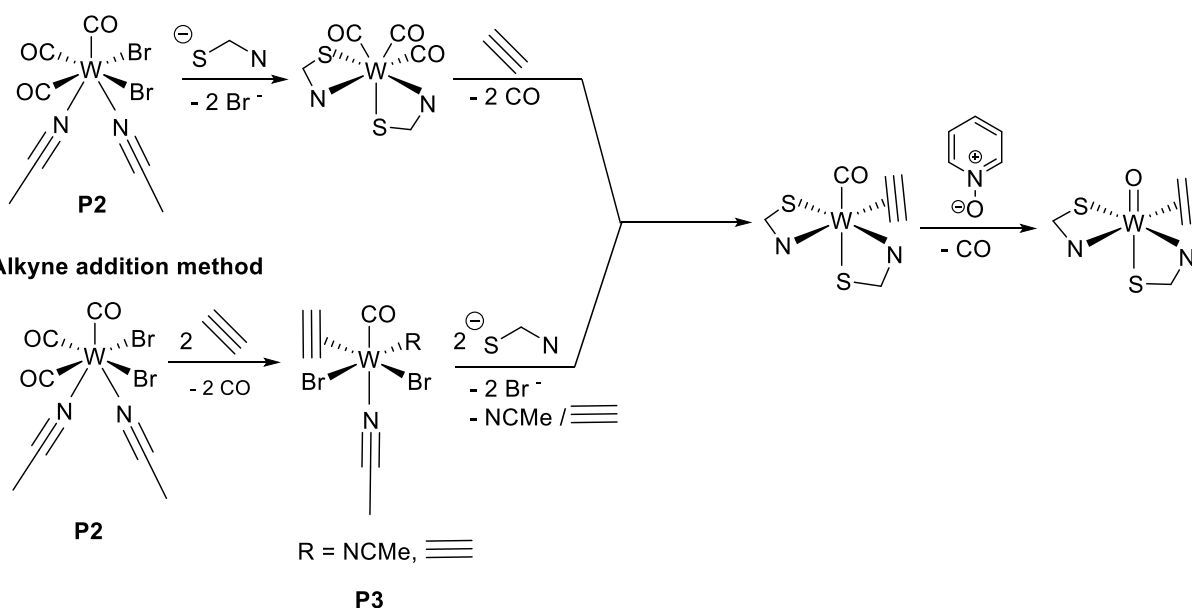
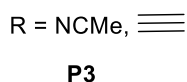
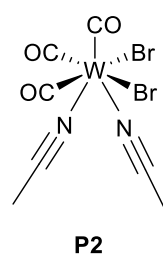
The aim of this master thesis is to synthesize new structural-functional models for *Acetylene Hydratase* based on the S, N-ligands 4-methylpyridine-2-thiolate (**L1**) and 4,6-dimethylpyrimidine-2-thiolate (**L2**). Both ligands were chosen as they are less prone to disulfide formation than SPhoz, because of the present tautomeric equilibrium between thiole and thione.^[98] Therefore they are expected to be more stable in an aqueous environment which is necessary for enzyme-like acetylene hydration. Furthermore, both ligands create a sulfur-rich coordination sphere comparable to the native enzyme. The route used for the synthesis of the desired tungsten-oxo-alkyne complexes is presented in Scheme 10. Starting from the precursors $[\text{W}_2\text{Br}_4(\text{CO})_7]$ (**P1**), $[\text{WBr}_2(\text{CO})_3(\text{NCMe})_2]$ (**P2**) and $[\text{WBr}_2(\text{CO})(\text{H}\equiv\text{H})_2(\text{NCMe})]$ (**P3**) tungsten-oxo-acetylene complexes of 4-methylpyridine-2-thiolate (**L1**) and 4,6-dimethylpyrimidine-2-thiolate (**L2**) should be synthesized via $[\text{W}(\text{CO})_3\text{L}_2]$ and $[\text{W}(\text{CO})_3(\text{H}\equiv\text{H})\text{L}_2]$.^[90,92,93] **P3** is only known within the Möscher-Zanetti group and was isolated in a mixture with $[\text{WBr}_2(\text{CO})(\text{H}\equiv\text{H})(\text{NCMe})_2]$.^[92] The reactivity of the

target complexes of the type $[\text{WO}(\text{H}\equiv\text{H})\text{L}_2]$ towards acetylene hydration as well as nucleophiles (methyl lithium, piperidine, sodium methanolate) will be investigated.

Ligand addition method

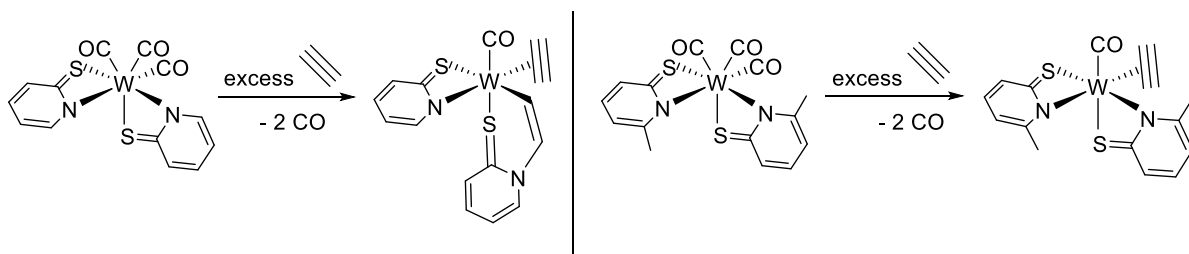


Alkyne addition method



Scheme 10. Synthesis of tungsten-oxo-alkyne complexes.

Moreover preliminary results show that if complex $[\text{W}(\text{CO})_3(\text{SPy})_2]$ is treated with excess acetylene, insertion of another acetylene moiety into the W-N bond to $[\text{W}(\text{CO})(\text{H}\equiv\text{H})(=\text{SPy})(\text{SPy})]$ is observed, whereas $[\text{W}(\text{CO})_3(6\text{-Me-SPy})_2]$ reacts to $[\text{W}(\text{CO})(\text{H}\equiv\text{H})(6\text{-Me-SPy})_2]$ under acetylene atmosphere (Scheme 11). Additionally L. M. Peschel et al. showed that $[\text{W}(\text{CO})(\text{H}\equiv\text{H})(\text{SPy})_2]$ is accessible via the ligand addition method starting from precursor **P3** (Scheme 10).^[92] Using $[\text{W}(\text{CO})(\text{H}\equiv\text{H})(4\text{-Me-SPy})_2]$ as model compound, the influence of the methyl group (electronic vs. steric) on the acetylene insertion into the W-N bond is to be studied.



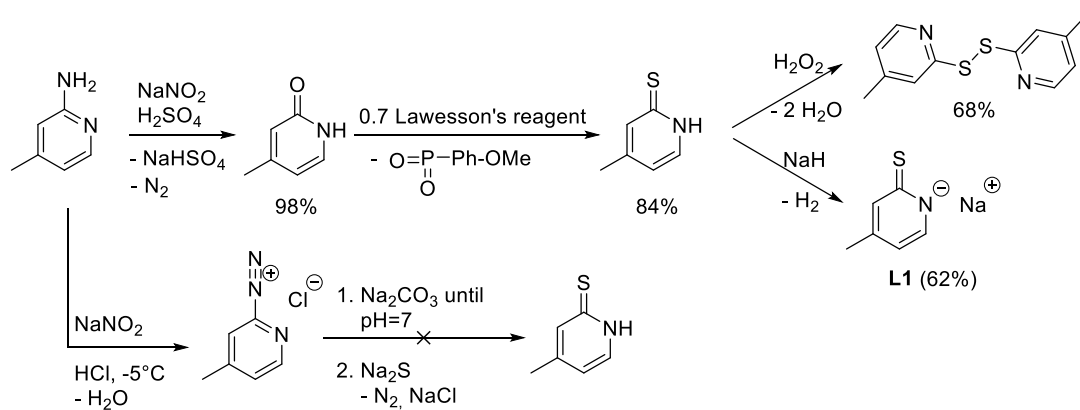
Scheme 11. Acetylene insertion into the W-N bond.

3. RESULTS AND DISCUSSION

3.1 LIGAND SYNTHESIS

3.1.1 SYNTHESIS OF SODIUM 4-METHYLPYRIDINE-2-THIOLATE

The synthetic route used for the preparation of sodium 4-methylpyridine-2-thiolate is presented in Scheme 12. Commercially available 2-amino-4-methylpyridine was converted, according to literature, into 4-methylpyridine-2-on via diazotisation at 0 – 5 °C and subsequent reaction of the formed diazonium salt with water.^[99] 4-Methylpyridine-2-on was obtained in high purity after 15 min. at 95 °C as a colorless powder in 98% yield.



Scheme 12. Synthesis of sodium 4-methylpyridine-2-thiolate (L1) and its corresponding disulfide.

Treatment of 4-methylpyridine-2-on with Lawesson's reagent to introduce the thioketone moiety is also well known in literature.^[100] According to the literature protocol a reaction time of 14 h at reflux (toluene) using 0.6 equiv. Lawesson's reagent should lead to full conversion.^[100] In our hands, however, 0.6 equiv. Lawesson's reagent and 15 h reflux (toluene) lead to approximately 90% conversion, according to GC-MS measurements. In order to get full conversion, additional 0.2 equiv. Lawesson's reagent were added and the suspension was refluxed again overnight. After extraction according to the literature procedure,^[100] 4-methylpyridine-2-thione was obtained as a yellow powder in a purity sufficient for further use in 84% yield. Deprotonation of 4-methylpyridine-2-thione with sodium hydride in

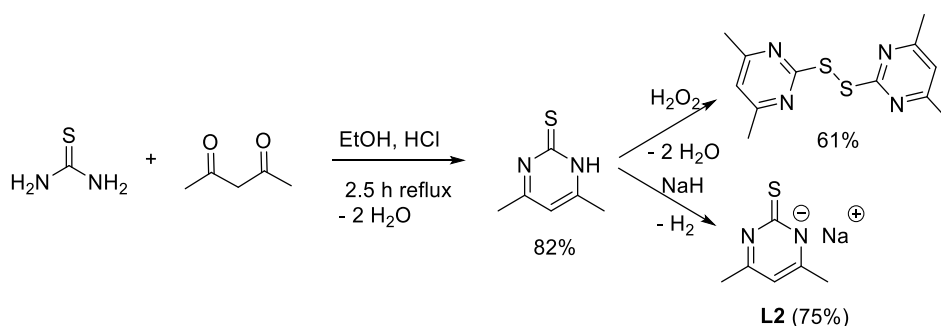
tetrahydrofuran gave the ligand salt sodium 4-methylpyridine-2-thiolate (**L1**). After precipitation with heptane and washing with tetrahydrofuran the ligand salt **L1** was obtained as a white powder in 62% yield. The incomplete conversion observed using the literature procedure for the synthesis of 4-methylpyridine-2-thione is also reflected by the published yields, which are approximately 30% lower than for the 3-methyl and 6-methyl derivatives.^[100]

Additionally the corresponding disulfide was synthesized as reference material (Scheme 12), as thioles are prone to disulfide formation under oxidizing conditions. 4-Methylpyridine-2-thione was treated with 5.9 equiv. hydrogen peroxide to obtain 1,2-bis(4-methylpyridine-2-yl)disulfide after extraction with dichloromethane as a colorless powder in 67% yield.

In principle, a second reaction pathway for the synthesis of 4-methylpyridine-2-thione should be feasible: The electrophilic diazonium salt could be directly converted into the thione using a sulfur-nucleophile like sodium sulfide (Scheme 12). Careful neutralization of the reaction solution before reacting with sodium sulfide is necessary to avoid the formation of H₂S. However, synthesis of 4-methylpyridine-2-thione was not successful via this reaction pathway.

3.1.2 SYNTHESIS OF SODIUM 4,6-DIMETHYLPYRIMIDINE-2-THIOLATE

The synthesis of sodium 4,6-dimethylpyrimidine-2-thiolate (**L2**) is summarized in Scheme 13. Thiourea and acetylacetone are reacted in an HCl-mediated condensation reaction to 4,6-dimethylpyrimidine-2-thione according to a modified literature procedure.^[101]



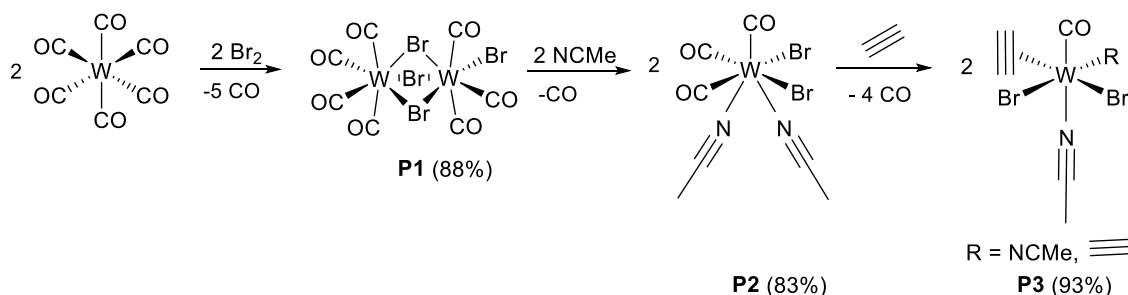
Scheme 13. Synthesis of sodium 4,6-dimethylpyrimidine-2-thiolate (**L2**) and its corresponding disulfide.

In contrast to the literature procedure, the corresponding pyrimidinium salt precipitates due to the strongly acidic reaction conditions as yellow needles after 2.5 hours of reflux in ethanol.^[101] Therefore, the pH of the suspension was adjusted to 7-8 before work-up. After extraction with dichloromethane 4,6-dimethylpyrimidine-2-thione was obtained as a yellow powder in 82% yield. It was further deprotonated using sodium hydride in tetrahydrofuran. The obtained sodium 4,6-dimethylpyrimidine-2-thiolate (**L2**) was precipitated with heptane and the isolated precipitate was washed with diethyl ether and tetrahydrofuran to obtain the ligand salt **L2** as an off-white powder in 75% yield.

Again, the corresponding disulfide was synthesized as reference material (Scheme 13). 4,6-Dimethylpyrimidine-2-thione was treated with 6.3 equiv. hydrogen peroxide to obtain 1,2-bis(4,6-dimethylpyrimidine-2-yl)disulfide after extraction with dichloromethane as a colorless powder in 61% yield.

3.2 TUNGSTEN(II) PRECURSOR SYNTHESIS

The syntheses of the tungsten(II) precursors **P1-P3** are summarized in Scheme 14. The precursor $[W_2Br_4(CO)_7]$ (**P1**) was synthesized according to a literature procedure. Literature-known precursor $[WBr_2(CO)_3(NCMe)_2]$ (**P2**) could be obtained by a different approach.^[91] Instead of synthesis via $[W(CO)_3(NCMe)_3]$,^[91,92] precursor **P1** was reacted to compound **P2** by stirring it in acetonitrile. **P2** was isolated as a dark red powder in 83% yield.



Scheme 14. Synthesis of tungsten(II) precursors **P1-P3**.

Similarly to the literature-known bis-alkyne precursors $[\text{WBr}_2(\text{CO})(\text{R}-\equiv\text{R})_2(\text{NCMe})]$ ($\text{R} = \text{CH}_3, \text{Ph}, \text{CH}_2\text{Cl}$) unpublished results of the Möscher-Zanetti group show that also the bis-acetylene precursor $[\text{WBr}_2(\text{CO})(\text{H}-\equiv\text{H})_2(\text{NCMe})]$ (**P3**) is accessible.^[92,95] For the synthesis of **P3**, **P2** was dissolved in dichloromethane. The solution was subsequently purged with acetylene for 30 min and stirred under an acetylene atmosphere for another hour. The product precipitated as a blue-grey powder and was isolated in 92% yield.

All precursors **P1-P3** are instable towards air and moisture. **P1** and **P2** are soluble in chlorinated solvents, **P2** is also soluble in acetonitrile. The bis-acetylene precursor **P3** has a very poor solubility in all solvents and is soluble in chlorinated solvents and acetonitrile in minor amounts.

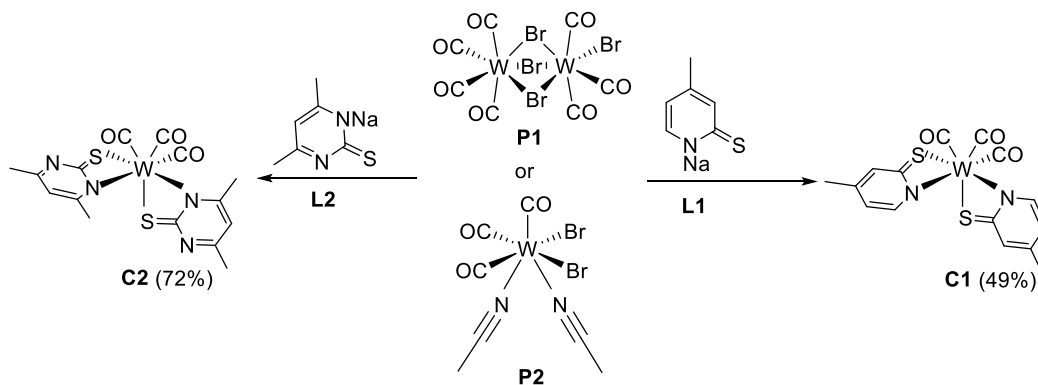
The obtained IR data of **P1-P3** is in good agreement to the literature values.^[90,91] As shown by results of Peschel et al. **P3** is obtained in a mixture of $[\text{WBr}_2(\text{CO})(\text{H}-\equiv\text{H})_2(\text{NCMe})]$ and $[\text{WBr}_2(\text{CO})(\text{H}-\equiv\text{H})(\text{NCMe})_2]$.^[92] As separation of the two products is not possible because of the poor solubility, the ^1H NMR spectrum in CD_2Cl_2 reveals three acetylenic protons approximately in the ratio 1 : 0.9 : 1 at 10.87, 11.00 and 11.30 ppm, respectively. Due to poor solubility the product could only be partly dissolved for NMR measurements. The $\text{C}\equiv\text{O}$ and $\text{N}\equiv\text{C}$ stretching frequencies of the two products are in the range expected from literature values for the published bis-alkyne precursors of the type $[\text{WBr}_2(\text{CO})(\text{R}-\equiv\text{R})_2(\text{NCMe})]$ ($\text{R} = \text{CH}_3, \text{Ph}, \text{CH}_2\text{Cl}$).^[95]

3.3 COMPLEX SYNTHESIS

3.3.1 SYNTHESIS OF $[\text{W}(\text{CO})_3\text{L}_2]$

Salt metathesis reaction of **L1** and **L2** with **P1** or **P2** in dichloromethane was performed to afford $[\text{W}(\text{CO})_3(4\text{-Me-SPy})_2]$ (**C1**) and $[\text{W}(\text{CO})_3(\text{Me-SPym})_2]$ (**C2**) (Scheme 15). In both reactions a precipitate of NaBr was formed, which was removed via filter cannulation. Both complexes were obtained in moderate yields: **C1** in 49 % as analytically pure orange-red crystals, which were obtained from a saturated solution in dichloromethane/heptane at $-20\text{ }^\circ\text{C}$, and **C2** in 72% yield as an orange powder. However, except of one bath, **C2** was always obtained in a mixture with presumably bridged side products. Nevertheless, the product mixture could be used

for further steps without any problems. Both **C1** and **C2** are highly soluble in chlorinated solvents, acetonitrile and ethyl acetate. Moderate solubility is observed in tetrahydrofuran and benzene, whereas in diethyl ether and aliphatic hydrocarbons both complexes are poorly soluble.



Scheme 15. Synthesis of $[\text{W}(\text{CO})_3\text{L}_2]$ ($\text{L} = \text{Me-SPym}, 4\text{-Me-SPy}$).

Complexes **C1** and **C2** were characterized by NMR and IR spectroscopy (Table 5). As compounds **C1** and **C2** do not display a mirror plane, two sets of ligand signals would be expected in the corresponding ^1H NMR spectra. However, only one set of ligand signals is revealed for both compounds, which Baker and co-workers attributed to fluxionality in solution.^[102] The IR bands of both complexes are summarized in Table 5 and compared to the IR bands of the published complexes $[\text{W}(\text{CO})_2(\text{S-Phoz})_2]$, $[\text{W}(\text{CO})_3(\text{SPy})_2]$ and $[\text{W}(\text{CO})_3(\text{SPym})_2]$.^[67,102,103] Compound **C1** reveals only two out of three expected CO stretching frequencies, which can be attributed to two electronically equivalent CO ligands, as shown by its crystal structure.

Table 5. Measured $\text{C}\equiv\text{O}$ stretching frequencies and comparison to literature IR data.

Complex	Year	IR $\nu_{\text{C}\equiv\text{O}}$ [cm^{-1}]	Reference
$[\text{W}(\text{CO})_3(4\text{-Me-SPy})_2]$ (C1)	2011	1881	This work
$[\text{W}(\text{CO})_3(\text{Me-SPym})_2]$ (C2)	2014	1903 1822	This work
$[\text{W}(\text{CO})_3(\text{SPym})_2]$	2029	1941	[102]
$[\text{W}(\text{CO})_2(\text{S-Phoz})_2]$	1919	1811	[67]
$[\text{W}(\text{CO})_3(\text{SPy})_2]$	2022	1928	[103]

Attempted cyclovoltammetry measurements were found to be inconclusive.

The crystal structure of **C1** is depicted in Figure 8 and the crystal data is given in Table 12.

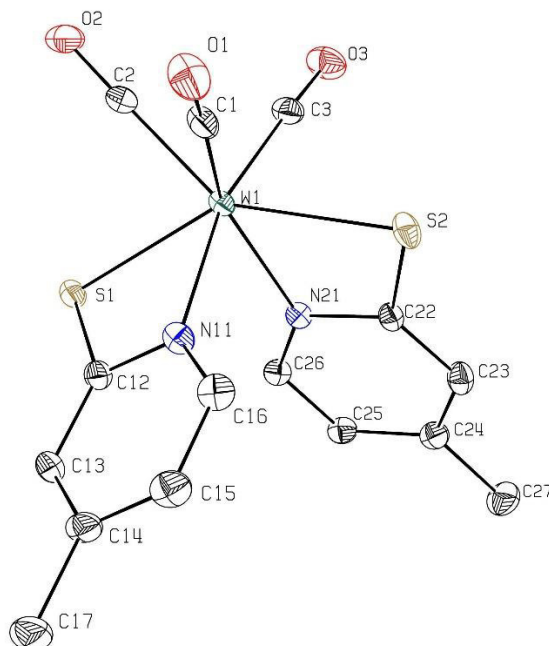


Figure 8. Molecular structure of $[W(CO)_3(4\text{-Me-SPy})_2]$ (**C1**) showing the atomic numbering scheme. Probability ellipsoids are drawn at 50% probability level. Hydrogen atoms are omitted for clarity reasons.

The structure of **C1** is approximately a capped trigonal prism with two ligands **L1** in *S-S-trans* orientation [S1-W1-S2 bond angle is 141.931(19)°].

Table 6. Selected bond lengths [Å] and bond angles [°] of **C1**.

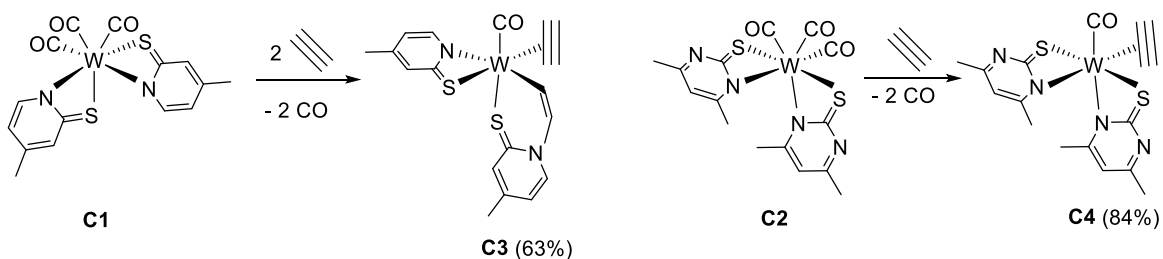
W1-C1	1.985(2)	W1-N11	2.204(2)
W1-C2	1.983(2)	W1-N21	2.2109(18)
W1-C4	2.013(2)	C1-O1	1.145(3)
W1-S1	2.5081(6)	C2-O2	1.160(3)
W1-S2	2.5389(6)	C4-O3	1.145(3)
W1-C1-O1	175.9(2)	W1-C2-O2	179.0(2)
W1-C4-O3	177.6(2)	S1-W1-S2	141.931(19)
S1-W1-N11	64.90(5)	N21-W1-S2	65.07(5)
N11-W1-N21	81.91(7)		

Table 6 summarizes selected bond lengths and bond angles of compound **C1**. Comparison with the literature-known tungsten-triscarbonyl complex $[\text{W}(\text{CO})_3(\text{SPy})_2]$ revealed similar bond lengths and angles.^[103] Thus, one CO ligand is different in terms of bond lengths (C2-O2: 1.160(3) Å) compared to the two other CO ligands (C4-O3/C1-O1: 1.145(3) Å).^[103] This result is also in accordance with the measured IR spectrum (see Table 5), where two CO bands were observed at 2011 and 1881 cm^{-1} .

The number of nitrogens in an aromatic ring system leads to less electron density in these systems and the methyl groups enhance the electron density because of the +I effect. This effect is apparent upon comparing pKa values of pyrrole (pKa = 23.0), pyrazole (pKa = 19.8) and imidazole (pKa = 18.6),^[104] as well as of the CO stretching frequencies of **C1**, $[\text{W}(\text{CO})_3(\text{SPy})_2]$, **C2** and $[\text{W}(\text{CO})_3(\text{SPym})_2]$ (Table 5). Hence, **L1** donates more electron density to the tungsten center, so that a stronger π – backbonding of the metal center to the CO ligand is expected. As π – backbonding leads to population of the π_p^* – orbital of the CO, the stretching frequency in **C1** should be at lower wavenumbers than in **C2**. The observed wavenumbers of **C1** and **C2** (Table 5) both follow this rule.

3.3.2 SYNTHESIS OF $[\text{W}(\text{CO})(\text{H}\equiv\text{H})\text{L}_2]$

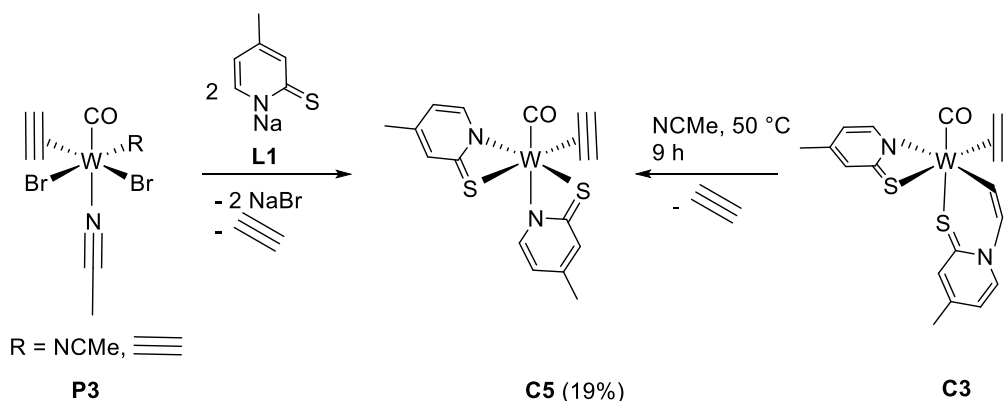
As depicted in Scheme 16, both complexes **C1** and **C2** coordinate acetylene under substitution of two CO molecules. Complete conversion of **C1** to $[\text{W}(\text{CO})(\text{H}\equiv\text{H})(=4\text{-Me-SPy})(4\text{-Me-SPy})]$ (**C3**) at rt was observed after 12 h, where insertion of one molecule of acetylene into the W-N bond and coordination of one acetylene occurred. Highly interestingly, **C2** completely reacted to $[\text{W}(\text{CO})(\text{H}\equiv\text{H})(\text{Me-SPym})_2]$ (**C4**) without insertion within 2.5 h stirring under acetylene atmosphere.



Scheme 16. Reactivity of **C1** and **C2** under acetylene atmosphere.

After work-up and recrystallization from dichloromethane overlaid with heptane both products were obtained in high purity as determined by elemental analysis. **C4** was obtained in 84% yield as violet crystalline needles, whereas **C3** was isolated in 63% yield as a maroon powder.

Additionally, the complex $[\text{W}(\text{CO})(\text{H}\equiv\text{H})(4\text{-Me-SPy})_2]$ (**C5**) was synthesized via the ligand addition method starting from the acetylene precursor mixture **P3** (Scheme 17). In the reaction of **P3** to **C5** nitrogen was purged through the solution to remove the formed acetylene. Analytically pure **C5** was obtained after work-up and recrystallization from dichloromethane overlaid with heptane as dark green crystals in 19% yield. The relatively low yield of **C5** can be explained by the partial formation of **C3** with formed acetylene.



Scheme 17. Synthetic routes towards $[\text{W}(\text{CO})(\text{H}\equiv\text{H})(4\text{-Me-SPy})_2]$ (**C5**).

Alternatively, **C5** can be synthesized via acetylene elimination from **C3** (Scheme 17). Complete conversion of **C3** into **C5** was observed after 9 hours of stirring in acetonitrile at 50 °C. Because of the elevated temperature necessary for acetylene elimination this route is more prone to the formation of side products. An attempt to prepare **C5** by preventing acetylene insertion using a shorter reaction time and a lower temperature was unsuccessful.

Compounds **C3** - **C5** are well soluble in chlorinated solvents, ethyl acetate and acetonitrile, partly soluble in benzene and insoluble in n-pentane and n-heptane. They can be well separated from each other by crystallization from

dichloromethane/heptane. The solubility of **C3** in dichloromethane is lower than the solubility of **C5**.

As shown in Table 7 two acetylenic NMR signals were observed for **C4** - **C5**, which points towards a non-rotating acetylene. In the case of $[W(CO)(H\equiv H)(4\text{-Me-SPy})_2]$ (**C5**) the presence of at least two dynamic isomers was observed, a summary of all theoretically possible isomers is given in Figure 9.

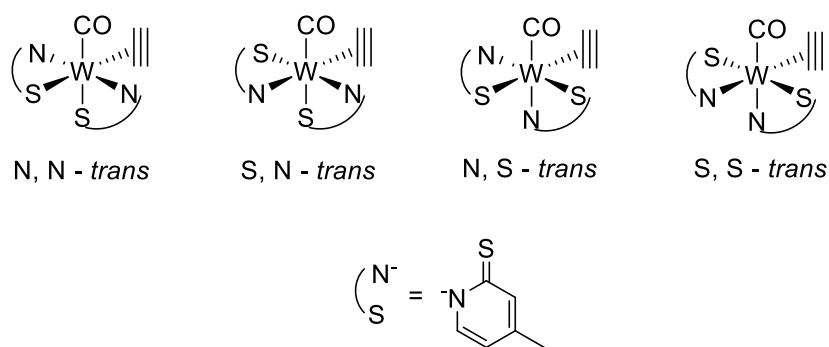


Figure 9. Possible isomers of compound **C5**.

Table 7. Summary of ^1H , ^{13}C and IR – data for **C4-C5**.

	^1H NMR		^{13}C NMR	IR	Lit.
	[ppm]		[ppm]	[cm^{-1}]	
	$\delta(\text{H}\equiv\text{H})$	$\delta(\equiv)$	$\delta(\text{CO})$	$\nu_{\text{C}\equiv\text{O}}$	
C3	12.91	198.43	232.62	1907	This work
	11.99	193.07			
C4	13.79	206.03	234.26	1916	This work
	12.47	203.72			
C5	13.61 (a)	177.88 (a)	241.39 (a)	1907	This work
	13.62 (b)	170.96 (a)	239.71 (b)		
	12.30 (a)	177.91 (b)			
	12.31 (b)	170.07 (b)			
$[W(\text{H}\equiv\text{H})(\text{CO})(\text{SPhoz})_2]$	12.22	200.0	235.28	2069	[67]
	11.57	193.1			

NMR data was measured in CD_2Cl_2 . The isomers formed in **C5** are assigned with indices (a) and (b).

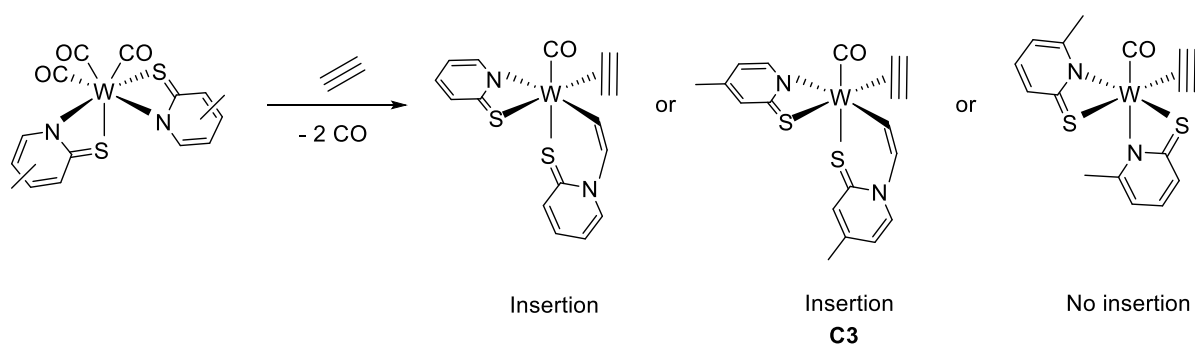
The existence of these isomers could be proven via ^1H NMR spectroscopy: Analytically pure complex **C5** dissolved in different solvents gave different ratios of aromatic proton signals of the two ligand sets in the respective spectra (CDCl_3 1 : 0.4, C_6D_6 1 : 0.2, CD_2Cl_2 1 : 0.5 and 0.06 equiv. of a 3rd acetylene and ligand-containing species).

As described in section 3.3.1, 4-Me-SPy (**L1**) is a stronger donor than Me-SPym (**L2**), hence **L1** leads to weaker CO bonds and to acetylenes with less electron density.^[104] In comparison to **C5** the CO stretching frequencies of **C4** are therefore found at higher wavenumbers and the acetylenic signals in ^1H and ^{13}C NMR spectra are shifted to lower field. Additionally the ^{13}C NMR signal of CO in **C4** is shifted to lower field compared to **C5**, because of the lower electron density at the CO (Table 7).

Unexpectedly, the π – backbonding to the CO and the acetylene seems to be stronger in **C5** than in **C3** according to the ^{13}C NMR shifts of acetylene and CO (Table 7). This might be attributed to the extended π -system in **C3** formed by acetylene insertion. Nevertheless, the acetylenic ^1H NMR shifts point towards the opposite direction, meaning a lower electron density at the acetylene of **C5** compared to **C3** (Table 7). Therefore, acetylenic ^1H NMR shifts might be affected by various electronic influences, whereas ^{13}C NMR and IR data both point in the same direction.

However, lower electron density on the acetylene, meaning a shift of ^1H and ^{13}C NMR signals to lower field, is in principle desirable, because this would favor a nucleophilic attack of a water molecule towards an activated acetylene to form acetaldehyde according to the mechanistic proposals of the Hillier, Bayse and Himo group.^[22–24]

In contrast to $[\text{W}(\text{CO})_3(\text{Me-SPym})_2]$ (**C2**), $[\text{W}(\text{CO})_3(4\text{-Me-SPy})_2]$ (**C1**) undergoes acetylene insertion into the W-N bond, presumably to minimize ring strain, additionally to acetylene coordination to form $[\text{W}(\text{CO})(\text{H}\equiv\text{H})(=4\text{-Me-SPy})(4\text{-Me-SPy})]$ (**C3**). It is assumed that acetylene insertion into the W-N bond of **C2** is mainly prevented by the steric bulk created by the methyl groups ortho to the ring-nitrogen coordinated to the tungsten center. This is shown by the fact that **C1** undergoes acetylene insertion, whereas insertion is not observed in $[\text{W}(\text{CO})_3(6\text{-Me-SPy})_2]$ (Scheme 18).^[92] Electronic effects can be assumed to play a minor role in this reactivity, as methyl groups ortho and para to the pyridine-N are known to be electronically similar.^[105]



Scheme 18. Distinct reactivity of tungsten(II) – tris(carbonyl) – thiopyridine complexes under acetylene atmosphere.^[92]

This finding of acetylene insertion into W-N bonds is crucial for biomimetic model compounds for *Acetylene Hydratase*, as insertion can be regarded as an intramolecular nucleophilic attack. Therefore these studies are important steps towards successful functional modelling of *Acetylene Hydratase*.

Acetylene insertion into M-X bonds is also rarely reported in literature and until yet an acetylene insertion into W-N bonds has not been observed. For mononuclear transition metal complexes acetylene insertion into Re-P, Pt-X (X = Br, I) and Co-X (X = Cl, Br, I) bonds have been reported, as summarized in Figure 10.^[106–109]

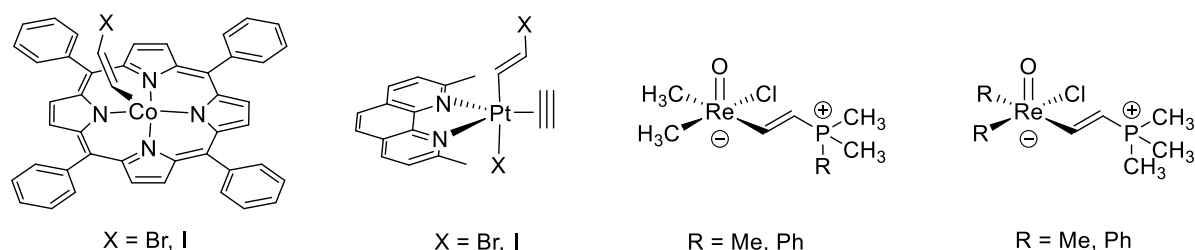


Figure 10. Summary of literature-known examples of acetylene insertion into an M-X bond.^[106–109]

A solution of $[W(CO)(H\equiv C-H)(=4\text{-Me-SPy})(4\text{-Me-SPy})]$ (**C3**) and $[W(CO)(H\equiv C-H)(\text{Me-SPym})_2]$ (**C4**) in dichloromethane was overlaid with heptane to obtain dark maroon and dark violet single crystals, respectively, suitable for X-ray diffraction analysis. Dark green needles suitable for diffraction measurements of $[W(CO)(H\equiv C-H)(4\text{-Me-SPy})_2]$ (**C5**) were obtained from a saturated solution in acetonitrile at $-35\text{ }^\circ\text{C}$. The molecular structures showing the atomic numbering schemes of **C3** and **C5** are

depicted in Figure 11 and of **C4** in Figure 12. The crystal data for **C3-C5** is given in the appendix (Table 12 for **C3**, Table 13 for **C4** and **C5**).

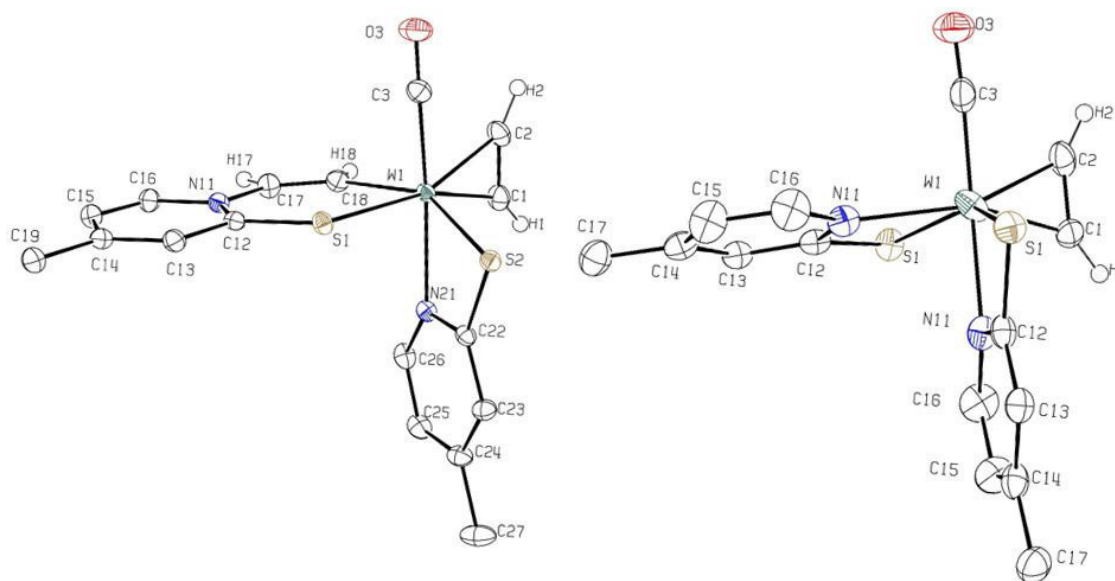


Figure 11. Molecular structures of $[W(CO)(H\equiv H)(=4\text{-Me-SPy})(4\text{-Me-SPy})]$ (**C3**) (left) and $[W(CO)(H\equiv H)(4\text{-Me-SPy})_2]$ (**C5**) (right) showing the atomic numbering scheme. Probability ellipsoids are drawn at 50% probability level. Except on the acetylene ligands, hydrogen atoms as well as the second orientation of the carbonyl and the acetylene ligand in **C5** were omitted for clarity reasons.

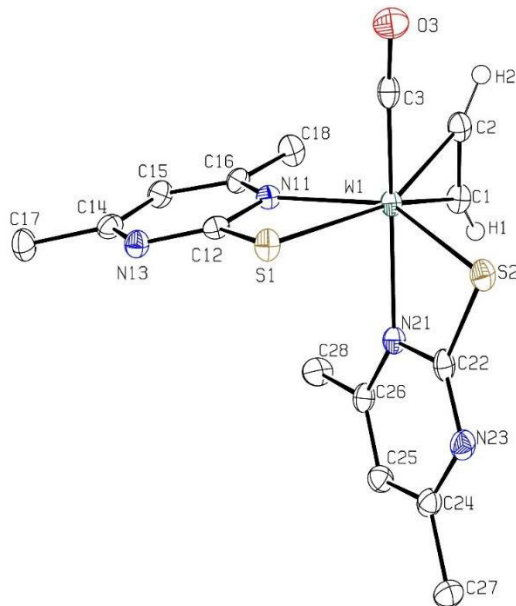


Figure 12. Molecular structure of $[W(CO)(H\equiv H)(\text{Me-SPym})_2]$ (**C4**) showing the atomic numbering scheme. Probability ellipsoids are drawn at 50% probability level. Except on the acetylene ligand, hydrogen atoms are omitted for clarity reasons.

All three structures show a distorted octahedral coordination sphere, in which the center of **C2** and **C1** bond occupies one of the six coordination sites. Interestingly $[\text{W}(\text{CO})(\text{H}\equiv\text{H})(4\text{-Me-SPy})_2]$ (**C5**) crystallized in an approximately *S-S-trans* motif, whereas $[\text{W}(\text{CO})(\text{H}\equiv\text{H})(\text{Me-SPym})_2]$ (**C4**) and $[\text{W}(\text{CO})(\text{H}\equiv\text{H})(=4\text{-Me-SPy})(4\text{-Me-SPy})]$ (**C3**) crystallized as the *S-S-cis* isomers. In **C5** the carbonyl ligand and the acetylene ligand are disordered over two orientations and were therefore refined with site occupation factors of 0.5, as the complex has a two-fold rotation axis.

In Table 8 selected bond lengths and angles of **C3-C5** are given. Noticeable is the larger C1-C2-H2 bond angle of the inserted product **C3** compared to **C4** and **C5**. This points towards a lower metallacyclic character of the acetylene ligand in **C3** and might be explained with the inserted acetylene, as the extended π -system in **C3** can donate additional electron density to the tungsten center. The complex bearing the electron-poor Me-SPym ligand **C4** has a shorter C3-O3 bond length compared to **C5**, which is an indicator for a higher electron density at the tungsten center in the case of **C5** (stronger π – backbonding into π_p^* - orbital). However, these findings are not reflected by ^1H and ^{13}C NMR data (Table 7). Therefore it might also be attributed to a different stereoelectronic situation in the inserted complex **C3** compared to **C4** and **C5**.

Table 8 also shows a comparison of $\text{C}\equiv\text{C}$ and $\text{C}\equiv\text{O}$ bond lengths and $\text{C}\equiv\text{C-H}$ angles of **C3-C5** with other tungsten(II)-carbonyl-acetylene complexes. The found bond lengths and angles in **C3-C5** are comparable to η^2 bound acetylene in the complex $[\text{W}(\text{CO})(\text{H}\equiv\text{H})(\text{S}_2\text{CNEt}_2)_2]$.^[66] The recently published compound $[\text{W}(\text{CO})(\text{H}\equiv\text{H})(\text{SPhoz})_2]$ reveals a larger $\text{C}\equiv\text{C}$ bond length as well as a lower $\text{C}\equiv\text{C-H}$ bond angle than **C3-C5**. This finding correlates with the higher electron density of the SPhoz ligand compared to SPym and 4-Me-SPy.

Table 8. Comparison of C≡C and C≡O bond lengths and C≡C-H angles of **C4-C5** with literature values.

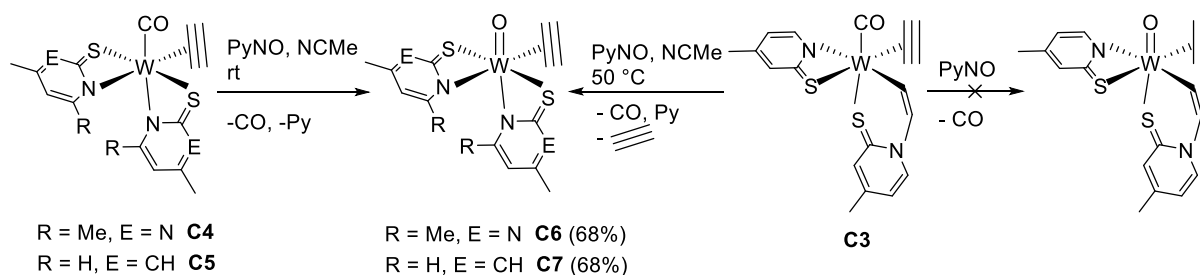
	C≡C-H [°]		C≡O [Å]	C≡C [Å]	Reference
C3	147.6(5)	C1-C2-H2	1.157(3)	1.308(3)	This work
	139.5(14)	C2-C1-H1			
C4	141.9(6)	C1-C2-H2	1.153(5)	1.309(4)	This work
	147.5(9)	C2-C1-H1			
C5	143.8	C1-C2-H2	1.142(16)	1.302(1 2)	This work
	144.4	C2-C1-H1			
[W(CO)(H≡-H)	136.1	H-C1-C2	1.16	1.29	[66]
(S ₂ CNEt ₂) ₂]	130.2	H-C2-C1			
[W(CO)(H≡-H)	122.7(15)		1.160(2)	1.327	[67]
(SPhoz) ₂]	146.9(16)				
Free acetylene	180			1.196	[110]
Free ethylene	120			1.324	[110]

The synthesized complexes all show a significantly reduced triple bond character of the C≡C bond in the range of free ethylene (1.324 Å).^[110] This finding is also reflected by the significant downfield shift of acetylenic NMR signals compared to free acetylene (Table 7) and supports the consideration of activating acetylene towards a nucleophilic attack, as a significant amount of the electron density of the C≡C triple bond is donated to the tungsten center.

Furthermore, acetylene insertion into the W-N bond has a slight influence on the C=S bond length: a shortened C12-S1 bond length is observed in **C3** (1.720(2) Å) compared to **C5** (1.749(3) Å). The shortened C12-S1 bond in **C3** compared to **C5** is attributed to an enhanced electron delocalization by the inserted acetylene. Because of the coordination to the tungsten center, all C-S bond lengths are significantly enlarged compared to free thiopyridine (C-S: 1.68 Å).^[111]

3.3.3 OXIDATION OF $[W(CO)(H\equiv H)L_2]$ TO $[WO(H\equiv H)L_2]$

The synthesis of tungsten-oxo-acetylene complexes is relevant for modeling *Acetylene Hydratase*, as its crystal structure shows an oxygen-donor ligand bound to the tungsten center.^[21] Tungsten-carbonyl complexes can be oxidized to the corresponding oxo-complexes using $Mo_2O_3[S_2P(OEt)_2]_4$, molecular oxygen, peracids or *N*-oxides like pyridine-*N*-oxide (Py*N*-O) or trimethylamine-*N*-oxide (TMAO) as oxygen-atom transfer agents.^[57,67,77,80,97,112] Therefore, the oxidation of **C3**, **C4** and **C5** was examined according to Scheme 19.



Scheme 19. Oxidation of **C4**, **C3** and **C5**.

For the oxidation of **C4** to **C6** as well as for the oxidation of **C5** to **C7** pyridine-*N*-oxide (1.1 and 1.05 equiv. respectively) was used. Both oxidations were conducted overnight in acetonitrile and were accompanied by a color change from violet (**C4**) and green (**C5**) to maroon (**C6**) and bright brown (**C7**), respectively. After evaporation of acetonitrile excess pyridine-*N*-oxide and side products were removed by washing the residue with diethyl ether. Both compounds **C6** and **C7** were isolated in 68% yield as maroon (**C6**) and bright brown (**C7**) powders. Complexes **C6** and **C7** are moderately soluble in chlorinated solvents, acetonitrile and ethyl acetate and insoluble in diethyl ether, pentane and heptane.

For the oxidation of **C4** to $[WO(H\equiv H)(Me-SPym)_2]$ (**C6**) Py*N*-O, TMAO and molecular oxygen as oxidants were investigated. It was found that molecular oxygen did not react with **C4** at atmospheric pressure, even at 55°C. Py*N*-O and TMAO were both capable of oxidizing **C4** to **C6**, albeit the oxidation using TMAO as oxidant is more prone to side-reactions.

Complex **C3** did not react to the corresponding oxo-complex using Py*N*-O, TMAO and molecular oxygen at atmospheric pressure as oxidant, rather than to $[WO(H\equiv H)(4-$

Me-SPy)₂] (**C7**) (Scheme 19). As described in section 3.3.2, compound **C3** undergoes acetylene elimination to complex **C5**. Formed **C5** can then be oxidized in situ to **C7**. The optimal reaction conditions for the oxidation of **C3** to **C7** were determined via a screening experiment and were found using pyridine-*N*-oxide in acetonitrile at 50 °C. Using these conditions complete conversion was obtained after 9 hours reaction time. However, the direct oxidation of **C5** to **C7** is more selective as with elevated temperature necessary to promote acetylene elimination.

Table 9 summarizes ¹H and ¹³C NMR data of **C6** and **C7** together with related literature known compounds. As for compound **C5**, the formation of isomers was observed and proven by the ¹H NMR measurement of a single crystal of **C6** and **C7** respectively. For both compounds a major isomer and approx. 10% of a minor isomer (in dichloromethane) were observed. Additionally approximately 5% of a third ligand containing tungsten species were detected in the ¹H NMR in CD₂Cl₂ of compound **C7**. The acetylenic NMR shifts of **C6** and **C7** are in the same range as literature-known oxo-tungsten complexes. The dithiocarbamate complexes [WO(H≡C)(S₂CNR₂)₂] (R = Et, Me) cannot be compared to **C6** and **C7** as the published NMRs were not measured in CD₂Cl₂.^[57]

Table 9. ^1H and ^{13}C NMR data of **C6**, **C7** and comparison to literature known tungsten(IV)-oxo-acetylene compounds.

	^1H NMR [ppm]	^{13}C NMR [ppm]	Lit.
	$\delta(\text{H}\equiv\text{H})$	$\delta(\equiv)$	
[WO(H \equiv H)(Me-SPym) $_2$] (C6)	11.25 (a)	158.15	This work
	10.95 (a)	157.02	
	10.70 (b)		
	11.03 (b)		
[WO(H \equiv H)(4-Me-SPy) $_2$] (C7)	10.94 (a)	158.08	This work
	10.95 (a)	154.65	
	11.03 (b)		
	11.06 (b)		
[Tp'WO(H $_2$ O)(H \equiv H)](OTf)	12.01	156.8	[78]
	10.63	148.2	
[WO(H \equiv H)(S-Phoz) $_2$]	10.60 - 10.47	152.90	[67]
		151.85	
[W(CO)(H \equiv H)(Me-SPym) $_2$] (C3)	13.79	206.03	This work
	12.47	203.72	
[W(CO)(H \equiv H)(4-Me-SPy) $_2$] (C5)	13.61 (a)	177.91 (b)	This work
	13.62 (b)	177.88 (a)	
	12.30 (a)	170.96(a)	
	12.31 (b)	170.07 (b)	

NMR data was measured in CD_2Cl_2 at 25 °C. Isomers are assigned with indices (a) and (b).

All oxidations were monitored using IR spectroscopy: the carbonyl stretchings of **C3**, **C4** and **C5** decreased during the course of the reaction and characteristic W=O stretchings at 933 cm^{-1} (**C6**) and 945 cm^{-1} (**C7**), respectively, appeared. Cyclovoltammetry measurements of **C6** and **C7** were found to be inconclusive.

[WO(H \equiv H)(Me-SPym) $_2$] (**C6**) and [WO(H \equiv H)(4-Me-SPy) $_2$] (**C7**) were crystallized from a solution in ethyl acetate overlaid with heptane at -35 °C as bright yellow crystals and as light brown crystals respectively. The crystallographic data for **C6** and **C7** can be found in the appendix in Table 14. The crystal structures of complexes **C6** and **C7**, showing the atomic numbering scheme, are depicted in Figure 13. Both

complexes crystallized in a distorted octahedral structure. Like their corresponding carbonyl complexes **C4** and **C5**, **C6** crystallized as the S-N-*trans* isomer, whereas in **C7** an S-S-*trans* arrangement was found.

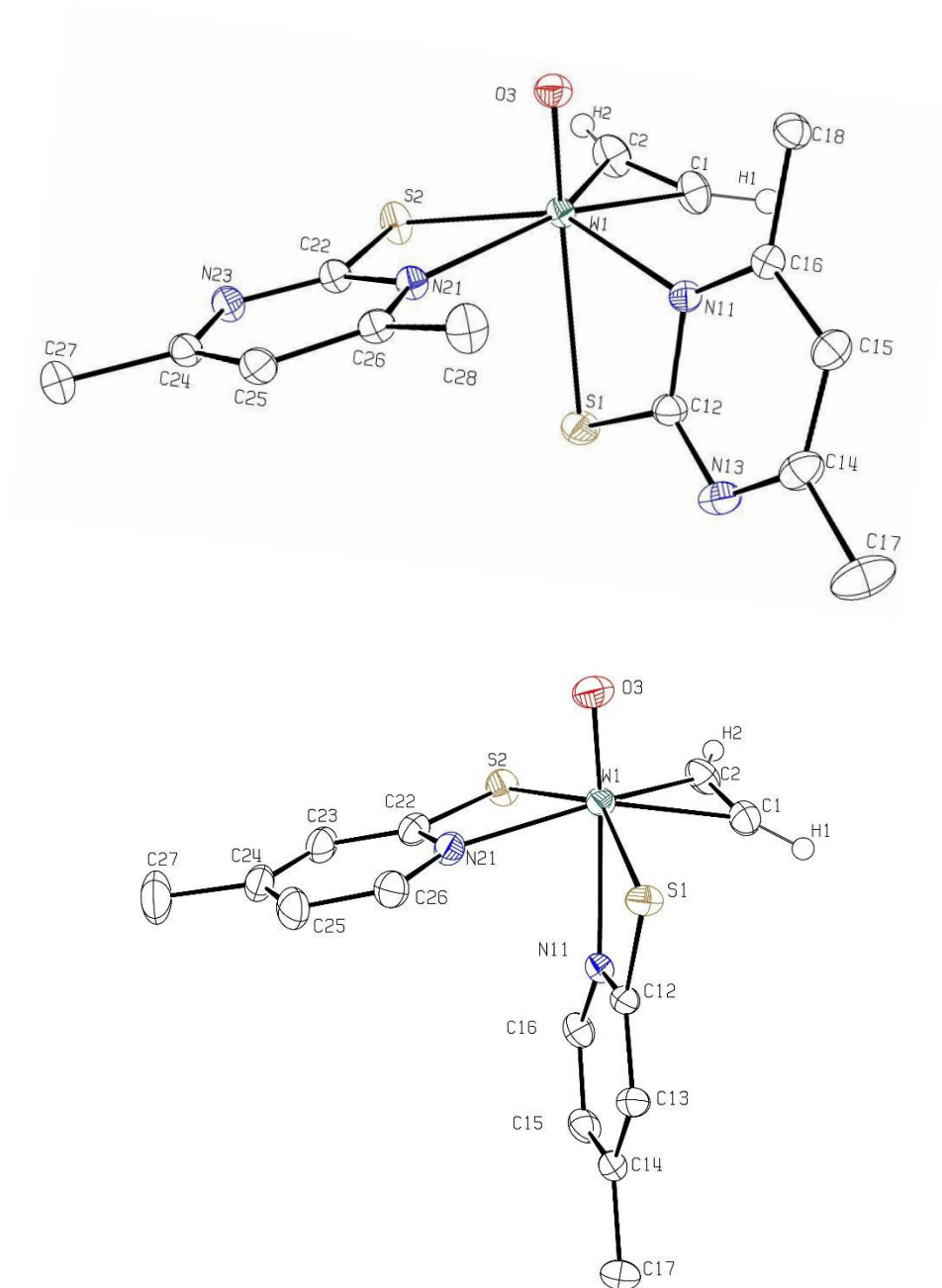


Figure 13. Molecular structures of $[\text{WO}(\text{H}\equiv\text{H})(\text{Me-SPym})_2]$ (**C6**) (top) and $[\text{WO}(\text{H}\equiv\text{H})(4\text{-Me-SPy})_2]$ (**C7**) (bottom) showing the atomic numbering scheme. Probability ellipsoids are drawn at 50% probability level. Except on the acetylene ligand, hydrogen atoms are omitted for clarity reasons.

Table 10 shows a comparison of selected bond lengths and angles of **C6** and **C7** with their corresponding carbonyl complexes. As expected, the acetylenic $\text{C}\equiv\text{C}$ bond

length of [WO(H≡H)(Me-SPym)₂] (**C6**) is significantly shorter than the C≡C bond length of [WO(H≡H)(4-Me-SPy)₂] (**C7**), which can be explained by lower π -electron backdonation into π^* of acetylene because of the electron-poorer pyrimidine system **C7**.

Table 10. Selected bond lengths [Å] and bond angles [°] of **C6-C7** and comparison to their carbonyl complexes **C4-C5**.

	Carbonyl complexes			Oxo complexes	
	C3	C4	C5	C6	C7
C1-C2	1.308(3)	1.309(4)	1.302(12)	1.276(3)	1.280(3)
C1-W1	2.031(2)	2.020(3)	2.090(13)	2.0911(17)	2.095(2)
C2-W1	2.0505(19)	2.040(3)	2.078(7)	2.0810(16)	2.093(2)
W1-O3	-	-	-	1.7178(14)	1.7204(17)
C1-C2-H2	147.6(5)	141.9(6)	143.8	149.3(16)	142.7(7)
C2-C1-H1	139.5(14)	147.5(9)	144.4	141.2(9)	143.9(5)

According to measured bond lengths and angles (Table 10), a slightly lower metallacyclic character of [WO(H≡H)(SPhoz)₂] is observed, which is reflected by a larger C≡C bond and smaller C≡C-H angles of **C6**, **C7** compared to [WO(H≡H)(SPhoz)₂]. Compared to free acetylene (C≡C: 1.196 Å), the acetylene bonds in **C6** and **C7** are significantly enlarged and are in the range between free acetylene and free ethylene (1.324 Å). Together with the drastic downfield shift of acetylenic ¹H and ¹³C NMR signals compared to free acetylene (1.91 ppm in the ¹H NMR and 71.8 ppm in the ¹³C NMR in CDCl₃) these results point towards a drastic increase in acidity of the protons and nucleophilicity of the acetylenic carbons (Table 9).^[113] These findings are important, as nucleophilic attack and protonation on the coordinated acetylene are discussed as key steps in mechanistic proposals.^[21,23,24]

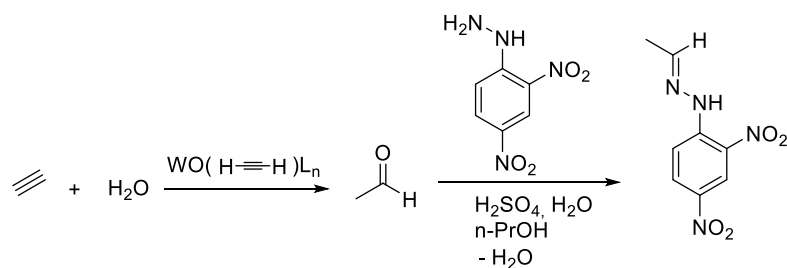
In comparison to the ¹H NMR spectra of the corresponding carbonyl-complexes **C4** and **C5** the acetylenic protons of **C6** and **C7** are significantly shifted towards higher field (Table 9). Similarly to the ¹H NMR shifts, also the signals of the acetylene in the ¹³C NMR are significantly shifted upfield compared to acetylenic shifts of the corresponding carbonyl derivatives (Table 9). These results indicate an increased electron density as well as an increased π -backbonding on acetylenic carbons of compounds **C6** and **C7** compared to their carbonyl derivatives. In contrast to that, the

C1-C2 bond lengths of **C6** and **C7** are shortened compared to **C4-C5** (Table 10), which is to be expected as oxidation of the metal center lowers the degree of π -backbonding. These contrary findings are attributed to the different coordination of acetylene in tungsten(II)-carbonyl-complexes **C4-C5** (parallel coordination of acetylene to CO) compared to their tungsten(IV)-oxo-complexes **C6-C7** (orthogonal coordination of oxo and acetylene), which leads to a totally different electronic situation in terms of orbital overlappings (Introduction, section 1.5).^[57,61] Additionally to that a very detailed study of the Chatt-Dewar Duncanson model for Au(I) alkyne complexes revealed that acetylenic bond lengths and angles cannot always be taken as an indicator for π -backbonding.^[114] This is demonstrated by the fact that, depending on the ligand system, a degree of π -backbonding of up to 50% has been calculated for Au(I) complexes, albeit alkyne bond lengths and angles as well as alkyne NMR signals are shifted only very slightly upon coordination to the metal center.^[29,114–117] As these results demonstrated for Au(I) alkyne complexes might also hold for **C3-C4**, a discussion of the degree of activation on the basis of NMR shifts and bond lengths and angles towards a nucleophilic attack is even more complex.

3.4 REACTIVITY OF [WO(H \equiv H)L₂]

3.4.1 CATALYTIC ACETYLENE HYDRATION

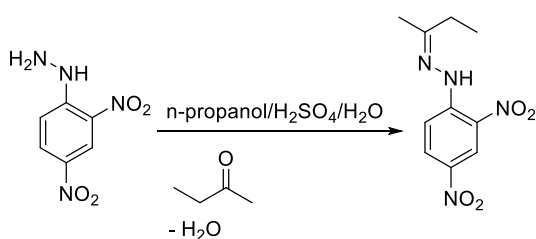
Catalytic acetylene hydration experiments were performed with the tungsten(IV) complexes [WO(H \equiv H)(Me-SPym)₂] (**C6**) and [WO(H \equiv H)(4-Me-SPy)₂] (**C7**) as well as with the tungsten(II) complexes [W(CO)(H \equiv H)(4-Me-SPy)₂] (**C5**), [W(CO)(H \equiv H)(=4-Me-SPy)(4-Me-SPy)] (**C3**) and [W(CO)(H \equiv H)(Me-SPym)₂] (**C4**). The experimental setup used for the study of catalytic acetylene hydration is similar to a published procedure from the Hintermann and Sarkar groups.^[84,87] Both used a stream of acetylene to transfer formed acetaldehyde (bp = 20 – 22 °C)^[118] from a catalyst-containing acetonitrile solution into a flask of 2,4-dinitrophenylhydrazine dissolved in aqueous HCl media.^[84,87] 2,4-Dinitrophenylhydrazine (Brady's reagent, DNP) is known to be a common detection reagent for aldehydes and ketones, as it forms the corresponding hydrazone (Scheme 20), which precipitates immediately from the solution.



Scheme 20. Precipitation of acetaldehyde using Brady's reagent.

The procedures used by the Hintermann and Sarkar groups were not reproducible, as the authors only stated the use of HCl media for the preparation of the Brady's reagent solution.^[84,87] We were not able to dissolve DNP in a 1:1 mixture of conc. HCl and water, nor precipitated acetaldehyde 2,4-dinitrophenylhydrazone from a solution of DNP in concentrated HCl. A procedure from "Organikum" using 2 mL H₂SO₄, 3 mL H₂O and 10 mL ethanol to dissolve 0.4 g 2,4-dinitrophenylhydrazine was found to dissolve the reagent completely and immediately precipitates the analyte.^[119] Nevertheless, this procedure had a major drawback, as commercially available ethanol contains the competing 2-butanone, which also reacts with DNP in the same way as acetaldehyde (Scheme 21). This could be easily overcome by the change to n-propanol.

A blank experiment using the setup described in Figure 14 with 0.1 mL acetaldehyde in 10 mL chloroform in a Schlenk flask proved the procedure to be suitable for acetaldehyde detection, as it led to immediate precipitation of acetaldehyde 2,4-dinitrophenylhydrazone.



Scheme 21. Schiff-base formation of 2-butanone and DNP.

For testing potential catalytic acetylene hydration activity, the complexes **C3-C7** were dissolved in 10 mL CDCl₃, instead of the NCM_e used by Sarkar and Hintermann,^[84,87] with 20 equiv. water in a 25 mL Schlenk flask which was then purged with acetylene.

The gas phase of the complex containing flask was then bubbled through a solution of 2,4-dinitrophenylhydrazine (Figure 14). Additionally, NMR samples were taken after 5, 10, 15, 30 and 45 min directly from the complex containing solution into a NMR tube equipped with a Young valve.

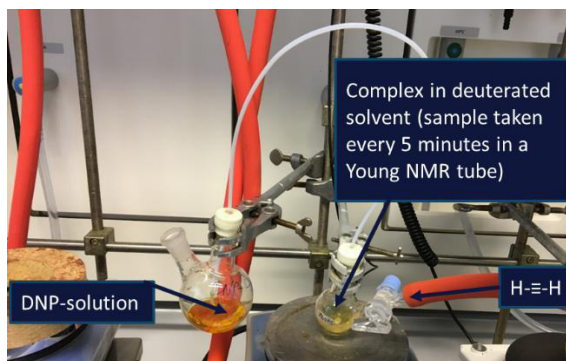


Figure 14. Experimental setup for the study of catalytic acetylene hydration.

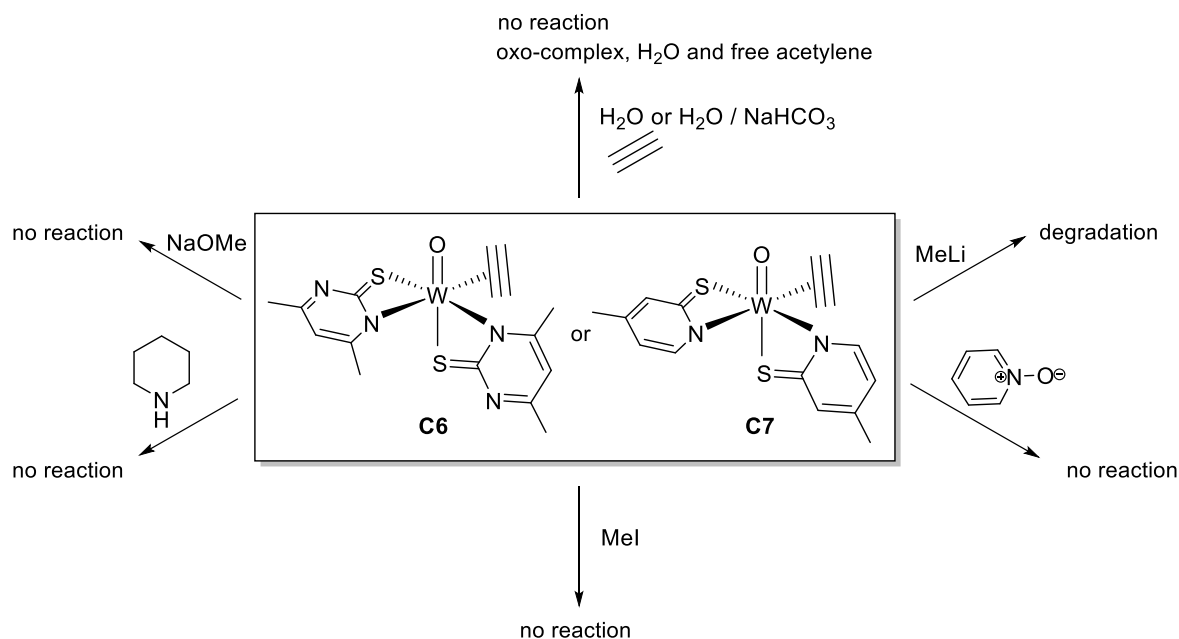
Using complexes **C3-C7** with H_2O or $\text{H}_2\text{O}/\text{NaHCO}_3$ as nucleophiles and the setup described above no acetylene hydration to acetaldehyde could be observed. The NMR samples taken directly from the solution revealed unreacted tungsten complex, acetylene (1.91 ppm in CDCl_3) as well as water.^[120]

However, it seems that the synthesized complexes **C3-C7** show the desired stability towards oxygen and water compared to $[\text{WO}(\text{H}\equiv\text{H})(\text{SPhoz})_2]$ and therefore do not degrade completely after one day with water and/or oxygen,^[67] but seem to be too stable for the desired reactivity towards water. The high stability of **C3-C7** can be attributed to a very tight coordination of the acetylene towards the tungsten center (strong σ -bonding as well as π -backbonding), which, however, makes a nucleophilic attack on the coordinated acetylene elusive. This strong interaction of the alkyne with the metal center is also demonstrated by a comparison of alkyne NMR shifts and bond lengths to cationic Au-alkyne complexes, which successfully catalyze a nucleophilic attack on alkynes.^[29,38,39,41] Whereas alkyne NMR shifts and bond lengths of **C3-C7** are dramatically different compared to the free alkyne, the cationic Au derivatives only show a very slight deviation,^[29,115–117] which has been attributed to an equal amount of σ -bonding and π -backbonding in Au(I) alkyne complexes.^[114] To conclude **C3-C7** show a desirable high stability towards water and oxygen and are therefore highly

suitable for structural studies on tungsten-alkyne complexes with a coordination sphere similar to *Acetylene Hydratase*.

3.4.2 REACTIVITY OF $[\text{WO}(\text{H}\equiv\text{H})\text{L}_2]$ WITH VARIOUS NUCLEOPHILES / ELECTROPHILES

The reactivity of $[\text{WO}(\text{H}\equiv\text{H})(\text{Me-SPym})_2]$ (**C6**) and $[\text{WO}(\text{H}\equiv\text{H})(4\text{-Me-SPy})_2]$ (**C7**) towards nucleophiles was investigated. The different nucleophiles and the performed experiments are summarized in Scheme 22.



Scheme 22. Investigated reactivity of **C6** and **C7** towards nucleophiles and electrophiles.

As already discussed in section 3.4.1, no reactivity of **C6** and **C7** with water under acetylene atmosphere was observed. Moreover, nucleophilic attack of sodium methanolate, piperidine and methyl lithium on complexes **C6** and **C7** as well as further oxidation with PyN-O were investigated. Therefore, the respective complex was dissolved in tetrahydrofuran and 1.0 equiv. of nucleophile was added. The addition of methyl lithium as a 1.6 M solution in diethyl ether led to an immediate change of color from bright brown to dark brown. No change of color was observed by the addition of 1.0 equiv. PyN-O to a solution of **C6** and **C7** in acetonitrile. To test the behavior of **C6** and **C7** towards electrophiles as well, an NMR experiment using 1.0 equiv. of a 5 vol% stock solution of methyl iodide in C_6D_6 was performed.

Further oxidation of **C6** and **C7** with 1 equiv. PyN-O showed no conversion, which reveals the high stability compared to $[\text{WO}(\text{H}\equiv\text{H})(\text{SPhoz})_2]$.^[67] Together with the obtained NMR and crystallographic data (section 3.3.3) this points towards a metallacyclic character of the η^2 acetylene bound to the tungsten center and therefore also towards a tungsten(VI) center in **C6** and **C7**.

Table 11. Summary of pKa values and nucleophilicity parameters of the nucleophiles used for the reactivity studies.

	pKa (DMSO)	Nucleophilicity parameter
H ₂ O	31.4 ^[121]	
H ₂ O/NaHCO ₃	10.25 ^[13]	10.47(H ₂ O) ^[122]
Me-Li	56 ^[104]	
Piperidine	11.22 ^[123]	15.6 (MeOH/NCMe) ^[124]
NaOMe	29.0 ^[121]	15.78 (MeOH) ^[125]

Methyl lithium together with **C6** or **C7** lead to the formation of a brown insoluble precipitate, which was identified as a variety of degradation products according to measured ¹H NMR spectra. This can be explained with the high basicity (pKa = 56) of methyl lithium.^[104] Reaction of **C6** or **C7** with piperidine or sodium methanolate revealed no reaction according to ¹H NMR spectroscopy. Similarly to the acetylene-hydration experiments in section 3.4.1 these results indicate that **C6** and **C7** display the desired enhanced stability, but seem too stable for any reactivity with the tested nucleophiles. This is surprising as $[\text{WO}(\text{H}\equiv\text{H})(\text{Me-SPym})_2]$ (**C6**) as well as $[\text{WO}(\text{H}\equiv\text{H})(4\text{-Me-SPy})_2]$ (**C7**) can be considered as 16-electron-complexes. Therefore a coordination of a nucleophile at the tungsten center in order to get the more stable 18-electron-complex seems favorable. Complexes $[\text{WO}(\text{H}\equiv\text{H})(\text{Me-SPym})_2]$ (**C6**) and $[\text{WO}(\text{H}\equiv\text{H})(4\text{-Me-SPy})_2]$ (**C7**) are presumably stabilized by steric bulk created by the coordinated ligands as well as by additional electron donation of the sulfur lone pair (section 3.3.3). A partial double bond character of the W-S bond was already proposed for $[\text{W}(\text{CO})_3(\text{SPy})_2]$.^[103]

As no reactivity with nucleophiles could be observed, the complexes were tested for potential electrophilic reactivity. Therefore methyl iodide was added to **C6** as well as **C7**. According to ¹H NMR measurements the addition of methyl iodide to both complexes did not lead to a reaction, as both complexes with their electron-poor

pyridine and piperidine ligand systems were developed for a nucleophilic attack on the coordinated acetylene.

4. CONCLUSION

Novel models for *Acetylene Hydratase* based on 4-methylpyridine-2-thiolate (**L1**, 4-Me-SPy) and 4,6-dimethylpyrimidine-2-thiolate (**L2**, Me-SPym) were developed. First, the two tricarbonyl complexes $[\text{W}(\text{CO})_3(\text{Me-SPym})_2]$ (**C2**) and $[\text{W}(\text{CO})_3(4\text{-Me-SPy})_2]$ (**C1**) were isolated starting from the literature-known precursors $[\text{W}_2\text{Br}_4(\text{CO})_7]$ (**P1**) or $[\text{WBr}_2(\text{CO})_3(\text{NCMe})_2]$ (**P2**).

While $[\text{W}(\text{CO})_3(6\text{-Me-SPy})_2]$ reacted under acetylene atmosphere to $[\text{W}(\text{CO})(\text{H}\equiv\text{H})(6\text{-Me-SPy})_2]$, $[\text{W}(\text{CO})_3(\text{SPy})_2]$ underwent acetylene insertion into the W-N bond to form $[\text{W}(\text{CO})(\text{H}\equiv\text{H})(=\text{SPy})(\text{SPy})]$.^[92] Using the ligand **L1** with the methyl group para to the pyridine-nitrogen we could demonstrate that acetylene insertion is mainly prevented by sterical hindrance as compound **C1** also showed acetylene insertion to the corresponding complex $[\text{W}(\text{CO})(\text{H}\equiv\text{H})(=4\text{-Me-SPy})(4\text{-Me-SPy})]$ (**C3**). However $[\text{W}(\text{CO})(\text{H}\equiv\text{H})(=4\text{-Me-SPy})(4\text{-Me-SPy})]$ (**C3**) was found to be in equilibrium with $[\text{W}(\text{CO})(\text{H}\equiv\text{H})(4\text{-Me-SPy})_2]$ (**C5**) and therefore undergoes complete acetylene elimination over time in solution. Additionally, complex **C2** also reacted readily with acetylene to form the novel and electron-poor compound $[\text{W}(\text{CO})(\text{H}\equiv\text{H})(\text{Me-SPym})_2]$ (**C4**), but did not undergo acetylene insertion into the W-N bond.

As *Acetylene Hydratase* is a tungsten(IV) dependent enzyme, the biologically relevant complexes $[\text{WO}(\text{H}\equiv\text{H})(\text{Me-SPym})_2]$ (**C6**) and $[\text{WO}(\text{H}\equiv\text{H})(4\text{-Me-SPy})_2]$ (**C7**) were synthesized from **C4** and **C5** respectively using pyridine-*N*-oxide as oxidant. Complex **C3** was found to be unreactive towards the oxidants pyridine-*N*-oxide, trimethylamine-*N*-oxide or molecular oxygen at atmospheric pressure, but underwent acetylene elimination to **C5**, which was subsequently oxidized to **C7**.

All compounds **C3-C7** show significantly downfield shifted acetylenic ^1H and ^{13}C NMR signals, which points towards a drastic increase in acidity and nucleophilicity on acetylenic carbons. Similar to that also the $\text{C}\equiv\text{C}$ bond lengths are considerably enlarged upon acetylene coordination and are between the bond lengths of free ethylene and free acetylene. Together with the $\text{C}\equiv\text{C}-\text{H}$ angles of **C3-C7**, which are between $141.2(9)^\circ$ and $149.3(16)^\circ$, this points towards a high metallacyclic character of the acetylene. Additionally oxidation of **C4** and **C5** to **C6** and **C7** increases the $\text{C}\equiv\text{C}$ bond length, as σ -bonding of the acetylene towards the metal center is strengthened. **C5** as well as its corresponding oxo-complex **C7** were crystallized as the *S-S-trans*

isomers, whereas **C3** was crystallized as the S-S-*cis* isomer. Therefore it might be the case that **C3** underwent isomerization to the S-S-*trans* isomer upon acetylene elimination. This finding might be crucial for further mechanistic studies as reactivity in acetylene hydration could be limited to one isomer. **C4** and **C6** were both crystallized as the S-S-*cis* isomers.

Furthermore the reactivity of **C6** and **C7** was intensively investigated. However, no reactivity was observed with sodium methanolate, piperide, water and water/NaHCO₃ as nucleophiles and with methyl iodide as electrophile. Also no reactivity of the carbonyl complexes **C4-C5** with water was observed. Degradation of **C6** and **C7** was observed with the strongly basic nucleophile methyl lithium. These findings might be attributed to the fact that **C6** and **C7** also did not react with a second equivalent of pyridine-*N*-oxide, which points towards a tungsten(VI) center with a high metallacyclic character of the strongly bound acetylene. This is also shown by the crystal structure of **C6** and **C7**, as the C≡C bond length is in the range of free ethylene and the C-C-H bond angle is significantly distorted.

To sum up, [WO(H≡H)(Me-SPym)₂] (**C6**) and [WO(H≡H)(4-Me-SPy)₂] (**C7**) show the desired stability towards oxygen and water but can both only serve as structural models for *Acetylene Hydratase*, as no reactivity in acetylene hydration experiments was observed. This can be attributed to the fact that the acetylene is too strongly coordinated in a metallacyclic manner to the tungsten center as Au-alkyne complexes, which successfully catalyze nucleophilic attacks on coordinated alkynes, only show very slight deviations of alkyne NMR shifts and bond lengths upon alkyne coordination.

5. EXPERIMENTAL SECTION

5.1 GENERAL

If not stated otherwise all manipulations were performed under an atmosphere of N₂ employing standard Schlenk and glovebox techniques. With the following exceptions, chemicals were purchased from commercial sources and were used without further purification. Acetylene 2.6 was purified by passing it through water and conc. H₂SO₄ and then dried with KOH and CaCl₂. Solvents were purified via a Pure Solv Solvent Purification system. Acidic residues were removed from silica gel by washing it with NEt₃.

All NMR spectra were measured on a Bruker Avance III 300 MHz spectrometer at 25 °C. ¹H and ¹³C NMR spectroscopy chemical shifts are given in ppm and are referenced to residual protons in the solvent. IR spectra were measured with a Bruker ALPHA-P Diamant ATR-FTIR spectrometer at a resolution of 2 cm⁻¹. Signal intensities are assigned according to their relative intensities as strong (s), medium (m) and weak (w). Most of the medium and weak intensities were omitted. All IR bands are listed in cm⁻¹ and were assigned according to literature values. Electron impact mass spectroscopy measurements have been performed using an Agilent Technologies 5975C inert XL MSD instrument equipped with a direct insertion probe. Elemental analysis were performed at the Graz University of Technology, Institute for Inorganic Chemistry using a Heraeus Vario Elementar automatic analyzer.

Electro-chemical measurements were performed under an inert atmosphere in a glovebox in dry solvents with a Gamry Instruments Reference 600 potentiostat using a three-electrode setup. Glassy carbon was used as the working electrode, platinum wire (99.99%) as the supporting electrode and silver wire immersed in a 0.01 M AgNO₃/0.1 M NBu₄(PF₆) CH₃CN solution, separated by a Vycor tip, as the reference electrode. NBu₄(PF₆) (0.1 M) was used as the supporting electrolyte.

[W₂Br₄(CO)₇] (**P1**) and 4-methylpyridine-2-on were synthesized according to previously published protocols in comparable yields.^[90,99] 4-Methylpyridine-2-thione and 4,6-dimethylpyrimidine-2-thione were synthesized according to modified literature procedures.^[100,101]

Crystal structure determination – General

All measurements were performed on a Bruker AXS SMART APEX 2 CCD diffractometer using monochromatized Mo K α radiation at 100 K. Structures were solved by direct methods (SHELXS-97) and refined by full-matrix least-squares techniques against F^2 (SHELXL-2014/6).^[126] The non-hydrogen atoms were refined with anisotropic displacement parameters without any constraints. The H atoms of the pyridine or pyrimidine rings were put at the external bisectors of the C–C–C angles at C–H distances of 0.95 Å and common isotropic displacement parameters were refined for the H atoms of the same ring. The H atoms of the methyl groups were refined with common isotropic displacement parameters for the H atoms of the same group and idealized geometries with tetrahedral angles, enabling rotation around the C–C bond, and C–H distances of 0.98 Å.

Crystal structure determination of C3-C7

The H atoms of the ethenidyl group and of the acetylene ligand were identified in a difference Fourier map, their C–H distances were fixed to 0.95 Å and refined with common isotropic displacement parameters for the H atoms of the same C1 unit without any constraints to the bond angles.

Crystal structure determination of C5

The carbonyl ligand and the ethyne ligand are disordered over two orientations and were refined with site occupation factors of 0.5 because the complex lies on a two-fold rotation axis.

Assay for the catalytic formation of acetaldehyde

The complexes **C3-C7** (0.20 mmol, 1.0 equiv.) were placed in a 100 mL Schlenk flask, dissolved in 10 mL dry CDCl₃ and water (4.30 mmol, 20.0 equiv.) was added. The mixture was stirred vigorously under a constant acetylene stream. The gas phase of the reaction mixture was passed through a solution of 2,4-dinitrophenylhydrazine (0.430 g, 2.17 mmol, 10.3 equiv.) in 2 mL conc. sulfuric acid, 3 mL water and 10 mL

n-propanol (see Figure 15). Additionally, NMR samples were taken directly from the CDCl_3 solution after 5, 10, 15, 30 and 45 min into a NMR tube equipped with a Young valve.

As a blank experiment 0.1 mL acetaldehyde were dissolved in 10 mL chloroform. The gas phase was constantly bubbled through a solution of the same mixture as in the reactivity study. A bright orange precipitate was immediately formed in the 2,4-dinitrophenylhydrazine solution, which was identified to be 1-(2,4-dinitrophenyl)-2-ethylidenehydrazone via ^1H NMR measurements.

^1H NMR (1-(2,4-dinitrophenyl)-2-ethylidenehydrazone, 300 MHz, CDCl_3 , *E* : *Z* isomer = 1 : 0.5) δ 11.18 (s, 1H, NH, *Z* isomer), 11.04 (s, 1H, NH, *E* isomer), 9.14 (dd, $J = 7.7, 2.6$ Hz, O=C-H, both isomers), 8.37 – 8.27 (m, 1H, arom. CH, both isomers), 7.96 (t, $J = 9.3$ Hz, 1H, arom. CH, both isomers), 7.57 (p, $J = 5.6$ Hz, 1H, arom. CH, *E* isomer), 7.11 (q, $J = 5.6$ Hz, 1H, arom. CH, *Z* isomer), 2.14 (d, $J = 5.4$ Hz, 3H, CH_3 , *E* isomer), 2.08 (d, $J = 5.6$ Hz, 3H, CH_3 , *Z* isomer).

When preparing the detection solution with commercially available ethanol, a bright orange precipitate was immediately formed, which was identified to be 1-(butan-2-ylidene)-2-(2,4-dinitrophenyl)hydrazone via ^1H NMR measurements.

^1H NMR (1-(butan-2-ylidene)-2-(2,4-dinitrophenyl)hydrazone, 300 MHz, CDCl_3 , *E* : *Z* isomer = 1 : 0.1) δ 11.20 (s, 1H, NH, *Z* isomer), 11.07 (s, 1H, NH, *E* isomer), 9.16 (d, $J = 2.5$ Hz, 1H, arom. CH, both isomers), 8.32 (m, 1H, arom. CH, both isomers), 7.99 (m, 1H, arom. CH, both isomers), 2.48 (q, $J = 5.7$ Hz, 2H, CH_2 , both isomers), 2.17 (s, 3H, CH_3 , *Z* isomer), 2.09 (s, 3H, CH_3 , *E* isomer), 1.32 – 1.18 (m, 3H, CH_3 , both isomers).

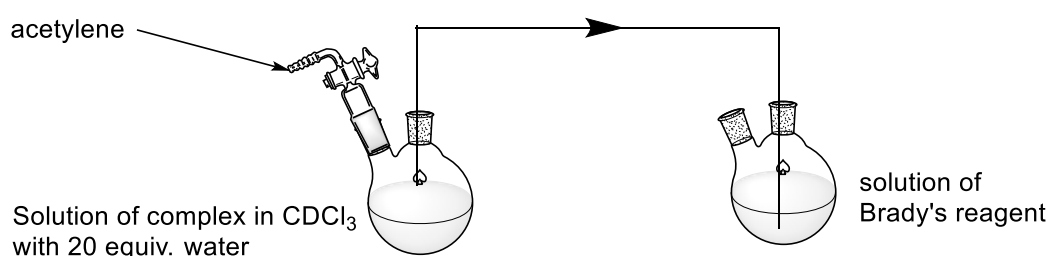


Figure 15. Setup for the catalytic formation and precipitation of acetaldehyde 2,4-dinitrophenylhydrazone.

5.2 PRECURSOR SYNTHESIS

Synthesis of $[\text{WBr}_2(\text{CO})_3(\text{NCMe})_2]$ (P2)

$[\text{W}_2\text{Br}_4(\text{CO})_7]$ (P1) (10.003 g, 11.40 mmol, 1.0 equiv.) was dissolved in 150 mL ice-cooled acetonitrile in a 250 mL Schlenk flask and cooled with an ice bath. A bubbler was placed onto the Schlenk flask and the solution was stirred for 2 h, whereby the orange-brown solution changed its color to dark yellow. The ice bath was removed and the mixture was stirred for additional 30 min. Approximately $\frac{3}{4}$ of the acetonitrile were evaporated and a red precipitate was formed. The supernatant solution was filtered off via cannula-filtration and after drying in vacuo 8.763 g (83%) of the product as a red powder were obtained.

IR ν = 2971 (w, C-H), 2918 (w, C-H), 2319 (m, $\text{N}\equiv\text{C}$), 2290 (m, $\text{N}\equiv\text{C}$), 2024 (s, $\text{C}\equiv\text{O}$), 2070 (s, $\text{C}\equiv\text{O}$), 1963 (s, $\text{C}\equiv\text{O}$).

Synthesis of a mixture of $[\text{WBr}_2(\text{CO})(\text{H}\equiv\text{H})_2(\text{NCMe})]$ with $[\text{WBr}_2(\text{CO})(\text{H}\equiv\text{H})(\text{NCMe})_2]$ (P3)

$[\text{WBr}_2(\text{CO})_3(\text{NCMe})_2]$ (P2) (1.026 g, 2.01 mmol, 1.0 equiv.) was dissolved in 60 mL dichloromethane in a 100 mL Schlenk flask. The solution was purged with acetylene for 1 h. After 30 min. a color change from dark red to grey-blue was observed. Approx. $\frac{1}{2}$ of the solvent were removed in vacuo. The product mixture was isolated via cannula-filtration as a blue-grey powder in 0.865 g (approx. 93%) yield. The ratio between $[\text{WBr}_2(\text{CO})(\text{H}\equiv\text{H})_2(\text{NCMe})]$ and $[\text{WBr}_2(\text{CO})(\text{H}\equiv\text{H})(\text{NCMe})_2]$ was estimated from ^1H NMR measurements in CD_2Cl_2 to be 1 : 0.9. Due to poor solubility the product was only partly dissolved in CD_2Cl_2 .

IR ν = 3097 (m, C-H), 3057 (m, C-H), 2969 (m, C-H), 2910 (m, C-H), 2325 (w, $\text{N}\equiv\text{C}$), 2306 (w, $\text{N}\equiv\text{C}$), 2095 (s, $\text{C}\equiv\text{O}$), 2080 (s, $\text{C}\equiv\text{O}$).

^1H NMR (300 MHz, CD_2Cl_2) δ 11.30 (s, 2H, $\equiv\text{H}$), 11.00 (s, 2H, $\equiv\text{H}$), 10.87 (s, 2H, $\equiv\text{H}$), 1.99 (s, 3H, CH_3).

5.3 LIGAND SYNTHESIS

Synthesis of 4-methylpyridine-2-thione

4-Methylpyridine-2-thione was synthesized using a modified literature procedure.^[100]

4-Methylpyridine-2-one (1.500 g, 13.75 mmol, 1.0 equiv.) and Lawesson's reagent (3.363 g, 8.25 mmol, 0.6 equiv.) were placed in a 250 mL Schlenk flask under ambient conditions. The flask was flushed with nitrogen and 80 mL of toluene were added. The suspension was stirred overnight under reflux. The next day additional 1.040 g (2.57 mmol, 0.2 equiv.) of Lawesson's reagent were added and the suspension was refluxed overnight. The suspension was extracted with 50 mL of a 1 M NaOH solution. The aqueous phase was acidified with acetic acid to pH 6-7 and was then extracted with 4x40 mL dichloromethane. The organic phases were combined and dried over MgSO₄. The solvent was removed in vacuo to give the product as a pale yellow powder in 1.437 g (84%) yield.

¹H NMR (300 MHz, CDCl₃) δ 13.59 (bs, 1H, S-H), 7.49 (s, 1H, arom. H), 7.41 (dd, *J* = 1.8, 0.9 Hz, 1H, arom. H), 6.63 (d, *J* = 6.4 Hz, 1H, arom. H), 2.26 (s, 3H, CH₃).

Synthesis of sodium 4-methylpyridine-2-thiolate (L1)

4-Methylpyridine-2-thione (2.864 g, 22.91 mmol, 1.0 equiv.) was suspended in 100 mL tetrahydrofuran in a 150 mL Schlenk tube. Sodium hydride (60% in mineral oil, 0.551 g, 22.90 mmol, 1.0 equiv.) was added spatula wise. A bubbler was placed on the Schlenk tube and the suspension was stirred at rt. After 1 h approx. 50 mL tetrahydrofuran were removed in vacuo and 20 mL heptane were added to precipitate the product. The precipitate was isolated via cannula-filtration. A second fraction precipitated in the filtrate and was also obtained via cannula-filtration. Both fractions were washed with 3x5 mL diethyl ether and were dried in vacuo. The fractions of colorless powder were combined to give 2.084 g (62%).

¹H NMR (300 MHz, DMSO-d₆) δ 7.66 (d, *J* = 5.1 Hz, 1H, arom. H), 6.79 (s, 1H, arom. H), 6.17 (d, *J* = 5.1 Hz, 1H, arom. H), 1.96 (s, 3H, CH₃).

Synthesis of 4,6-dimethylpyrimidine-2-thione

4,6-Dimethylpyrimidine-2-thione was synthesized using a slightly modified literature procedure.^[101]

Thiourea (7.674 g, 100.6 mmol, 1.0 equiv.) and acetylacetone (10.2 mL, 104.0 mmol, 1.0 equiv) were placed in a 250 mL round bottom flask and 60 mL ethanol were added. The suspension was heated to 80 °C. Conc. hydrochloric acid (16.8 mL) was added dropwise within 5 min with a syringe. After 2.5 h of stirring at 80 °C the product precipitated as yellow needles. The flask was cooled to rt and 70 mL of a saturated NaHCO₃ solution were added. The pH was adjusted to 7-8 by adding solid NaHCO₃. The solution was extracted with 8-50 mL dichloromethane. The organic layers were combined and dried over MgSO₄. The solvent was removed on a rotary evaporator to obtain 11.529 g (82%) of 4,6-dimethylpyridine-2-thione as a yellow powder.

¹H NMR (300 MHz, CDCl₃) δ 13.33 (bs, 1H, S-H), 6.48 (s, 1H, arom. H), 2.43 (s, 6H, CH₃).

Synthesis of sodium 4,6-dimethylpyrimidine-2-thiolate (L2)

4,6-Dimethylpyrimidine-2-thione (14.682 g, 104.7 mmol, 1.0 equiv) was placed in a 150 mL Schlenk tube. Tetrahydrofuran (100 mL) was added and the suspension was cooled with an ice bath. Sodium hydride (60% in mineral oil, 4.221 g, 104.7 mmol, 1.0 equiv.) was added spatula wise. A bubbler was placed onto the Schlenk tube and the suspension was stirred overnight at rt. Approx. half of the solvent was removed in vacuo and the product was precipitated with approx. 50 mL heptane. The precipitate was isolated via cannula-filtration and washed with 5-10 mL of diethyl ether, with 4-10 mL tetrahydrofuran and with 10-10 mL acetonitrile using an ultrasonic bath. 4,6-Dimethylpyrimidine-2-thiolate (12.711 g, 75%) was obtained as an off-white product.

¹H NMR (300 MHz, D₆C1SO) δ 6.20 (s, 1H, arom. H), 2.04 (s, 6H, CH₃).

Synthesis of 1,2-bis(4,6-dimethylpyrimidine-2-yl)disulfide as a reference material

4,6-Dimethylpyrimidine-2-thione (0.106 g, 0.75 mmol, 1.0 equiv.) was suspended in 10 mL water in a 25 mL Erlenmeyer flask. After the addition of hydrogen peroxide (30 % in water, 0.6 mL, 4.76 mmol, 6.3 equiv.) the solution was stirred for 5 min. The mixture was extracted with 5 mL dichloromethane and the organic phase was dried over MgSO₄. The solvent was removed in vacuo to obtain the product (0.063 g, 61%) as a colorless powder.

¹H NMR (300 MHz, CDCl₃) δ 6.76 (s, 2H, arom. H), 2.39 (s, 12H, CH₃).

Synthesis of 1,2-bis(4-methylpyridine-2-yl)disulfide as a reference material

4-Methylpyridine-2-thione (0.101 g, 0.81 mmol, 1.0 equiv.) was suspended in 10 mL water in a 25 mL Erlenmeyer flask. After the addition of hydrogen peroxide (30 % in water, 0.6 mL, 4.76 mmol, 5.9 equiv.) the solution was stirred for 5 min. The mixture was extracted with 5 mL dichloromethane and the organic phase was dried over MgSO₄. The solvent was removed in vacuo to obtain 0.068 g (67%) of product as a colorless powder.

¹H NMR (300 MHz, CDCl₃) δ 8.32 (d, *J* = 5.0 Hz, 2H, arom. H), 7.47 – 7.44 (m, 2H, arom. H), 6.92 (dd, *J* = 5.0, 0.7 Hz, 2H, arom. H), 2.30 (s, 6H, CH₃).

5.4 COMPLEX SYNTHESIS

Synthesis of [W(CO)₃(4-Me-SPy)₂] (C1)

[WBr₂(CO)₃(NCMe)₂] (**P2**) (0.209 g, 0.39 mmol, 1.0 equiv.) and sodium 4-methylpyridine-2-thiolate (**L1**) (0.133 g, 0.87 mmol, 2.2 equiv.) were placed into a 50 mL Schlenk flask and suspended in 20 mL dichloromethane. A bubbler was placed onto the flask and the suspension was stirred for 1 h, whereby the color changed from brownish to orange. Solids were removed via cannula-filtration. A brown impurity was precipitated by overlaying with 30 mL of heptane. The impurity was filtered off over a plug of Celite. Approx. 5 mL of solvent were removed and the orange solution was

again put into the -20 °C fridge. After 3 days orange-red crystals (0.098 g, 49%) were isolated by cannula-filtration.

^1H NMR (300 MHz, CD_2Cl_2) δ = 8.27 (d, J = 5.7, 2H, arom. H), 6.72 (m, 2H, arom. H), 6.66 (m, 2H, arom. H), 2.21 (s, 6H, CH_3).

^{13}C NMR (75 MHz, CD_2Cl_2) δ = 235.74 (s, CO), 176.46 (s, C-S), 150.69 (s, C- CH_3), 145.03 (s, CH), 128.29 (s, CH), 120.81 (s, CH), 21.66 (s, CH_3).

IR ν = 2922 (w, C-H), 2011 (s, $\text{C}\equiv\text{O}$), 1881 (s, $\text{C}\equiv\text{O}$), 1649 (w, $\text{C}\equiv\text{C}$).

Anal. Calcd for $\text{C}_{25}\text{H}_{12}\text{N}_2\text{O}_3\text{S}_2\text{W}$: C, 34.90; H, 2.34; N, 5.43; S, 12.42. Found: C, 35.22; H, 2.43; N, 5.50; S, 12.07.

Synthesis of $[\text{W}(\text{CO})_3(\text{Me-SPym})_2]$ (**C2**)

$[\text{W}_2\text{Br}_4(\text{CO})_7]$ (**P1**) (1.535 g, 1.70 mmol, 1.0 equiv.) and 4,6-dimethylpyrimidine-2-thiolate (**L2**) (1.161 g, 7.13 mmol, 4.2 equiv.) were placed in a 150 mL Schlenk tube and approx. 100 mL dichloromethane were added. A bubbler was placed onto the tube and the suspension was stirred for 45 min until CO evolution stopped. The suspension was filter-cannulated and the residue was washed with 10 mL dichloromethane using an ultrasonic bath. The filtrate was concentrated to approx. 20 mL and approx. 40 mL heptane were added. Further solvent was carefully evaporated in vacuo to obtain the product as an orange precipitate. The precipitate was isolated via cannula-filtration and was washed with 5 mL heptane to get 1.328 g (72%) of the product as an orange powder.

^1H NMR (300 MHz, CDCl_3) δ 6.65 (s, 2H, arom. H), 2.61 (s, 6H, CH_3), 2.37 (s, 6H, CH_3).

IR ν = 2955 (w, C-H), 2922 (w, C-H), 2852 (w, C-H), 2014 (m, CO), 1903 (s, CO), 1822 (m, CO).

Synthesis of [W(CO)(H≡H)(=4-Me-SPy)(4-Me-SPy)] (C3)

[W(CO)₃(4-MeSPy)₂] (**C1**) (0.532 g, 1.01 mmol, 1.0 equiv.) was placed in a 100 mL Schlenk flask and dissolved in 50 mL toluene. The suspension was purged with acetylene for 1.4 hours and stirred overnight. The next day the toluene was removed completely and the residue was dissolved in 20 mL dichloromethane. The solution was filtered through a 4 cm plug of silica gel in a Schlenk frit. The silica gel plug was washed with dichloromethane until the intense red-violet color of the filtrate vanished. The filtrate was concentrated to approx. 15 mL in vacuo and was overlaid with 30 mL heptane. Approximately half of the solvent was evaporated slowly to obtain a red-violet precipitate. The precipitate was isolated via cannula-filtration and washed with 5 mL heptane. The obtained product was dried in vacuo to give 0.326 g (63%) of [W(CO)(H≡H)(=4-Me-Spy)(4-MeSPy)] (**C3**) as a maroon powder. Single crystals suitable for diffraction analysis were obtained from a saturated solution in dichloromethane carefully overlaid with heptane (dichloromethane : heptane = 1 : 1).

¹H NMR (300 MHz, CD₂Cl₂) δ 12.91 (s, 1H, ≡-H), 11.99 (s, 1H, ≡-H), 8.08 (d, J = 5.6 Hz, 1H, arom. H), 7.73 – 7.56 (m, 3H, 2 arom. H + insert. CH), 6.77 – 6.70 (m, 2H, arom. H), 6.66 (m, 1H, arom. H), 6.50 (d, J = 10.9 Hz, 1H, insert. CH), 2.28 (s, 3H, CH₃), 2.25 (s, 3H, CH₃).

¹³C NMR (75 MHz, CD₂Cl₂) δ 232.62 (s, CO), 198.43 (s, ≡), 193.07 (s, ≡), 179.06 (s, C-S), 166.68 (s, insert. CH), 160.16 (s, C-S), 148.68 (s, C-CH₃), 147.56 (s, arom. CH), 145.27 (s, C-CH₃), 139.67 (s, insert. CH), 133.30 (s, arom. CH), 132.16 (s, arom. CH), 128.07 (s, arom. CH), 119.96 (s, arom. CH), 119.35 (s, arom. CH), 21.64 (s, CH₃), 20.83 (s, CH₃).

IR ν = 3046 (w, C-H), 1907 (s, C=O), 1632 (w, C≡C).

Anal. Calcd for C₂₇H₁₆N₂OS₂W · 0.1 CH₂Cl₂: C, 39.44; H, 3.14; N, 5.38; S, 12.31. Found: C, 39.37; H, 3.12; N, 5.29; S, 12.05.

EI-MS: m/z 432 [M⁺ - CO - 2 H≡H].

Synthesis of [W(CO)(H≡H)(Me-SPym)₂] (C4)

[W(CO)₃(Me-SPym)₂] (C2) (0.402 g, 0.74 mmol, 1.0 equiv.) were placed in a 100 mL Schlenk flask and dissolved in 60 mL dichloromethane. The flask was purged with acetylene under vigorous stirring for 45 min. The dark red suspension was filtered through an approx. 5 cm plug of silica gel in a Schlenk frit and eluted using 60 mL of acetonitrile. The dark red solution was concentrated to approx. 20 mL and carefully overlaid with 25 mL heptane. The next day the violet needle-shaped crystals were isolated and washed with 5 mL of pentane to obtain [W(CO)(H≡H)(Me-SPym)₂] (C4) in 84% (0.319 g) yield.

¹H NMR (300 MHz, CD₂Cl₂) δ 13.79 (s, 1H, ≡-H), 12.47 (s, 1H, ≡-H), 6.88 (s, 1H, arom. CH), 6.56 (s, 1H, arom. H), 2.44 (s, 3H, CH₃), 2.36 (s, 3H, CH₃), 1.93 (s, 3H, CH₃), 1.21 (s, 3H, CH₃).

¹³C NMR (75 MHz, CD₂Cl₂) δ 234.26 (s, CO), 206.03 (s, ≡), 203.72 (s, ≡), 184.90 (s, C-S), 176.27 (s, C-S), 170.17 (s, C-CH₃), 167.73 (s, C-CH₃), 165.58 (s, C-CH₃), 162.27 (s, C-CH₃), 117.68 (s, arom. CH), 116.30 (s, arom. CH), 26.01 (s, CH₃), 24.77 (s, CH₃), 24.07 (s, CH₃), 22.09 (s, CH₃).

IR ν = 3057 (w, C-H), 3015 (w, C-H), 1916 (s, C≡O), 1575 (C≡C).

EI-MS: *m/z* 488.03 [M⁺ - CO].

Anal. Calcd for C₂₅H₁₆N₄OS₂W: C, 34.90; H, 3.12; N, 10.85; S, 12.42. Found: C, 34.85; H, 3.04; N, 10.94; S, 12.25.

Synthesis of [W(CO)(H≡H)(4-Me-SPy)₂] (C5)

[WBr₂(CO)(H≡H)₂(NCMe)] (P3) (0.504 g) and sodium 4-methylpyridine-2-thiolate (0.350 g, 2.37 mmol) were placed in a 100 mL Schlenk flask, suspended in approx. 100 mL dichloromethane and nitrogen was immediately bubbled through the solution with a gas frit. Evaporated dichloromethane was continuously compensated. After 2 h the gas frit was removed and a spatula of silica gel was added. An olive-green solution was obtained via cannula-filtration. The solution was overlaid with 40 mL of heptane and the solvent was carefully removed under vacuo until a green powder precipitated. The powder was isolated via cannula-filtration and again dissolved in 20 mL dichloromethane. The solution was overlaid with 20 mL heptane. The brownish

residue, which precipitated overnight, was separated via cannula-filtration. The filtrate was placed in a -20 °C fridge overnight. The formed green needles were isolated from the solution via cannula-filtration to obtain the product in 19% (0.100 g) yield. Single crystals suitable for diffraction measurements were obtained from a saturated acetonitrile solution at -35 °C.

¹H NMR (300 MHz, CD₂Cl₂, major : minor isomer = 1 : 0.5) δ 13.62 (s, 2H, ≡-H, major and minor isomer), 12.31 (s, 2H, ≡-H, major and minor isomer), 8.72 (d, *J* = 5.4 Hz, 1H, arom. H, major isomer), 8.45 (d, *J* = 5.8 Hz, 1H, arom. H, major isomer), 7.80 (d, *J* = 5.4 Hz, 1H, arom. H, minor isomer), 6.93 (m, 0.9 Hz, 2H, arom. H, major and minor isomer), 6.81 – 6.77 (m, 2H, arom. H, 2 minor isomer), 6.73 – 6.70 (m, 1H, arom. H, major isomer), 6.65 (dd, *J* = 5.8, 1.1 Hz, 1H, arom. H, major isomer), 6.57 – 6.53 (m, 2H, arom. H, major and minor isomer), 6.42 (dd, *J* = 5.9, 1.2 Hz, 1H, arom. H, major and minor isomer), 2.34 (s, 2H, CH₃, minor isomer), 2.29 (s, 3H, CH₃, major isomer), 2.20 (s, 2H, CH₃, minor isomer), 2.18 (s, 3H, CH₃, major isomer).

¹³C NMR (75 MHz, CD₂Cl₂) δ 241.39 (s, CO, major isomer), 239.71 (s, CO, minor isomer), 177.91 (s, ≡, minor isomer), 177.88 (s, ≡, major isomer), 170.96 (s, ≡, major isomer), 170.07 (s, ≡, minor isomer), 151.82 (s, C-S, major and minor isomer), 151.31 (s, C-S, major and minor isomer), 149.48 (s, C-CH₃, major and minor isomer), 148.01 (s, C-CH₃, major and minor isomer), 146.36 (s, arom. CH, major isomer), 145.56 (s, arom. CH, major isomer), 145.36 (s, arom. CH, minor isomer), 145.17 (s, arom. CH, minor isomer), 127.98 (s, arom. CH, minor isomer), 127.78 (s, arom. CH, minor isomer), 127.31 (s, arom. CH, major isomer), 126.88 (s, arom. CH, major isomer), 121.87 (s, arom. CH, minor isomer), 121.83 (s, arom. CH, major isomer), 119.43 (s, arom. CH, major and minor isomer), 22.02 (s, CH₃, minor isomer), 21.97 (s, CH₃, major isomer), 21.47 (s, CH₃, major isomer), 21.19 (s, CH₃, minor isomer).

IR ν = 2936 (w, C-H), 2677 (w, C-H), 1907 (s, C≡O), 1596 (w, C≡C).

Synthesis of [WO(H≡H)(Me-SPym)₂] (C6)

[W(CO)(H≡H)(Me-SPym)₂] (C5) (1.817 g, 3.52 mmol, 1.0 equiv.) and pyridine-*N*-oxide (0.351 g, 3.70 mmol, 1.1 equiv.) of were placed in a 100 mL Schlenk flask and were suspended in 60 mL acetonitrile. The mixture was stirred with a bubbler overnight, whereby the color of the suspension changed from dark violet to bright yellow. The reaction mixture was evaporated until dryness. The product was washed with 5·5 mL diethyl ether using an ultrasonic bath to obtain the product as a bright yellow powder in 1.198 g (68%) yield. Single crystals suitable for X-ray diffraction analysis were obtained from a solution in ethyl acetate overlaid with heptane (ethyl acetate : heptane = 1 : 1).

¹H NMR (300 MHz, CD₂Cl₂, major : minor isomer = 1 : 0.1) δ 11.25 (s, 1H, ≡-H, major isomer), 11.03 (s, 1H, ≡-H, minor isomer), 10.95 (s, 1H, ≡-H, major isomer), 10.70 (s, 1H, ≡-H, minor isomer), 6.98 (s, 1H, arom. H, major isomer), 6.90 (s, 2H, arom. H, major and minor isomer), 6.35 (s, 1H, arom. H, minor isomer), 3.03 (s, 3H, CH₃, minor isomer), 2.56 (s, 3H, CH₃, major isomer), 2.47 (s, 6H, CH₃, major and minor isomer), 2.44 (s, 6H, CH₃, major and minor isomer), 2.05 (s, 6H, CH₃, major and minor isomer).

¹³C NMR (75 MHz, CD₂Cl₂) δ 181.41 (s, C-S, major and minor isomer), 179.05 (s, C-S, major and minor isomer), 170.90 (s, C-CH₃, major and minor isomer), 170.06 (s, C-CH₃, major and minor isomer), 165.97 (s, C-CH₃, major and minor isomer), 163.00 (s, C-CH₃, major and minor isomer), 158.15 (s, ≡, major and minor isomer), 157.02 (s, ≡, major and minor isomer), 119.26 (s, arom. CH, minor isomer), 118.56 (s, arom. CH, major isomer), 116.83 (s, arom. CH, major isomer), 115.52 (s, arom. CH, minor isomer), 46.50 (s, CH₃, minor isomer), 24.89 (s, CH₃, major isomer), 24.75 (s, CH₃, major and minor isomer), 24.73 (s, CH₃, major and minor isomer), 21.20 (s, CH₃, major and minor isomer).

IR ν = 3057 (w, C-H), 3015 (w, C-H), 1916 (s, CO), 1575 (w, C≡C), 933 (s, W=O).

Synthesis of [WO(H≡H)(4-Me-SPy)₂] (C7)

[W(CO)(H≡H)(4-MeSPy)₂] (C5) (0.500 g, 1.03 mmol, 1.0 equiv.) and pyridine-*N*-oxide (0.108 g, 1.13 mmol, 1.1 equiv.) were placed in a 100 mL Schlenk flask and suspended in 20 mL acetonitrile. A bubbler was placed onto the Schlenk flask. The suspension was stirred overnight whereafter the color changed from violet-red to dark ochreous. The acetonitrile was evaporated completely in vacuo and the residue was washed with 5·5 mL diethyl ether to obtain the product as a light brown powder in 68% (0.333 g) yield. Single crystals suitable for X-ray diffraction analysis were obtained from a saturated solution in ethyl acetate carefully overlaid with heptane (ethyl acetate : heptane = 1 : 1) at -35 °C.

¹H NMR (300 MHz, CD₂Cl₂, major : minor isomer = 1 : 0.1) δ 11.06 (s, 1H, ≡-H, minor isomer), 11.03 (s, 1H, ≡-H, minor isomer), 10.95 (s, 1H, ≡-H, major isomer), 10.94 (s, 1H, ≡-H, major isomer), 9.02 (d, *J* = 5.4 Hz, 1H, arom. H, major isomer), 8.64 (d, *J* = 6.0 Hz, 1H, arom. H, minor isomer), 7.54 (d, *J* = 5.5 Hz, 1H, arom. H, minor isomer), 7.35 (d, *J* = 5.6 Hz, 1H, arom. H, major isomer), 7.02 (s, 1H, arom. H, minor isomer), 6.98 (s, 1H, arom. H, minor isomer), 6.94 (m, 4H, arom. H, 2 major and 2 minor isomer), 6.85 – 6.79 (m, 1H, arom. H, major isomer), 6.34 (dd, *J* = 5.7, 0.9 Hz, 1H, arom. H, major isomer), 2.35 (s, 6H, CH₃, 2 minor isomer), 2.30 (s, 3H, CH₃, major isomer), 2.09 (s, 3H, CH₃, major isomer).

¹³C NMR (75 MHz, CD₂Cl₂) δ 176.98 (s, C-S, major and minor isomer), 168.26 (s, C-S, major and minor isomer), 158.08 (s, ≡, major and minor isomer), 154.65 (s, ≡, major and minor isomer), 153.80 (s, C-CH₃, major isomer), 150.55 (s, C-CH₃, minor isomer), 149.67 (s, C-CH₃, major and minor isomer), 143.21 (s, arom. CH, major and minor isomer), 142.77 (s, arom. CH, major isomer), 142.33 (s, arom. CH, minor isomer), 130.07 (s, arom. CH, minor isomer), 128.27 (s, arom. CH, minor isomer), 127.99 (s, arom. CH, major isomer), 127.58 (s, arom. CH, major isomer), 122.28 (s, arom. CH, minor isomer), 121.84 (s, arom. CH, major isomer), 120.06 (s, arom. CH, minor isomer), 119.31 (s, arom. CH, major isomer), 22.13 (s, CH₃, major and minor isomer), 21.49 (s, CH₃, major and minor isomer).

IR ν = 3085 (w, C-H), 3048 (w, C-H), 1598 (w, C≡C), 945 (s, W=O).

6. REFERENCES

- [1] M. Eckert, G. Fleischmann, R. Jira, H. M. Bolt, K. Golka (Eds.) *"Acetaldehyde" in Ullmann's Encyclopedia of Industrial Chemistry*, Wiley-VCH Verlag GmbH, Weinheim, **2007**.
- [2] Y. Ogata, A. Kawasaki, N. Okumura, *J. Am. Chem. Soc.* **1965**, *30*, 1636.
- [3] R. Longley, W. S. Emerson, A. Blardinelli, *Org. Synth.* **1954**, *34*, 29.
- [4] S. F. Marrian, *Chem. Rev.* **1948**, *43*, 149.
- [5] A. W. Budiman, J. S. Nam, J. H. Park, R. I. Mukti, T. S. Chang, J. W. Bae, M. J. Choi, *Catal. Surv. Asia* **2016**, *20*, 173.
- [6] a) J. Smidt, W. Hafner, R. Jira, J. Sedlmeier, R. Sieber, R. Rüttinger, H. Kojer, *Angew. Chem.* **1959**, *71*, 176; b) R. Jira, *Angew. Chem. Int. Ed.* **2009**, *48*, 9034; c) J. Smidt, W. Hafner, R. Jira, R. Sieber, J. Sedlmeier, A. Sabel, *Angew. Chem. Int. Ed.* **1962**, *1*, 80.
- [7] D. Chadwick, J. Goode (Eds.) *Novartis Foundation symposium, Vol. 285*, John Wiley, Chichester, England, Hoboken, NJ, **2010**.
- [8] D. W. Crabb, S. Liangpunsakul in *Novartis Foundation symposium, Vol. 285* (Eds.: D. Chadwick, J. Goode), John Wiley, Chichester, England, Hoboken, NJ, **2010**, pp. 4–22.
- [9] B. M. Rosner, B. Schink, *J. Bacteriol.* **1995**, *177*, 5767.
- [10] B. K. Burgess, D. J. Lowe, *Chem. Rev.* **1996**, *96*, 2983.
- [11] B. Schink, *Arch. Microbiol.* **1985**, *142*, 295.
- [12] L. E. Bevers, P.-L. Hagedoorn, W. R. Hagen, *Coord. Chem. Rev.* **2009**, *253*, 269.
- [13] A. F. Holleman, E. Wiberg, N. Wiberg, *Lehrbuch der anorganischen Chemie*, de Gruyter, Berlin, **2007**.
- [14] A. Kletzin, *FEMS Microbiol. Rev.* **1996**, *18*, 5.
- [15] a) R. R. Schrock, A. H. Hoveyda, *Angew. Chem. Int. Ed.* **2003**, *42*, 4592; b) A. Szymańska, W. Nitek, M. Oszejca, W. Łasocha, K. Pamin, J. Połtowicz, *Catal. Lett.* **2016**, *146*, 998; c) J. K. Lam, C. Zhu, K. V. Bukhryakov, P. Müller, A. Hoveyda, R. R. Schrock, *J. Am. Chem. Soc.* **2016**, *138*, 15774.
- [16] M. K. Johnson, D. C. Rees, M. W. W. Adams, *Chem. Rev.* **1996**, *96*, 2817.
- [17] R. H. Holm, E. I. Solomon, A. Majumdar, A. Tenderholt, *Coord. Chem. Rev.* **2011**, *255*, 993.
- [18] R. Hille, *Trends Biochem. Sci.* **2002**, *27*, 360.
- [19] P. M. H. Kroneck, *J. Biol. Inorg. Chem.* **2016**, *21*, 29.
- [20] O. Einsle, H. Niessen, D. J. Abt, G. Seiffert, B. Schink, R. Huber, A. Messerschmidt, P. M. H. Kroneck, *Acta crystallogr. F* **2005**, *61*, 299.
- [21] G. Seiffert, M. G. Ullmann, A. Messerschmidt, B. Schink, P. M. H. Kroneck, O. Einsle, *Proc. Natl. Acad. Sci. USA* **2007**, *107*, 3073.
- [22] R.-Z. Liao, J.-G. Yu, F. Himo, *Proc. Natl. Acad. Sci. USA* **2010**, *107*, 22523.
- [23] S. Antony, C. A. Bayse, *Organometallics* **2009**, *28*, 4938.
- [24] M. A. Vincent, I. H. Hillier, G. Periyasamy, N. A. Burton, *Dalton Trans.* **2010**, *39*, 3816.
- [25] R.-Z. Liao, F. Himo, *ACS Catal.* **2011**, *1*, 937.
- [26] R.-Z. Liao, W. Thiel, *J. Chem. Theory Comput.* **2012**, *8*, 3793.
- [27] R.-Z. Liao, W. Thiel, *J. Comput. Chem.* **2013**, *34*, 2389.
- [28] R.-Z. Liao, W. Thiel, *J. Phys. Chem. B* **2013**, *117*, 3954.
- [29] A. Fürstner, *Angew. Chem. Int. Ed.* **2018**, 4215-4233.

- [30] M. Beller, J. Seayad, A. Tillack, H. Jiao, *Angew. Chem. Int. Ed.* **2004**, *43*, 3368.
- [31] a) S. Cacchi, *J. Organomet. Chem.* **1999**, *576*, 42; b) I. Nakamura, Y. Yamamoto, *Chem. Rev.* **2004**, *104*, 2127.
- [32] F. Alonso, I. P. Beletskaya, M. Yus, *Chem. Rev.* **2004**, *104*, 3079.
- [33] a) J. Li, M. John, L. Ackermann, *Chem. Eur. J.* **2014**, *20*, 5403; b) B. M. Trost, Y. H. Rhee, *J. Am. Chem. Soc.* **2003**, *125*, 7482; c) B. M. Trost, Y. H. Rhee, *J. Am. Chem. Soc.* **2002**, *124*, 2528; d) B. M. Trost, M. T. Rudd, M. G. Costa, P. I. Lee, A. E. Pomerantz, *Org. Lett.* **2004**, *6*, 4235.
- [34] F. E. McDonald, *Chem. Eur. J.* **1999**, *5*, 3103.
- [35] S. Elgafi, L. D. Field, B. A. Messerle, *J. Organomet. Chem.* **2000**, *607*, 97.
- [36] a) B. Gabriele, G. Salerno, A. Fazio, R. Pittelli, *Tetrahedron* **2003**, *59*, 6251; b) I. Kadota, L. M. Lutete, A. Shibuya, Y. Yamamoto, *Tetrahedron Lett.* **2001**, *42*, 6207.
- [37] B. Liu, J. K. de Brabander, *Org. Lett.* **2006**, *8*, 4907.
- [38] A. S. K. Hashmi, *Acc. Chem. Res.* **2014**, *47*, 864.
- [39] S. Samala, A. K. Mandadapu, M. Saifuddin, B. Kundu, *J. Org. Chem.* **2013**, *78*, 6769.
- [40] S. Antoniotti, E. Genin, V. Michelet, J.-P. Genêt, *J. Am. Chem. Soc.* **2005**, *127*, 9976.
- [41] A. S. K. Hashmi, S. Schäfer, M. Wölfle, C. Diez Gil, P. Fischer, A. Laguna, M. C. Blanco, M. C. Gimeno, *Angew. Chem. Int. Ed.* **2007**, *46*, 6184.
- [42] F. E. McDonald, K.S. Reddy, *J. Organomet. Chem.* **2001**, *617-618*, 444.
- [43] P. Wipf, T. H. Graham, *J. Org. Chem.* **2003**, *68*, 8798.
- [44] X. Meng, S. Kim, *Synlett* **2012**, *23*, 1960.
- [45] J. W. Hartman, L. Sperry, *Tetrahedron Lett.* **2004**, *45*, 3787.
- [46] H. Kucükbay, B. Cetinkaya, S. Guesmi, P. H. Dixneuf, *Organometallics* **1996**, *15*, 2434.
- [47] a) E. Genin, S. Antoniotti, V. Michelet, J.-P. Genêt, *Angew. Chem. Int. Ed.* **2005**, *44*, 4949; b) X. Li, A. R. Chianese, T. Vogel, R. H. Crabtree, *Org. Lett.* **2005**, *7*, 5437.
- [48] H. Nakagawa, Y. Okimoto, S. Sakaguchi, Y. Ishii, *Tetrahedron Lett.* **2003**, *44*, 103.
- [49] Y. Kataoka, O. Matsumoto, K. Tani, *Organometallics* **1996**, *15*, 5246.
- [50] Y. Fukuda, K. Utimoto, *J. Org. Chem.* **1991**, *56*, 3729.
- [51] a) D. N. Tran, N. Cramer, *Angew. Chem. Int. Ed.* **2011**, *50*, 11098; b) R. Zeng, G. Dong, *J. Am. Chem. Soc.* **2015**, *137*, 1408.
- [52] D. Masui, T. Kochi, Z. Tang, Y. Ishii, Y. Mizobe, M. Hidai, *J. Organomet. Chem.* **2001**, *620*, 69.
- [53] F. E. McDonald, C. C. Schultz, *J. Am. Chem. Soc.* **1994**, *116*, 9363.
- [54] T. Sordo, P. Campomanes, A. Diéguez, F. Rodríguez, F. J. Fañanás, *J. Am. Chem. Soc.* **2005**, *127*, 944.
- [55] J. Chatt, L. A. Duncanson, *J. Chem. Soc.* **1953**, 2939.
- [56] a) A. Dedieu, *Chem. Rev.* **2000**, *100*, 543; b) R. H. Crabtree, *The Organometallic Chemistry of the Transition Metals*, John Wiley & Sons, Inc, Hoboken, NJ, USA, **2005**.
- [57] J. L. Templeton, B. C. Ward, I. G. J.-J. Chen, J. W. McDonald, W. E. Newton, *Inorg. Chem.* **1981**, 1248.
- [58] J. L. Templeton, P. B. Winston, B. C. Ward, *J. Am. Chem. Soc.* **1981**, *103*, 7713.

- [59] H. Nuss, N. Claiser, S. Pillet, N. Lugan, E. Despagnet-Ayoub, M. Etienne, C. Lecomte, *Dalton Trans.* **2012**, 41, 6598.
- [60] C. Elschenbroich, *Organometallchemie*, Teubner, Wiesbaden, **2005**.
- [61] J. L. Templeton in *Advances in Organometallic Chemistry*, v.29 (Eds.: F. G. A. Stone, R. West), Elsevier textbooks, s.l., **1989**, pp. 1–100.
- [62] B. Fang, W. Ren, G. Hou, G. Zi, D.-C. Fang, L. Maron, M. D. Walter, *J. Am. Chem. Soc.* **2014**, 136, 17249.
- [63] V. Bachler, *J. Comput. Chem.* **2012**, 33, 1936.
- [64] G. Frenking, N. Fröhlich, *Chem. Rev.* **2000**, 100, 717.
- [65] a) C. C. Romão, W. A. Blättler, J. D. Seixas, G. J. L. Bernardes, *Chem. Soc. Rev.* **2012**, 41, 3571; b) E. R. Davidson, K. L. Kunze, F. B. C. Machado, S. J. Chakravorty, *Acc. Chem. Res.* **2002**, 26, 628.
- [66] L. Ricard, R. Weiss, W. E. Newton, G. J.-J. Chen, J. W. McDonald, *J. Am. Chem. Soc.* **1978**, 100, 1318.
- [67] L. M. Peschel, F. Belaj, N. C. Mösch-Zanetti, *Angew. Chem. Int. Ed.* **2015**, 54, 13018.
- [68] H. G. Alt, *J. Organomet. Chem.* **1977**, 127, 349.
- [69] H. G. Alt, J. Su Han, H. E. Maisel, *J. Organomet. Chem.* **1991**, 409, 197.
- [70] H. G. Alt, *J. Organomet. Chem.* **1983**, 256, C12-C14.
- [71] H. G. Alt, *J. Organomet. Chem.* **1985**, 288, 149.
- [72] H. G. Alt, H. E. Engelhardt, U. Thewalt, J. Riede, *J. Organomet. Chem.* **1985**, 288, 165.
- [73] H. G. Alt, J. S. Han, R. D. Rogers, U. Thewalt, *J. Organomet. Chem.* **1993**, 459, 209.
- [74] H. G. Alt, H. I. Hayen, *J. Organomet. Chem.* **1986**, 316, 105.
- [75] M. B. Wells, P. S. White, J. L. Templeton, *Organometallics* **1997**, 16, 1857.
- [76] R. J. Beattie, P. S. White, J. L. Templeton, *Organometallics* **2016**, 35, 32.
- [77] T. W. Crane, P. S. White, J. L. Templeton, *Organometallics* **1999**, 18, 1897.
- [78] T. W. Crane, P. S. White, J. L. Templeton, *Inorg. Chem.* **2000**, 39, 1081.
- [79] D. S. Frohnafel, S. Reinartz, P. S. White, J. L. Templeton, *Organometallics* **1998**, 17, 3759.
- [80] C. Khosla, A. B. Jackson, P. S. White, J. L. Templeton, *Organometallics* **2012**, 31, 987.
- [81] B. C. Ward, J. L. Templeton, *J. Am. Chem. Soc.* **1980**, 102, 1532.
- [82] P. Umland, H. Vahrenkamp, *Chem. Ber.* **1982**, 115, 3565.
- [83] J. R. Morrow, T. L. Tonker, J. L. Templeton, W. R. Kenan, *J. Am. Chem. Soc.* **1985**, 107, 6956.
- [84] J. Yadav, S. K. Das, S. Sarkar, *J. Am. Chem. Soc.* **1997**, 119, 4315.
- [85] S. K. Das, D. Biswas, R. Maiti, S. Sarkar, *J. Am. Chem. Soc.* **1996**, 118, 1387.
- [86] H. Sugimoto, H. Tsukube, *Chem. Soc. Rev.* **2008**, 37, 2609.
- [87] M. Schreyer, L. Hintermann, *Beilstein J. Org. Chem.* **2017**, 13, 2332.
- [88] M. Kersting, A. El-Kholi, U. Müller, K. Dehnicke, *Chem. Ber.* **1989**, 122, 279.
- [89] D. S. Williams, M. H. Schofield, R. R. Schrock, *Organometallics* **1993**, 12, 4560.
- [90] L. M. Peschel, J. A. Schachner, C. H. Sala, F. Belaj, N. C. Mösch-Zanetti, *Z. Anorg. Allg. Chem.* **2013**, 639, 1559.
- [91] P. K. Baker, M. B. Hursthouse, A. I. Karaulov, A. J. Lavery, K. M. A. Malik, D. J. Muldoon, A. Shawcross, *Dalton Trans.* **1994**, 3, 3493.
- [92] *Unpublished results of the Mösch-Zanetti group.*
- [93] P. K. Baker, S. G. Fraser, E. M. Keys, *J. Organomet. Chem.* **1986**, 309, 319.

- [94] G.J.-J. Chen, R. O. Yelton, J. W. McDonald, *Inorg. Chim. Acta* **1977**, *22*, 249.
- [95] P. K. Baker, D. J. Muldoon, *Polyhedron* **1994**, *20*, 2915.
- [96] J. L. Davidson, G. Vasapollo, *Dalton Trans.* **1985**, 2231.
- [97] S. Thomas, E. R. T. Tiekink, C. G. Young, *Inorg. Chem.* **2006**, *45*, 352.
- [98] C. Kashima, A. Katoh, M. Shimizu, Y. Omote, *Heterocycles* **1984**, *22*, 2591.
- [99] B. M. Adger, P. Ayrey, R. Bannister, M. A. Forth, Y. Hajikarimian, N. J. Lewis, C. O'Farrell, N. Owens, A. Shamji, *Perkin Trans.* **1988**, 2791.
- [100] O. S. Kanishchev, W. R. Dolbier, *Angew. Chem. Int. Ed.* **2015**, *54*, 280.
- [101] X. Chen, J.-Q. Qu, *Z. Anorg. Allg. Chem.* **2015**, *641*, 1301.
- [102] P. K. Baker, M. E. Harman, S. Hughes, M. B. Hursthouse, K. M. Abdul Malik, *J. Organomet. Chem.* **1995**, *498*, 257.
- [103] K. Sukcharoenphon, K. B. Capps, K. A. Abboud, C. D. Hoff, *Inorg. Chem.* **2001**, *40*, 2402.
- [104] F. G. Bordwell, *Acc. Chem. Res.* **1988**, *21*, 456.
- [105] C. Hansch, A. Leo, R. W. Taft, *Chem. Rev.* **1991**, *91*, 165.
- [106] D. Lappas, D. M. Hoffman, K. Folting, J. C. Huffman, *Angew. Chem. Int. Ed.* **1988**, *27*, 587.
- [107] D. M. Hoffman, J. C. Huffman, D. Lappas, D. A. Wierda, *Organometallics* **1993**, *12*, 4312.
- [108] M. Benedetti, V. Lamacchia, D. Antonucci, P. Papadia, C. Pacifico, G. Natile, F. P. Fanizzi, *Dalton Trans.* **2014**, *43*, 8826.
- [109] J. M. Fritsch, N. D. Retka, K. McNeill, *Inorg. Chem.* **2006**, *45*, 2288.
- [110] M. Takahashi, K. Sakamoto, *J. Phys. Chem. A* **2004**, *108*, 5710.
- [111] B. R. Penfold, *Acta Cryst.* **1953**, *6*, 707.
- [112] a) C. Lorber, J. P. Donahue, C. A. Goddard, E. Nordlander, R. H. Holm, *J. Am. Chem. Soc.* **1998**, *120*, 8102; b) A. A. Eagle, C. G. Young, E. R. T. Tiekink, *Aust. J. Chem.* **2004**, *57*, 269; c) K. Helmdach, A. Villinger, W. W. Seidel, *Z. Anorg. Allg. Chem.* **2015**, *641*, 2300.
- [113] a) J. M. A. Al-Rawi, A.-H. Khuthier, *Org. Magn. Reson.* **1981**, *15*, 285; b) R. J. Abraham, M. Reid, *Perkin Trans. 2* **2001**, 1195.
- [114] N. Salvi, L. Belpassi, F. Tarantelli, *Chem. Eur. J.* **2010**, *16*, 7231.
- [115] S. Flügge, A. Anoop, R. Goddard, W. Thiel, A. Fürstner, *Chem. Eur. J.* **2009**, *15*, 8558.
- [116] L. Rocchigiani, J. Fernandez-Cestau, G. Agonigi, I. Chambrier, P. H. M. Budzelaar, M. Bochmann, *Angew. Chem. Int. Ed.* **2017**, *56*, 13861.
- [117] R. E. M. Brooner, R. A. Widenhoefer, *Angew. Chem. Int. Ed.* **2013**, *52*, 11714.
- [118] M. B. Gravestock, W. S. Johnson, B. E. McCarry, R. J. Parry, B. E. Ratcliffe, *J. Am. Chem. Soc.* **1978**, *100*, 4274.
- [119] H. G.O. Becker, W. Berger, G. Domschke, E. Fanghänel, J. Faust, M. Fischer, F. Gentz, K. Gewalt, R. Gluch, R. Mayer et al., *Organikum. Organisch-chemisches Grundpraktikum*, Wiley-VCH Verlag GmbH, Weinheim, **2001**.
- [120] a) T. Zuschneid, H. Fischer, T. Handel, K. Albert, G. Häflinger, *Z. Naturforsch. B* **2004**, *59*, 1153; b) E. Kloster-Jensen, R. Tabacchi, *Tetrahedron Lett.* **1972**, *13*, 4023.
- [121] W. N. Olmstead, Z. Margolin, F. G. Bordwell, *J. Org. Chem.* **1980**, *45*, 3295.
- [122] S. Minegishi, H. Mayr, *J. Am. Chem. Soc.* **2003**, *125*, 286.
- [123] H. K. Hall, *J. Am. Chem. Soc.* **1957**, *79*, 5441.
- [124] T. B. Phan, M. Breugst, H. Mayr, *Angew. Chem. Int. Ed.* **2006**, *45*, 3869.
- [125] T. B. Phan, H. Mayr, *Can. J. Chem.* **2005**, *83*, 1554.

[126] a) G. M. Sheldrick, *Acta Crystallogr. A* **2008**, *64*, 112; b) G. M. Sheldrick, *Acta Crystallogr. C* **2015**, *71*, 3.

7. APPENDIX

7.1 CRYSTALLOGRAPHIC DATA AND STRUCTURE REFINEMENT

Table 12. Crystal data and structure refinement for $[W(CO)_3(4\text{-Me-SPy})_2]$ (**C1**) and $[W(CO)(H\equiv H)(=4\text{-Me-SPy})(4\text{-Me-SPy})]$ (**C3**).

Crystal data	C1	C3
Empirical formula	C ₂₅ H ₁₂ N ₂ O ₃ S ₂ W	C ₂₇ H ₁₆ N ₂ OS ₂ W
Formula weight	516.24	512.29
Crystal description	needle, red	block, red
Crystal size	0.28 x 0.18 x 0.13 mm	0.29 x 0.15 x 0.11 mm
Crystal system, space group	monoclinic, C 2/c	monoclinic, P 2 ₁ /c
Unit cell dimensions:	a = 30.255(4) Å b = 7.2572(9) Å c = 17.973(3) Å β = 121.289(5)°	a = 7.7201(8) Å b = 16.5422(18) Å c = 14.1069(14) Å β = 105.730(4)°
Volume	3372.3(8) Å ³	1734.1(3) Å ³
Z	8	4
Calculated density	2.034 mg/m ³	1.962 mg/m ³
F(000)	1968	984
Linear absorption coefficient μ	7.112 mm ⁻¹	6.906 mm ⁻¹
Max. and min. transmission	1.000 and 0.577	1.000 and 0.623
Unit cell determination	2.65° < θ < 35.77° 8318 reflections used at 100 K	2.88° < θ < 40.58° 9799 reflections used at 100 K
Data collection		
Scan type		φ and ω scans
Q range for data collection	2.28 to 35.00°	2.74 to 40.00°
Reflections collected / unique	16307 / 7398	38720 / 10718
Significant unique reflections	6412 with I > 2σ(I)	8811 with I > 2σ(I)
R(int), R(sigma)	0.0316, 0.0410	0.0501, 0.0472
Completeness to Q = 35.0°	99.8%	99.9%
Refinement		
Refinement method	Full-matrix least-squares on F ²	
Data / parameters / restraints	7398 / 214 / 0	10718 / 228 / 4
Goodness-of-fit on F ²	1.034	1.029
Final R indices [I > 2σ(I)]	R1 = 0.0240, wR2 = 0.0550	R1 = 0.0293, wR2 = 0.0640
R indices (all data)	R1 = 0.0307, wR2 = 0.0574	R1 = 0.0411, wR2 = 0.0691
Extinction expression		none
Largest Δ/σ in last cycle	0.001	0.001
Largest difference peak and hole	1.465 and -1.150e/Å ³	2.336 and -2.380e/Å ³

Table 13. Crystal data and structure refinement for [W(CO)(H≡H)(Me-SPym)₂] (**C4**) and [W(CO)(H≡H)(4-Me-SPy)₂] (**C5**).

Crystal data	C4	C5
Empirical formula	C ₂₅ H ₁₆ N ₄ OS ₂ W	C ₂₅ H ₁₄ N ₂ OS ₂ W
Formula weight	516.29	486.25
Crystal description	block, red	needle, green
Crystal size	0.19 x 0.19 x 0.16 mm	0.26 x 0.11 x 0.07 mm
Crystal system, space group	monoclinic, P 2 ₁ /c	orthorhombic, P c c n
Unit cell dimensions:	a = 14.6041(13) Å b = 8.2934(7) Å c = 15.8933(12) Å β = 117.315(4)°	a = 17.273(3) Å b = 6.7944(11) Å c = 13.531(2) Å
Volume	1710.3(3) Å ³	1587.9(5) Å ³
Z	4	4
Calculated density	2.005 mg/m ³	2.034 mg/m ³
F(000)	992	928
Linear absorption coefficient m	7.006 mm ⁻¹	7.536 mm ⁻¹
Max. and min. transmission	1.000 and 0.555	1.000 and 0.496
Unit cell determination	4.58° < θ < 30.74° 6500 reflections used at 100 K	2.34° < θ < 34.22° 4760 reflections used at 100 K
Data collection		
Scan type		φ and ω scans
Q range for data collection	2.58 to 30.00°	3.01 to 35.00°
Reflections collected / unique	12318 / 5003	12659 / 3486
Significant unique reflections	4164 with I > 2σ(I)	2699 with I > 2σ(I)
R(int), R(sigma)	0.0390, 0.0499	0.0457, 0.0430
Completeness to Q = 35.0°	99.9%	99.9%
Refinement		
Refinement method	Full-matrix least-squares on F ²	
Data / parameters / restraints	5003 / 225 / 2	3486 / 118 / 0
Goodness-of-fit on F ²	1.065	1.109
Final R indices [I > 2σ(I)]	R1 = 0.0301, wR2 = 0.0607	R1 = 0.0311, wR2 = 0.0638
R indices (all data)	R1 = 0.0400, wR2 = 0.0639	R1 = 0.0458, wR2 = 0.0695
Extinction expression		none
Largest Δ/σ in last cycle	0.002	0.001
Largest difference peak and hole	1.796 and -1.775e/Å ³	1.452 and -1.226e/Å ³

Table 14. Crystal data and structure refinement for [WO(H≡-H)(Me-SPym)₂] (**C6**) and [WO(H≡-H)(4-Me-SPy)₂] (**C7**).

Crystal data	C6	C7
Empirical formula	C ₂₄ H ₁₆ N ₄ OS ₂ W	C ₂₄ H ₁₄ N ₂ OS ₂ W
Formula weight	504.28	474.24
Crystal description	needle, colorless	block, colorless
Crystal size	0.25 x 0.11 x 0.09 mm	0.16 x 0.13 x 0.10 mm
Crystal system, space group	monoclinic, C 2/c	triclinic, P -1
Unit cell dimensions:	a = 19.236(2) Å b = 11.1271(13) Å c = 16.563(2) Å β = 109.575(5)°	a = 7.433(3) Å b = 7.930(3) Å c = 13.329(5) Å α = 94.702(8)° β = 98.065(7)° γ = 92.130(7)°
Volume	3340.4(7) Å ³	774.4(5) Å ³
Z	8	2
Calculated density	2.005 mg/m ³	2.034 mg/m ³
F(000)	1936	452
Linear absorption coefficient m	7.172 mm ⁻¹	7.724 mm ⁻¹
Max. and min. transmission	1.000 and 0.801	1.000 and 0.688
Unit cell determination	2.31° < θ < 35.55° 9248 reflections used at 100 K	2.58° < θ < 40.45° 8534 reflections used at 100 K
Data collection		
Scan type	φ and ω scans	f and w scans
Q range for data collection	2.15 to 35.00°	1.55 to 40.00°
Reflections collected / unique	39148 / 7350	18122 / 9584
Significant unique reflections	6332 with I > 2σ(I)	7852 with I > 2σ(I)
R(int), R(sigma)	0.0350, 0.0268	0.0387, 0.0516
Completeness to Q = 35.0°	100.0%	99.9%
Refinement		
Refinement method	Full-matrix least-squares on F ²	Full-matrix least-squares on F ²
Data / parameters / restraints	7350 / 216 / 2	9584 / 194 / 2
Goodness-of-fit on F ²	1.015	1.039
Final R indices [I > 2σ(I)]	R1 = 0.0187, wR2 = 0.0403	R1 = 0.0296, wR2 = 0.0678
R indices (all data)	R1 = 0.0261, wR2 = 0.0425	R1 = 0.0411, wR2 = 0.0720
Extinction expression	none	none
Largest Δ/σ in last cycle	0.003	0.002
Largest difference peak and hole	1.329 and -0.710e/Å ³	1.821 and -1.903e/Å ³